South Bay Pathology Society
December 2023

Disclosures
December 4, 2023

Dr. Greg Charville has disclosed a financial relationship as an advisory board member for Intuitive Surgical, Inc. The planners have determined that this relationship is not relevant to the clinical diagnostic case being presented. The remaining activity planners and faculty listed below have no relevant financial relationship(s) to disclose with ineligible companies whose primary business is producing, marketing, selling, re-selling, or distributing healthcare products used by or on patients.

Presenters/Faculty:
Armen Kharajian, MD
Greg Rumore, MD
Hubert Lau, MD
Margarita Munoz de Toro
David Bingham, MD
Susie Potterveld, MD
Ankur Sangoi, MD
Tyler Jankowski, MD

Activity Planners/Moderator:
Kristin Jensen, MD
Megan Troxell, MD, PhD
Dave Bingham, MD

23-1201

Armen Khararjian; Kaiser Permanente, Walnut Creek

Middle aged male who presented for screening colonoscopy

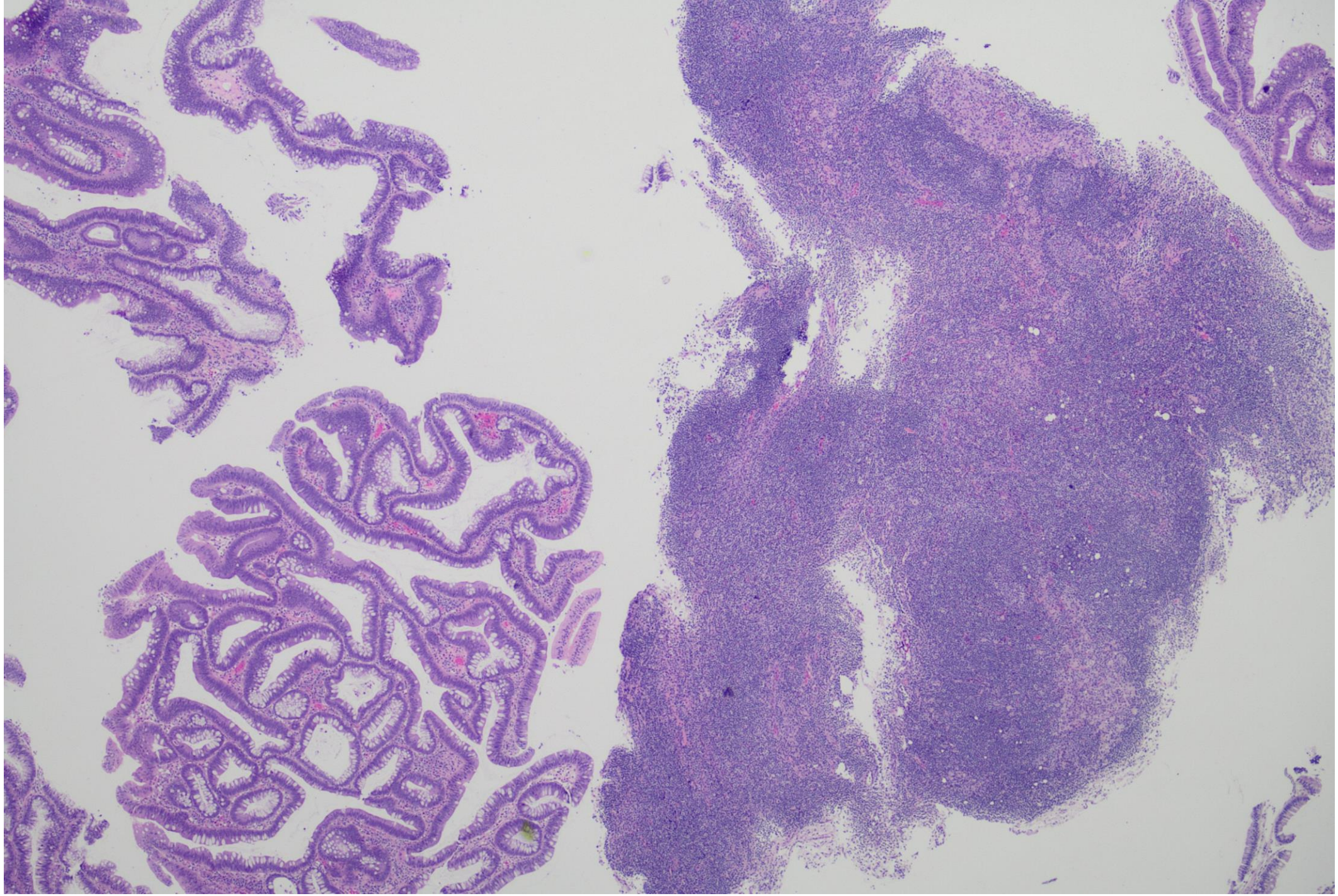

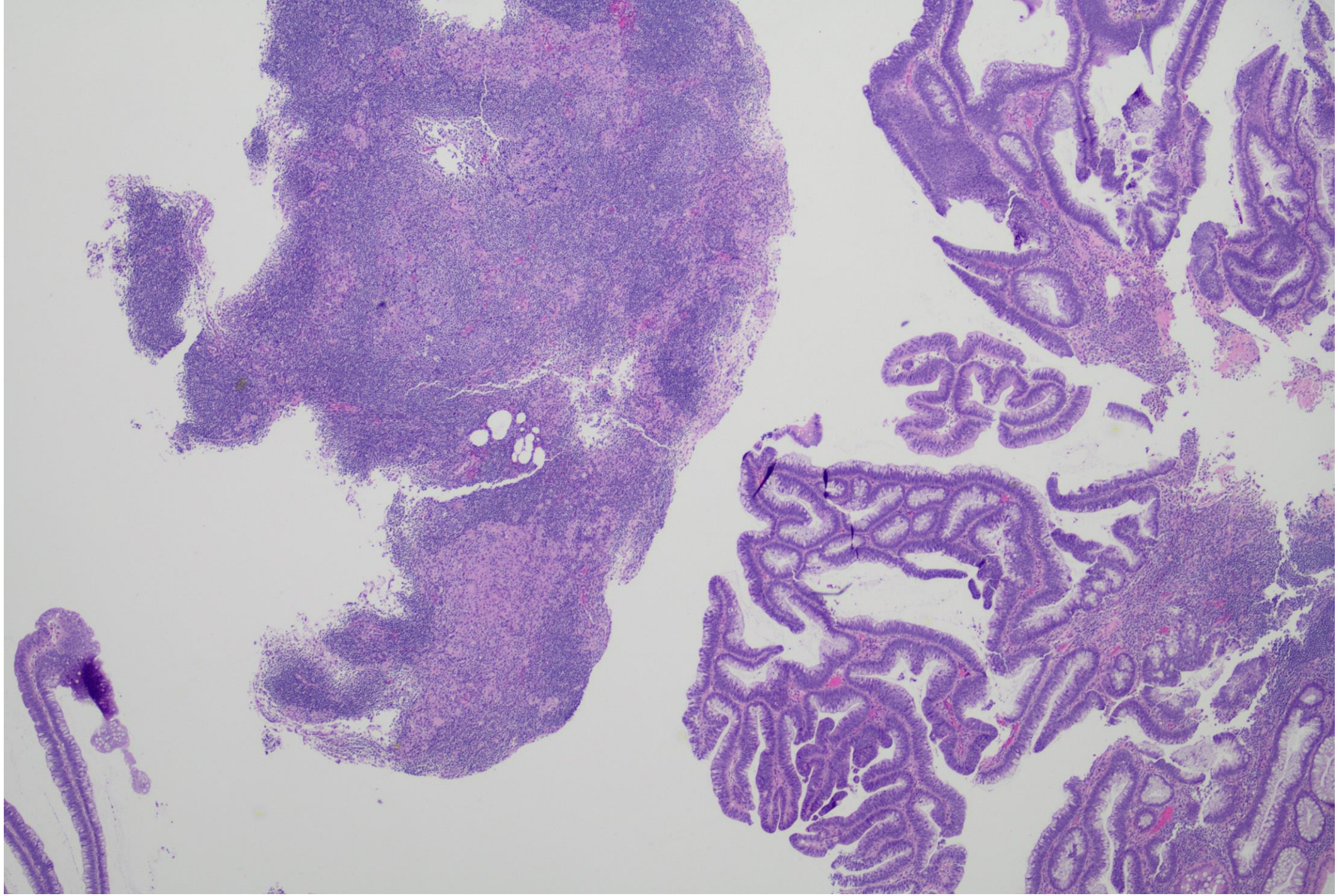

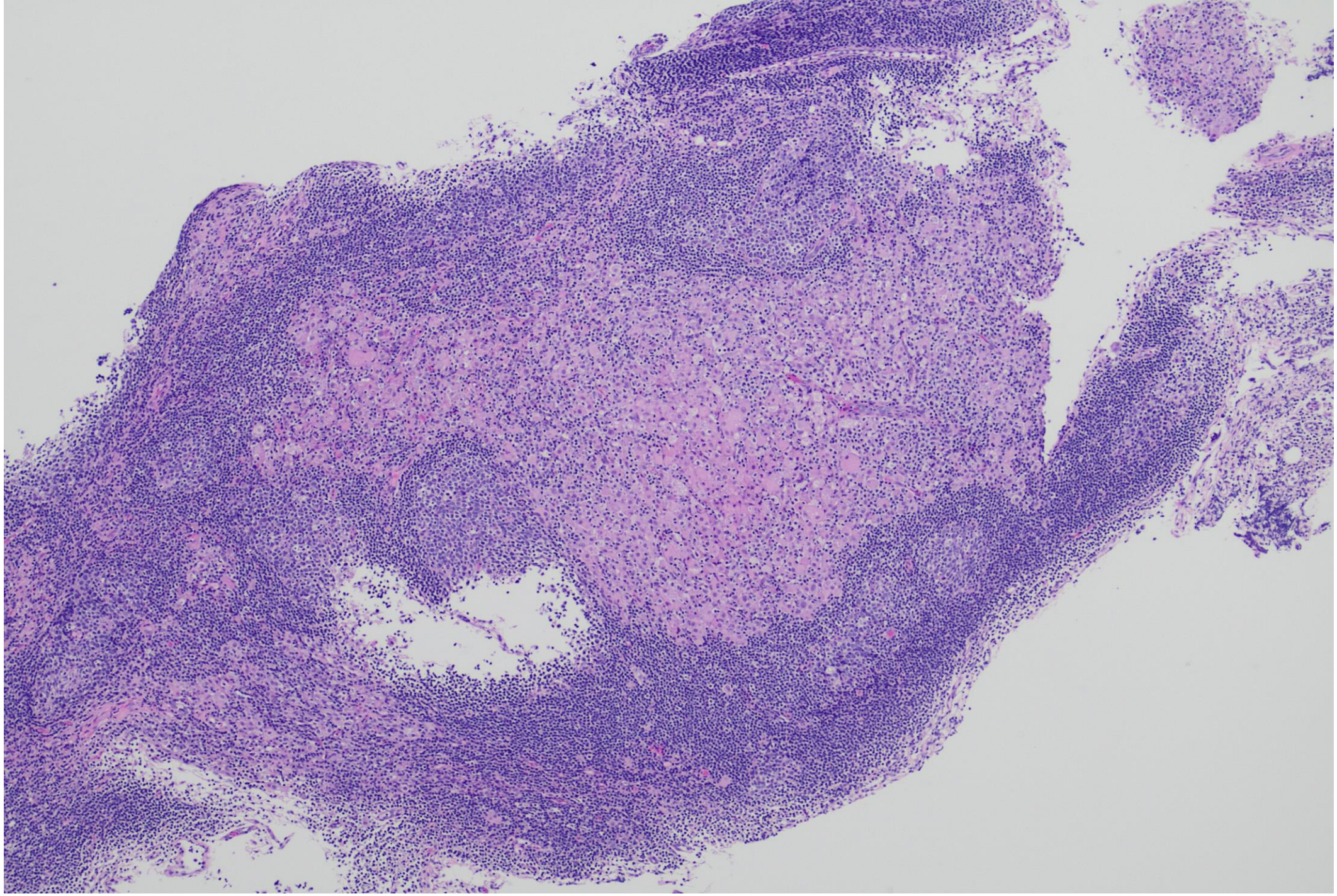

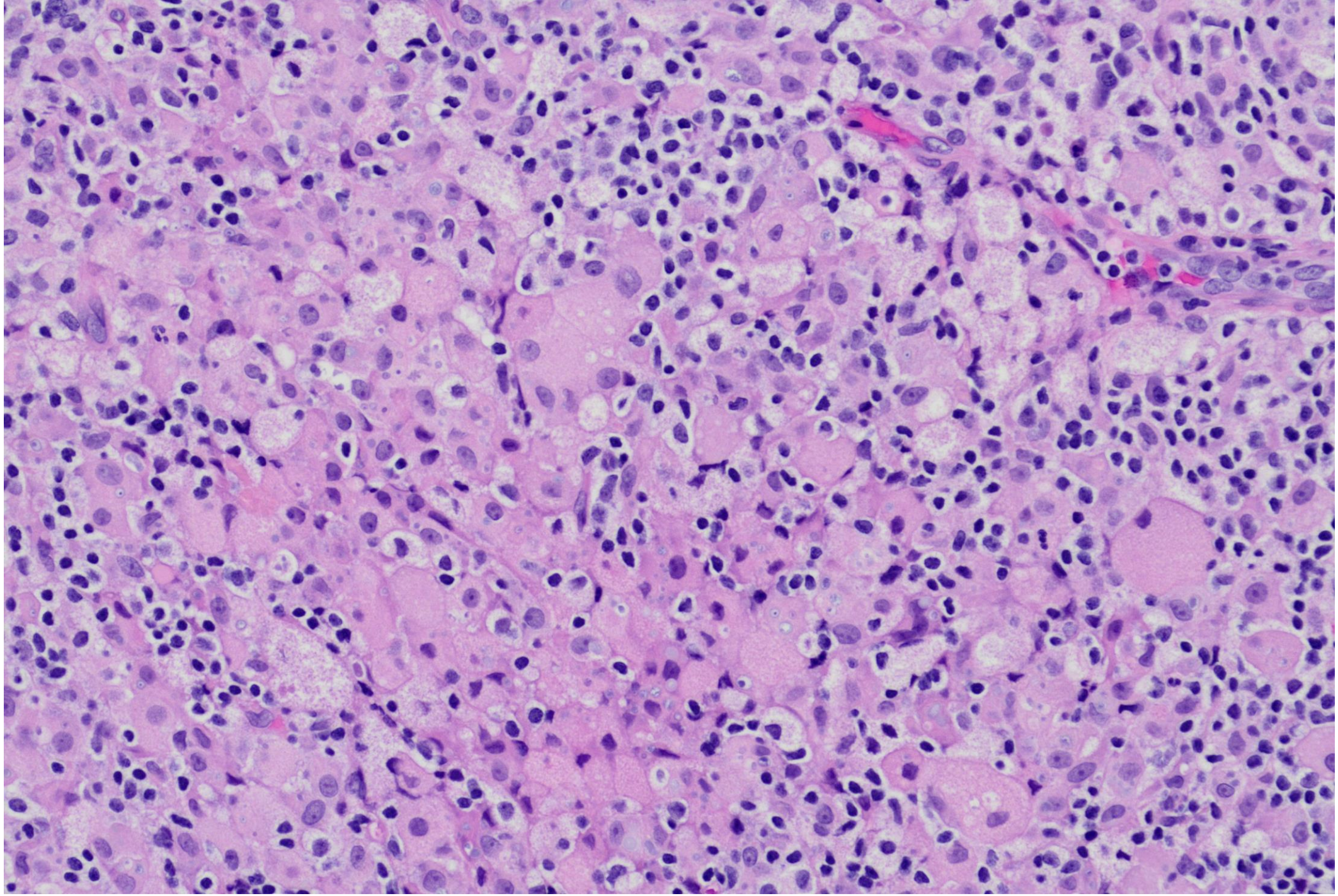

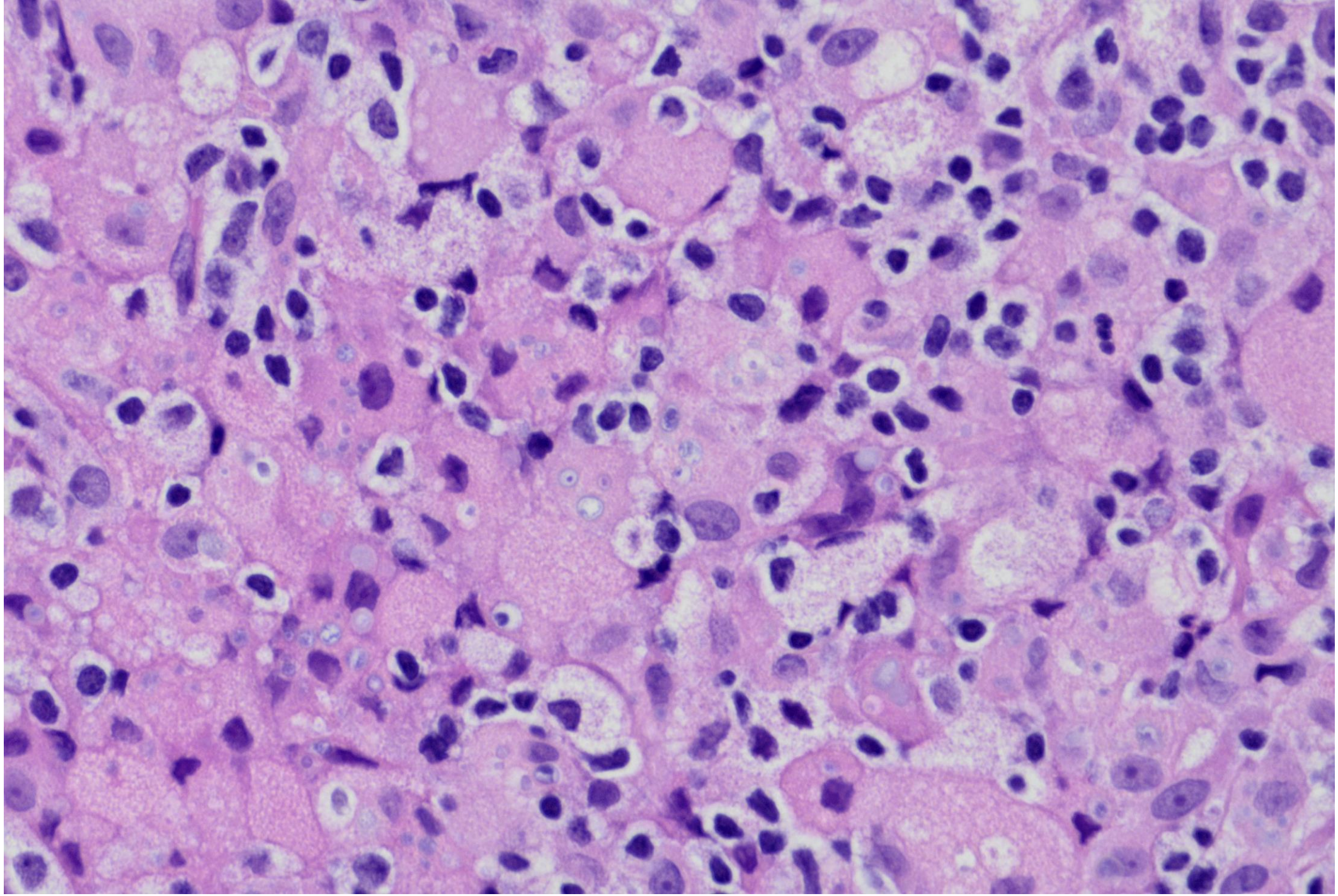

DIAGNOSIS?

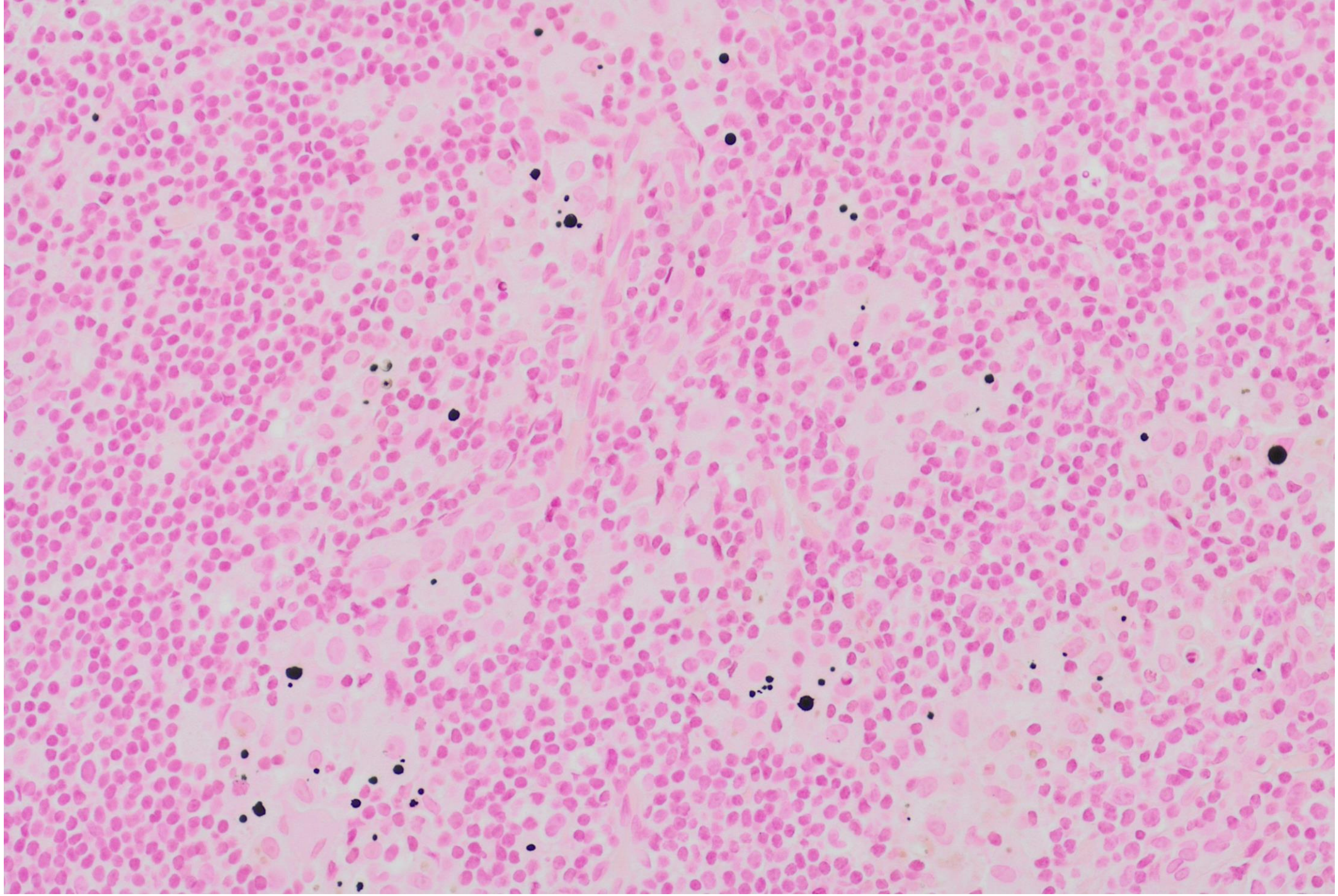

Malakoplakia

- Rare inflammatory condition that often occurs in immunocompromised individuals
- Due to defective inflammatory response (intraphagosomal digestion) to bacteria
- Often affects the GU tract (bladder)
- Can be seen in the colon and other sites

Key Features

- Clusters of macrophages often associated with prominent lymphoid aggregates
  - Clue at low power
- Higher power shows histiocytes (von Hansemann cells) with intracytoplasmic targetoid lesions (Michaelis-Gutmann bodies)
  - Stain with Von Kossa
    - Bacteria provide a nidus for the calcium phosphate crystals
- Treated with antibiotics and surgery

23-1202

Greg Rumore; Kaiser Permanente, Diablo Service Area

Late 20’s male with retrocaval adenopathy, anterior mediastinal mass and pleural effusion

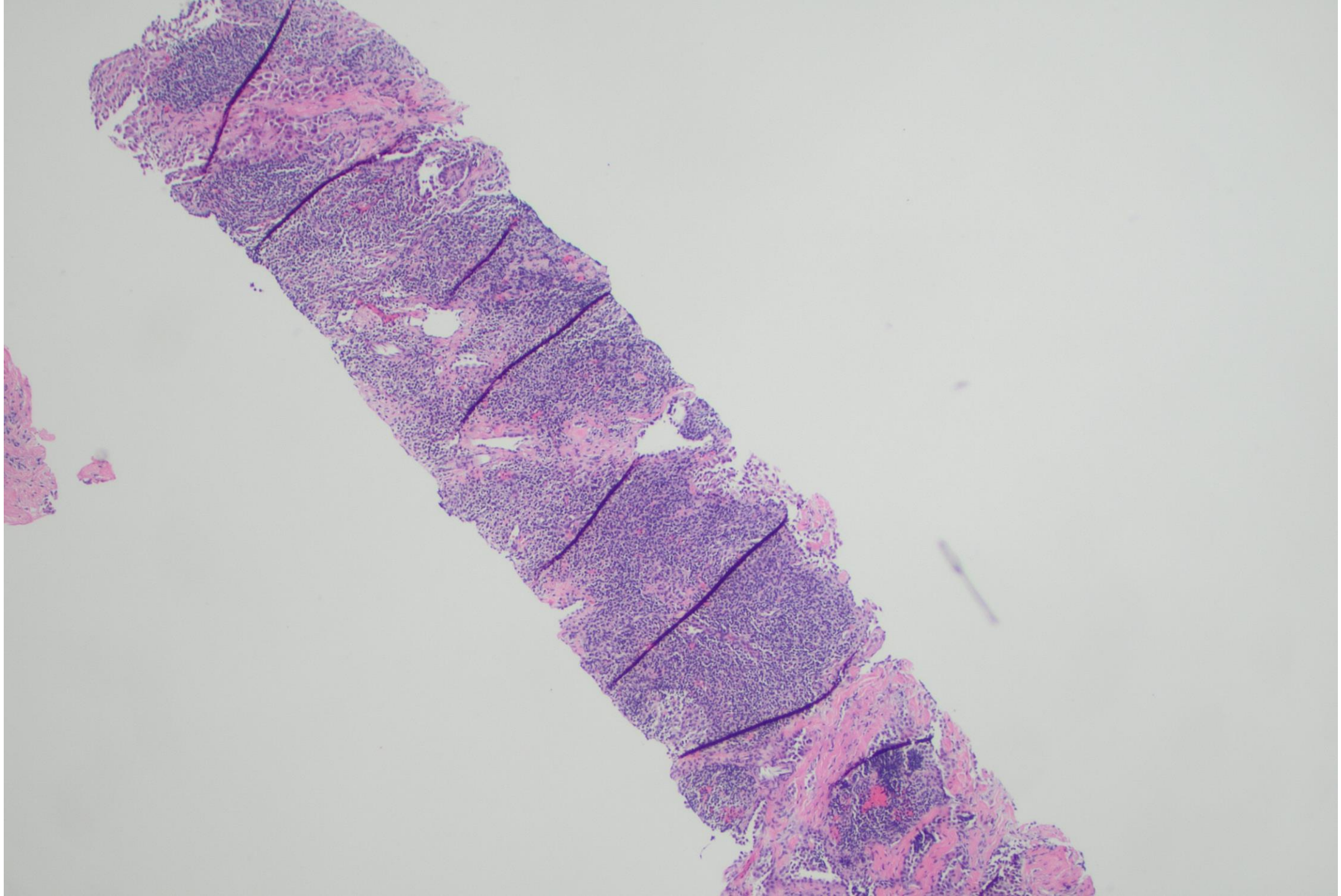

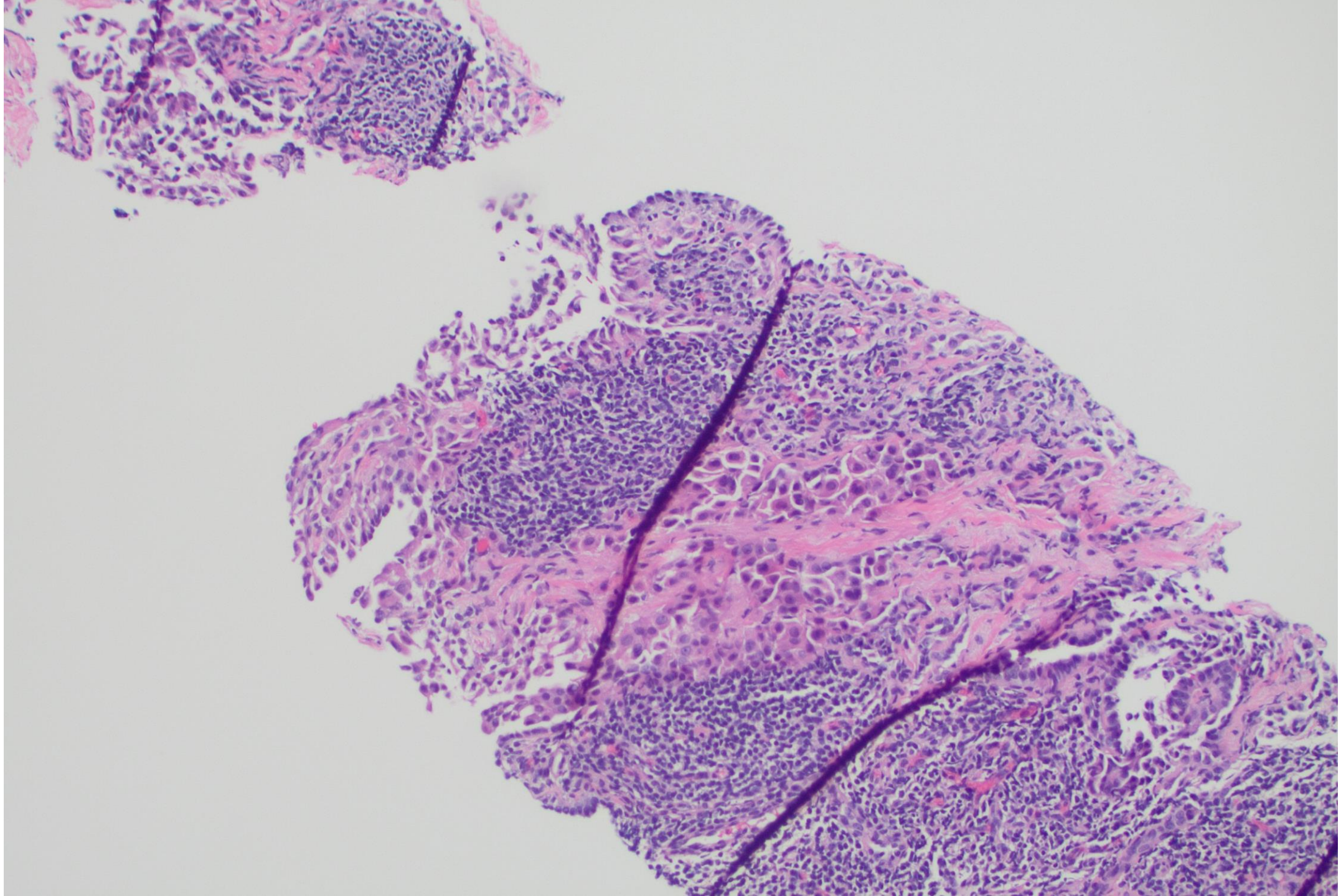

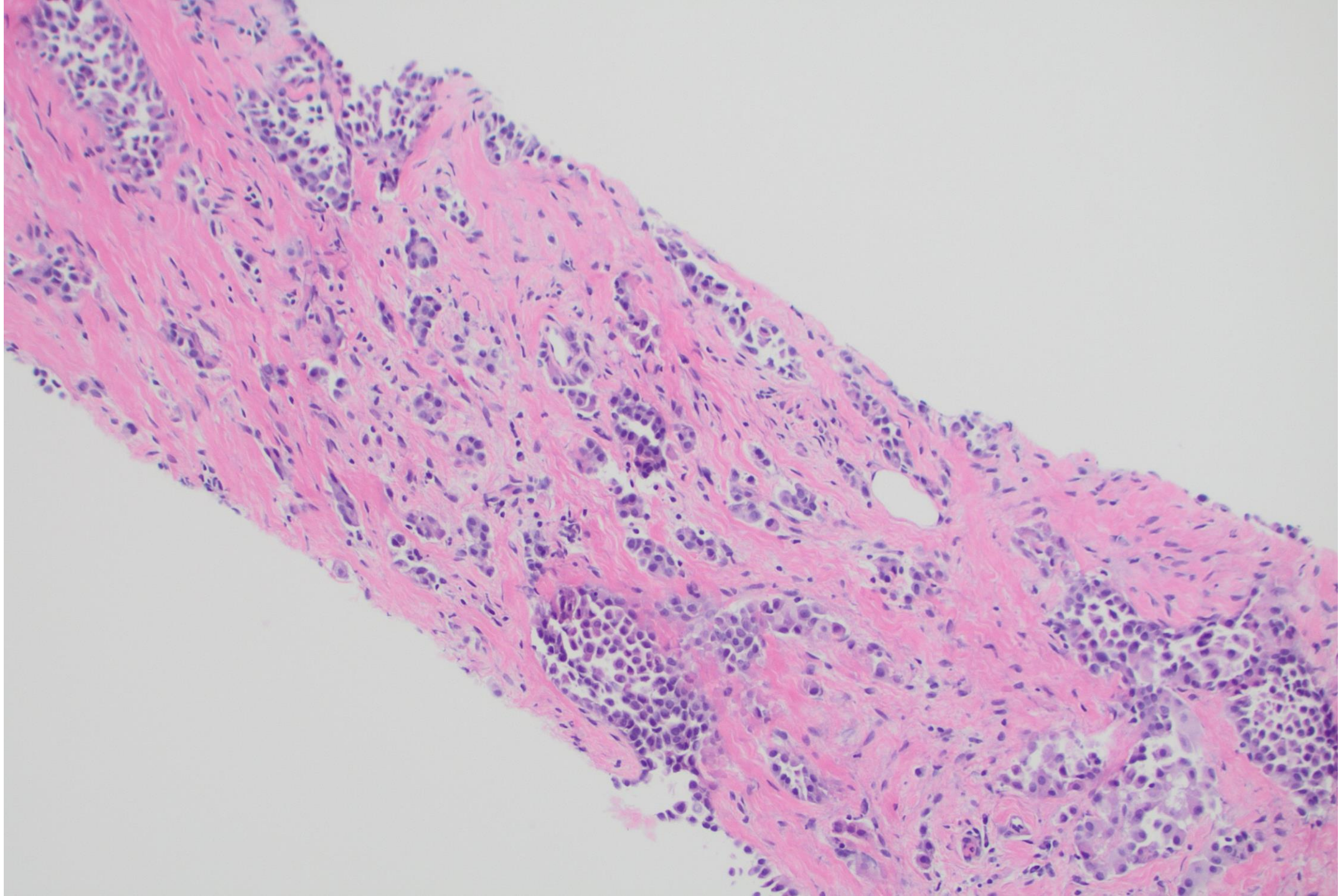

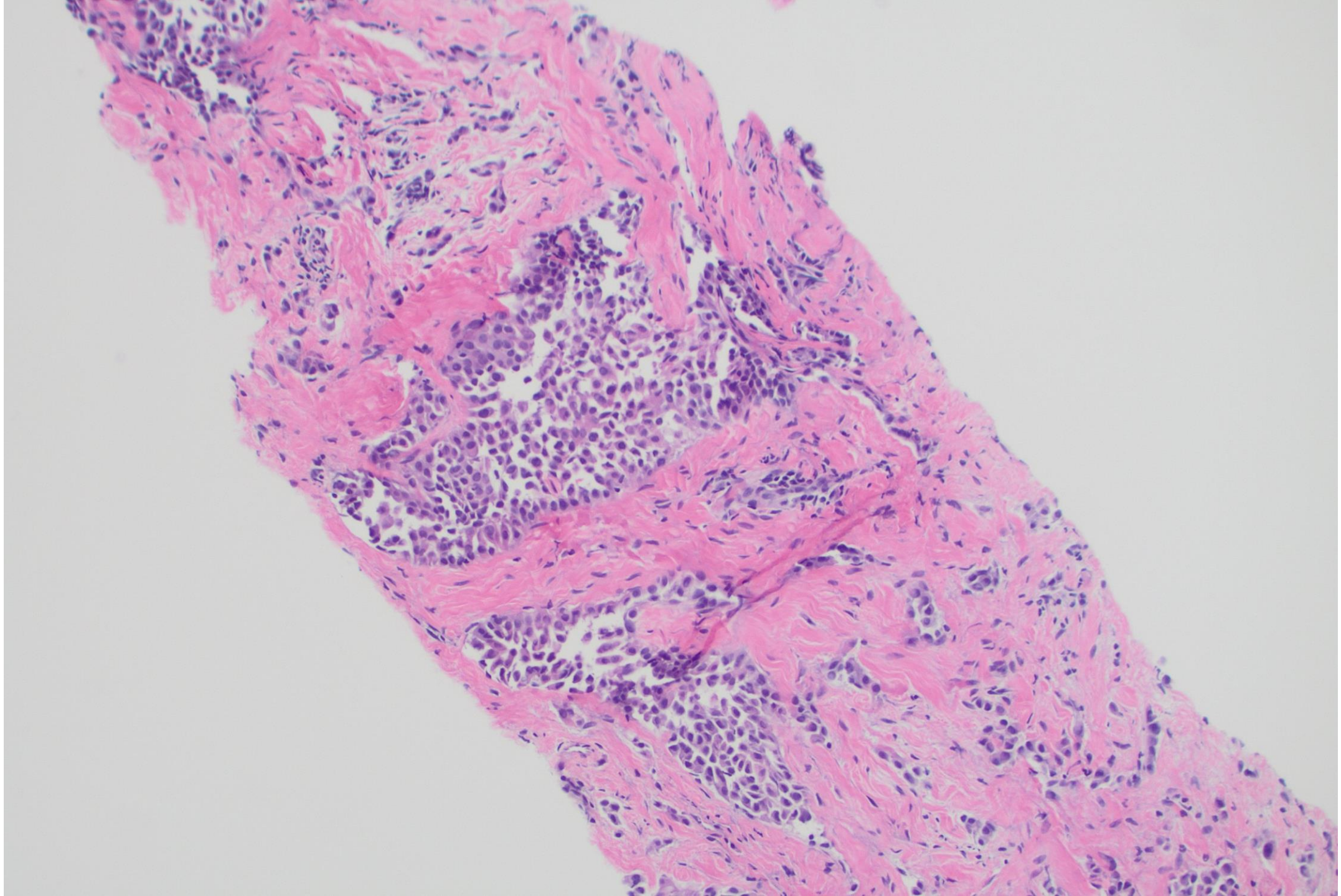

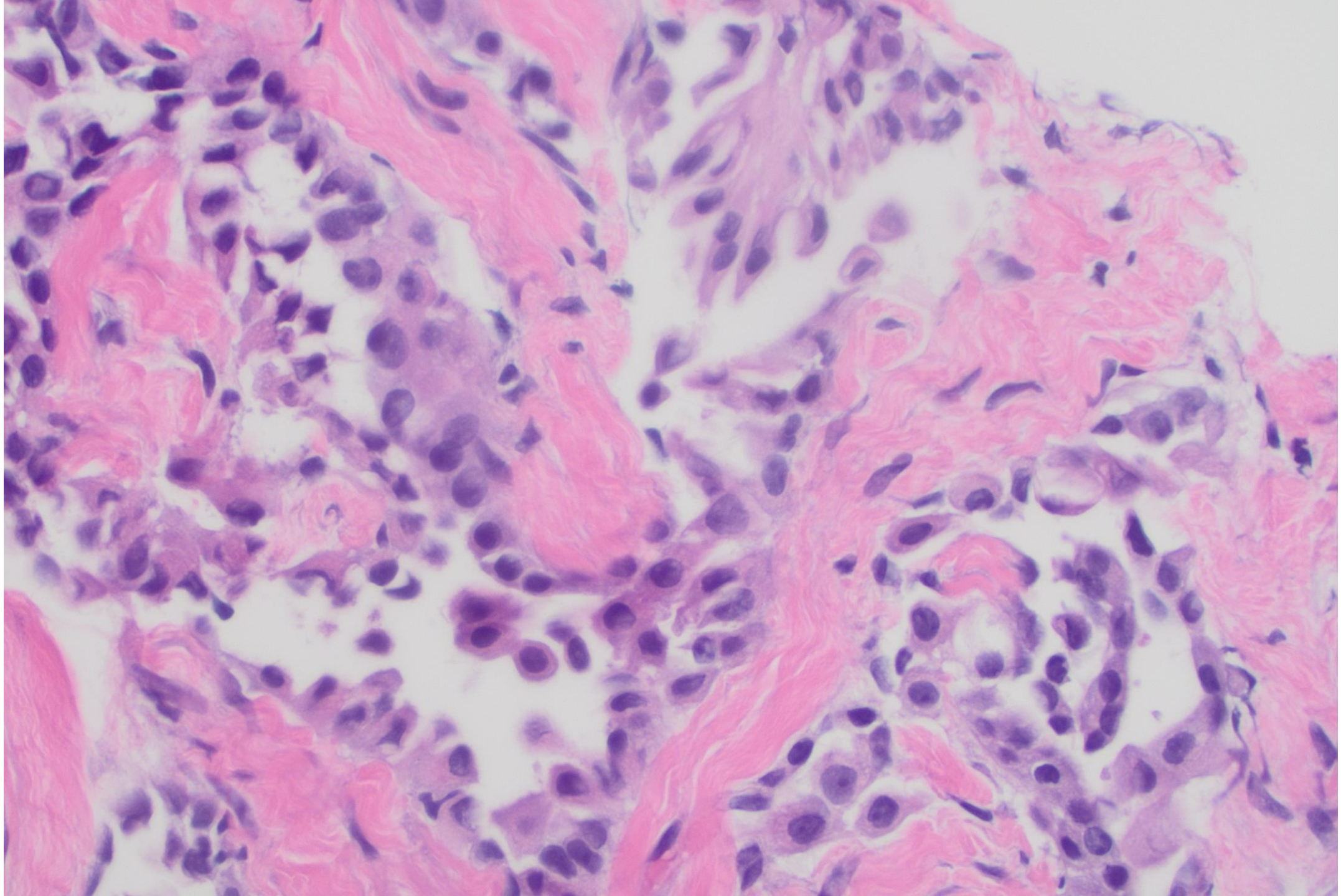

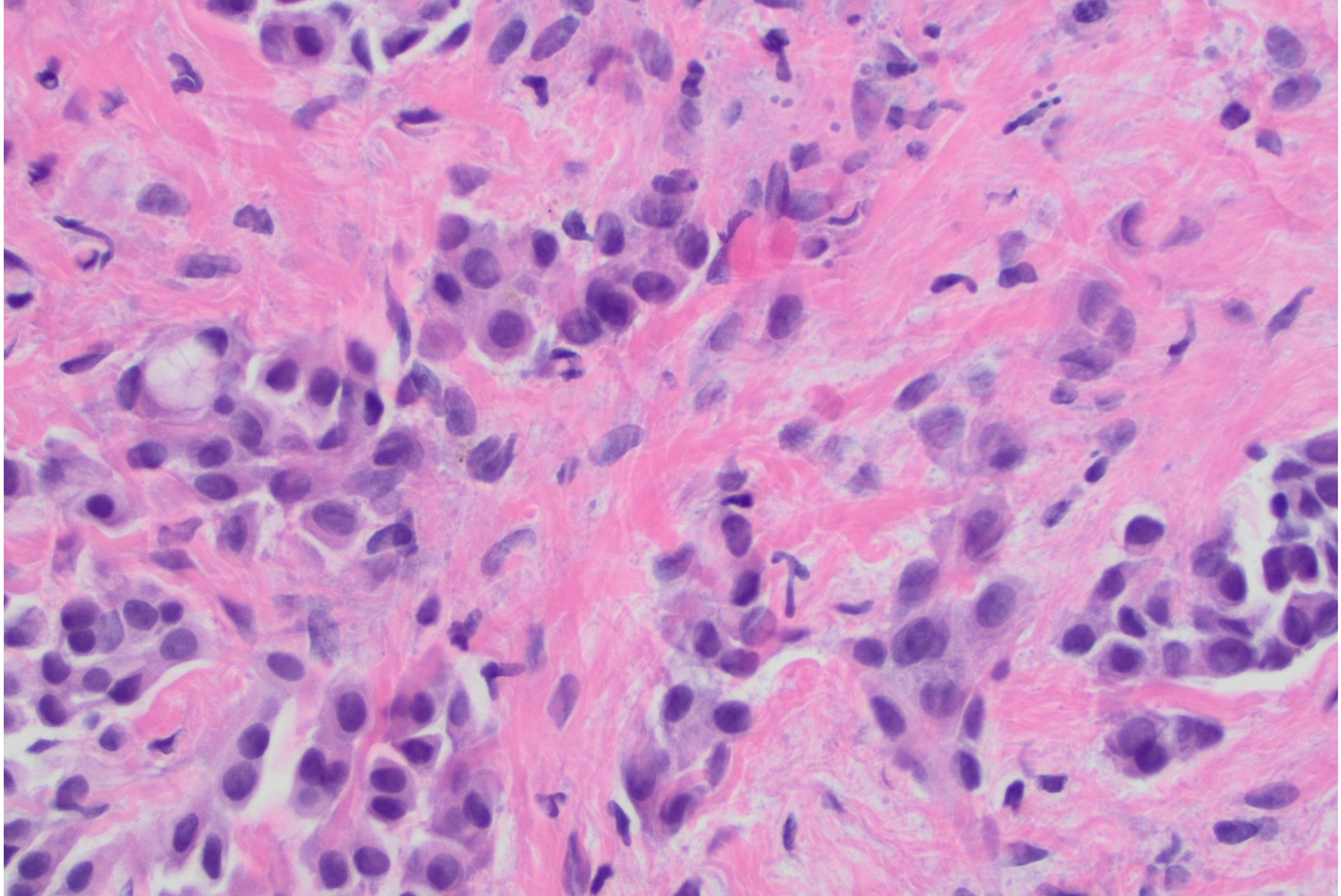

DIAGNOSIS?

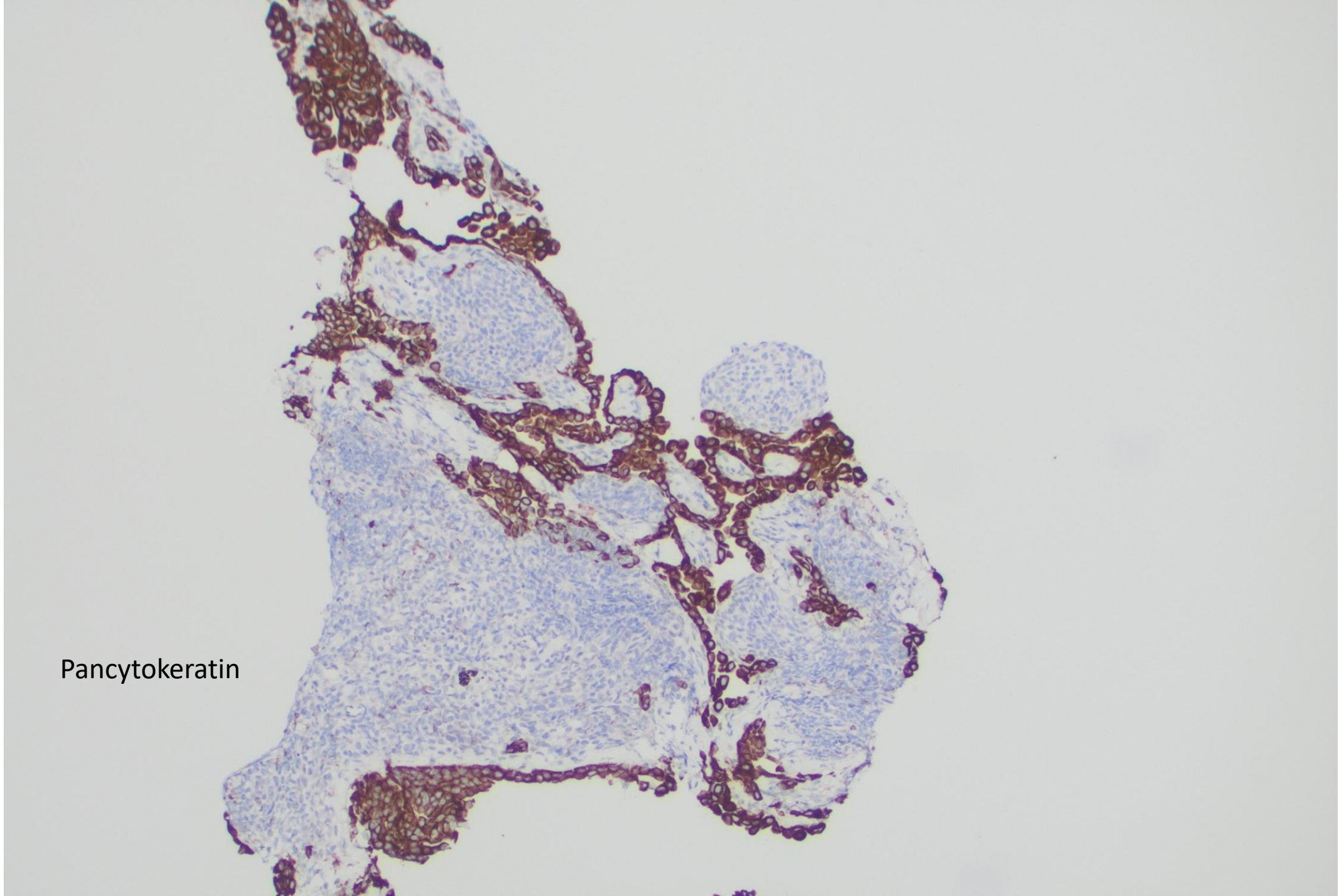

Pancytokeratin

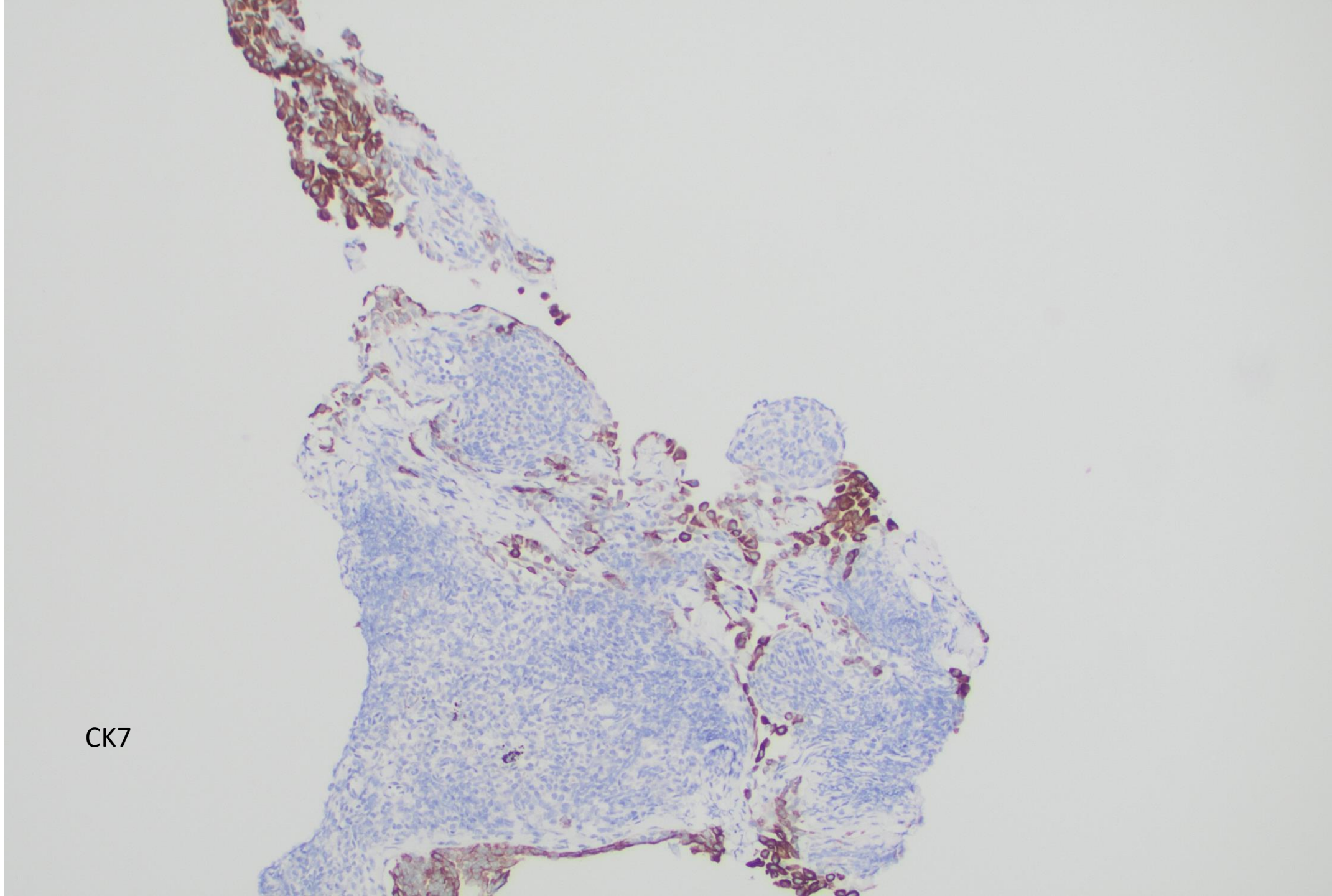
CK7

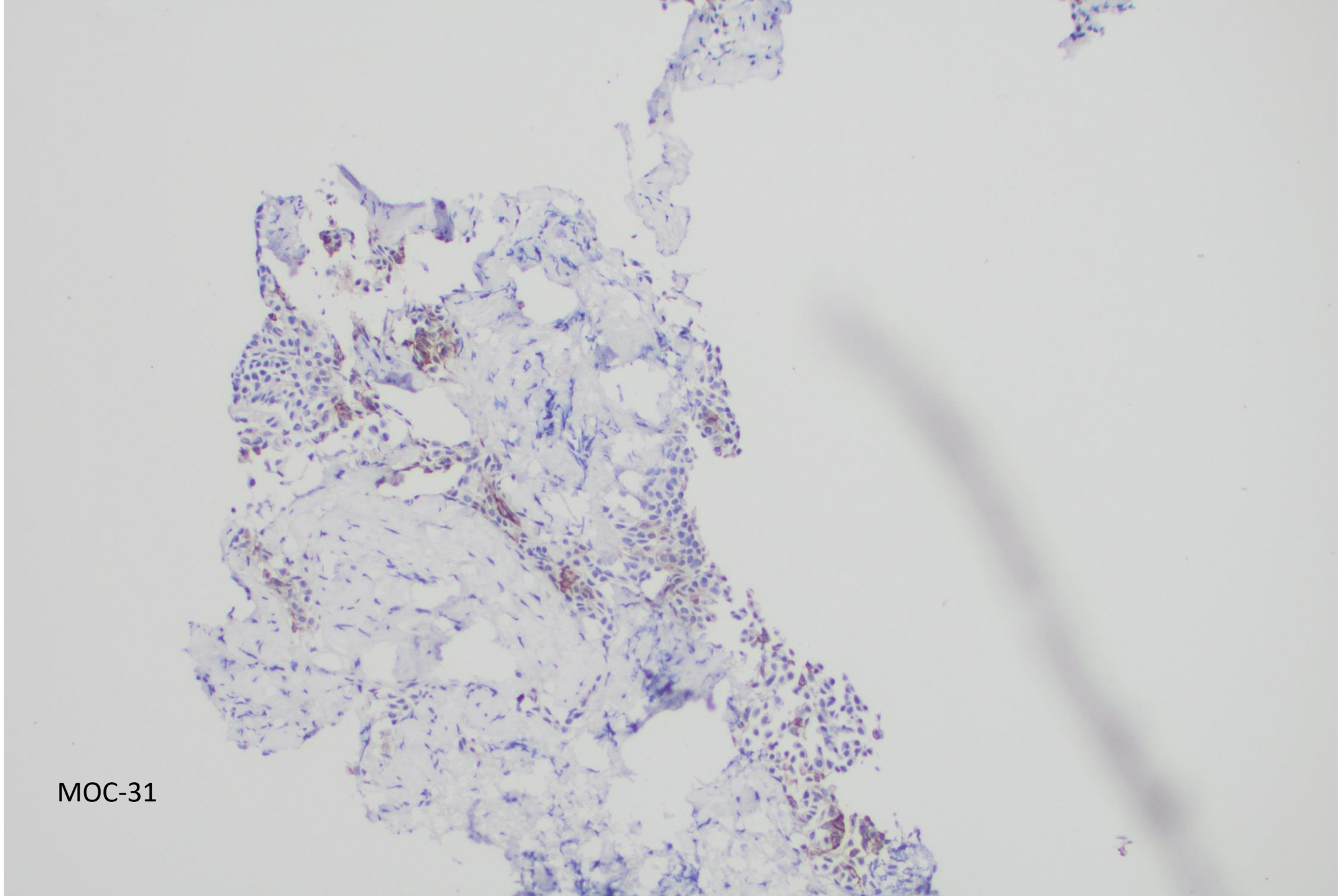
MOC-31

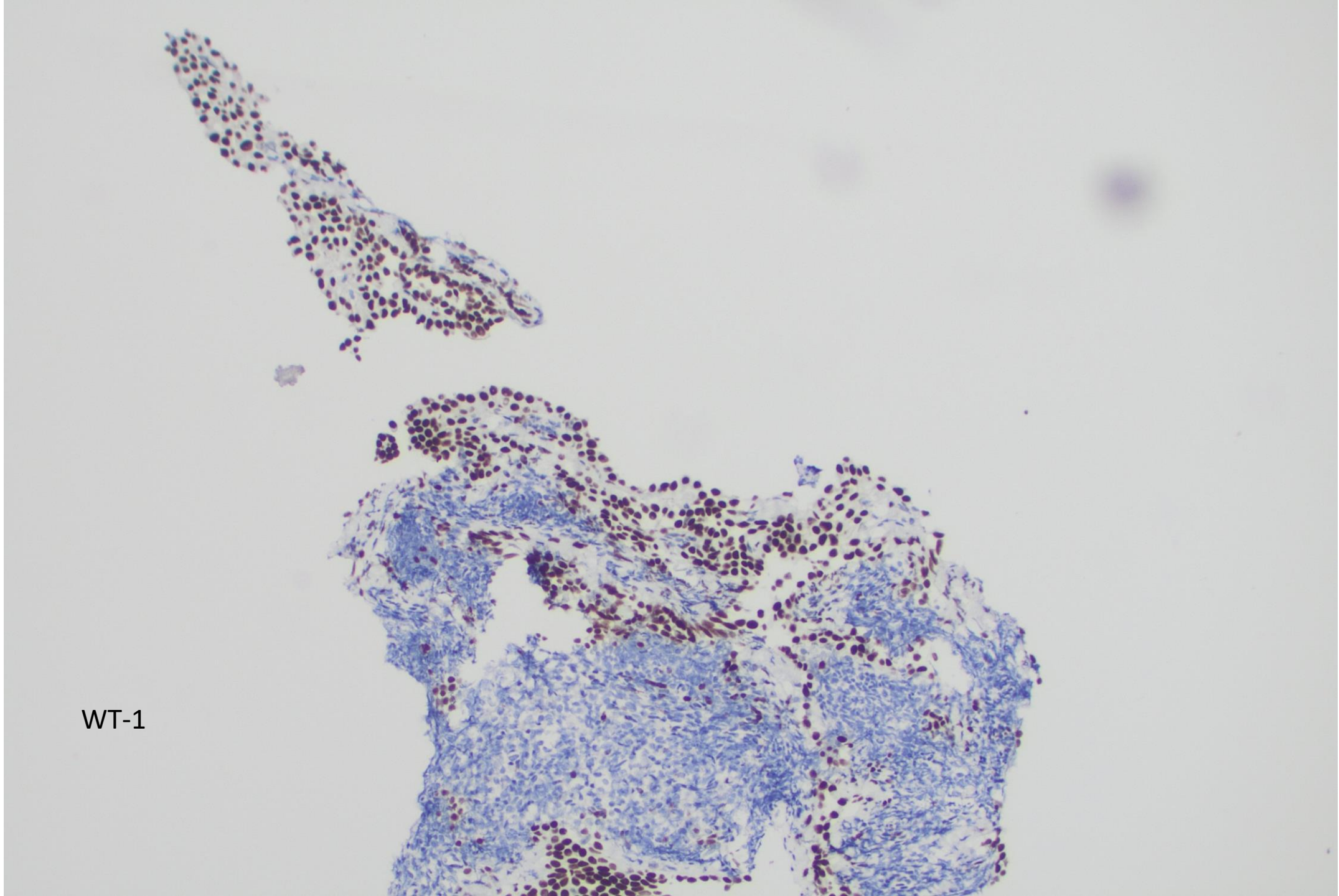
WT-1

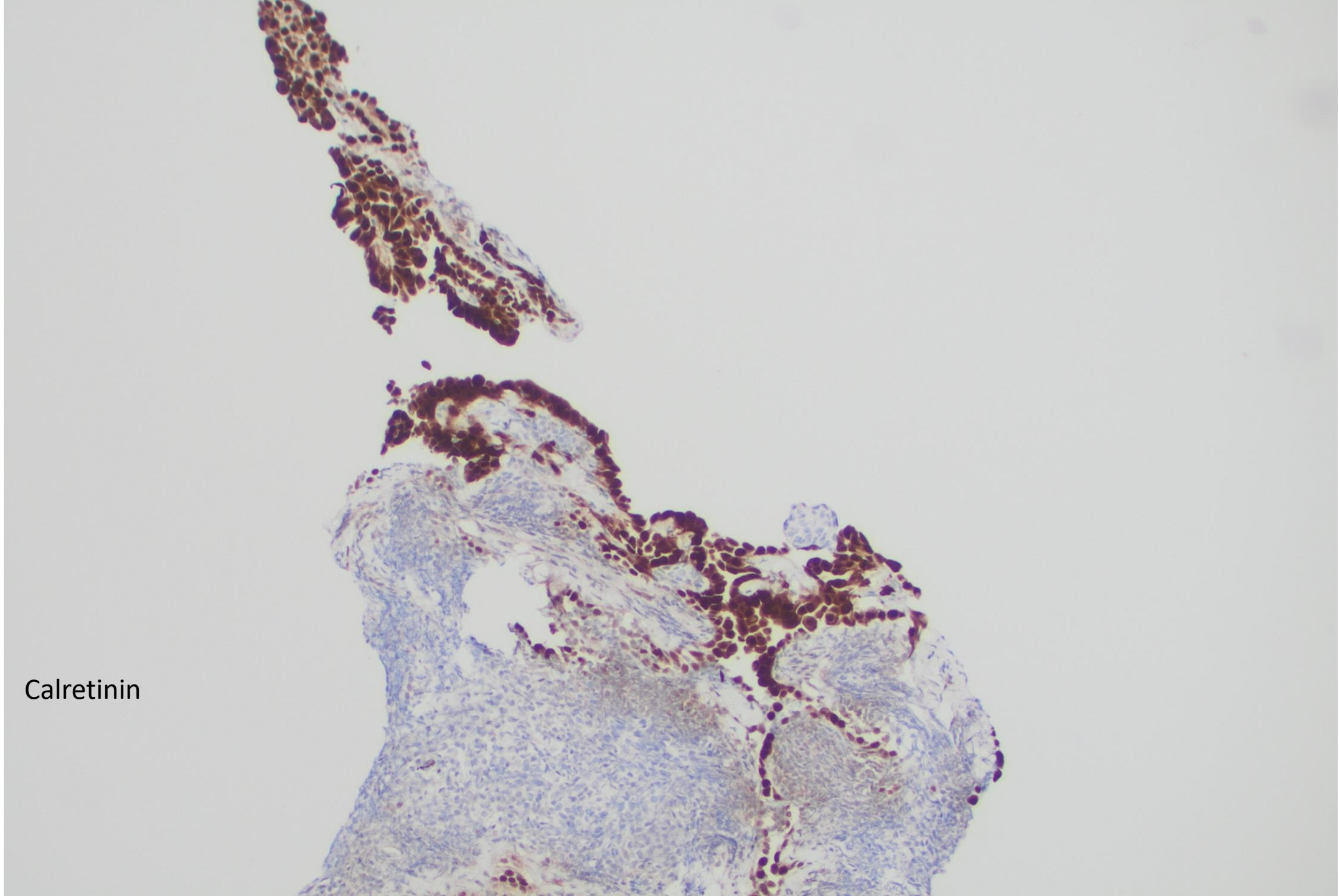

Calretinin

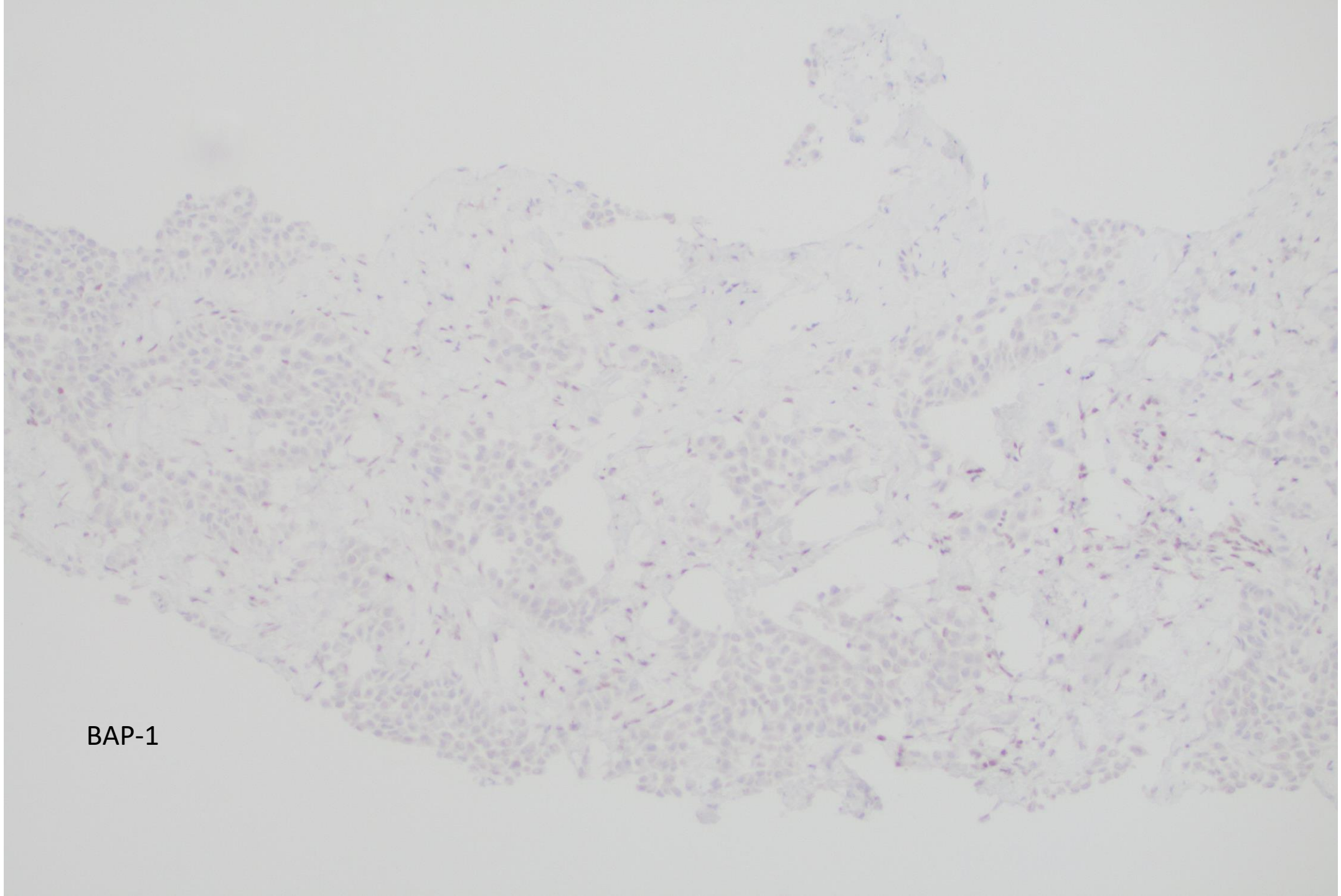
BAP-1

Mesothelioma with BAP1 inactivation

- History of “combined melanocytic proliferation with a BAP1 negative population”-2012 (MSKCC)
- Father with clear cell renal cell CA

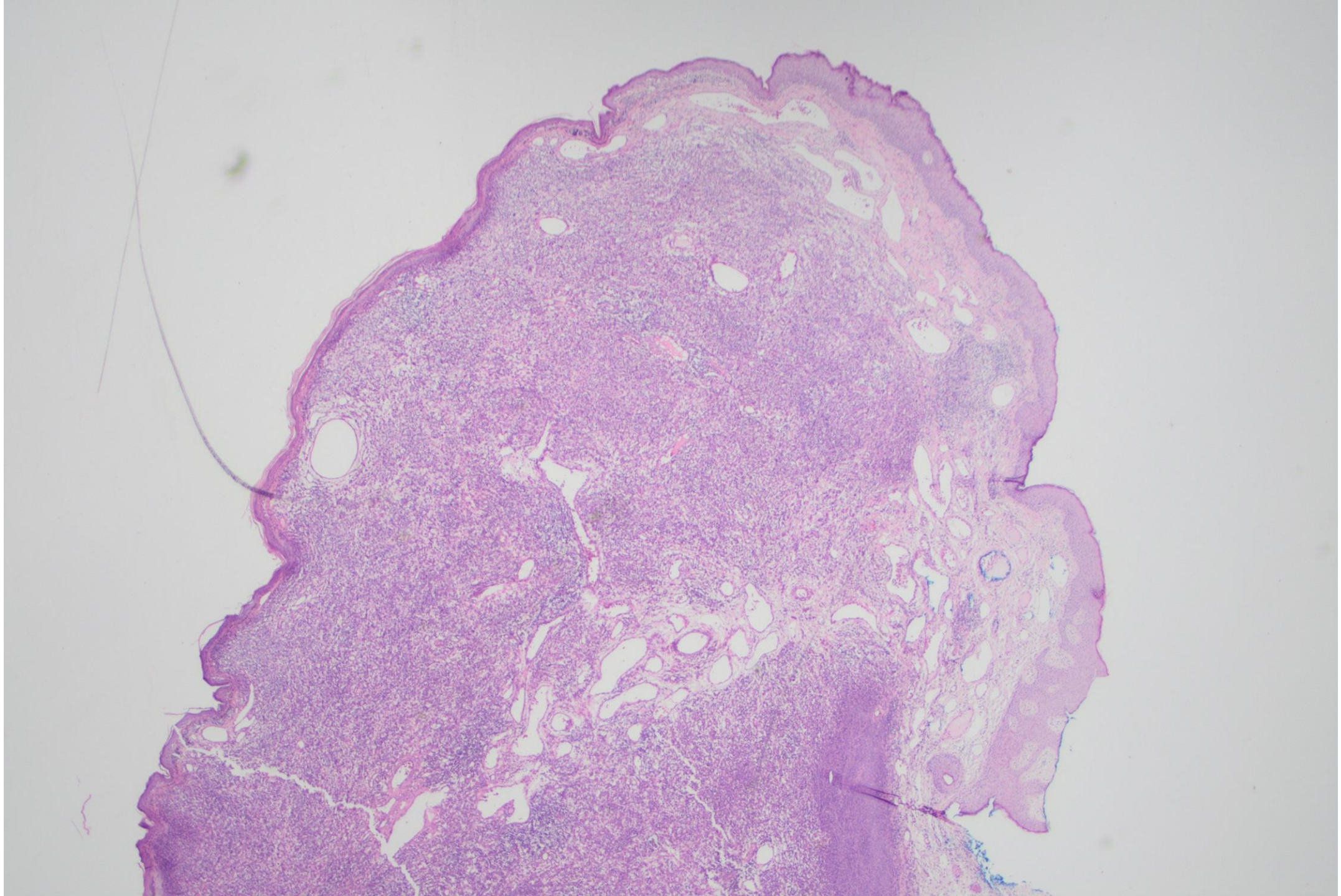

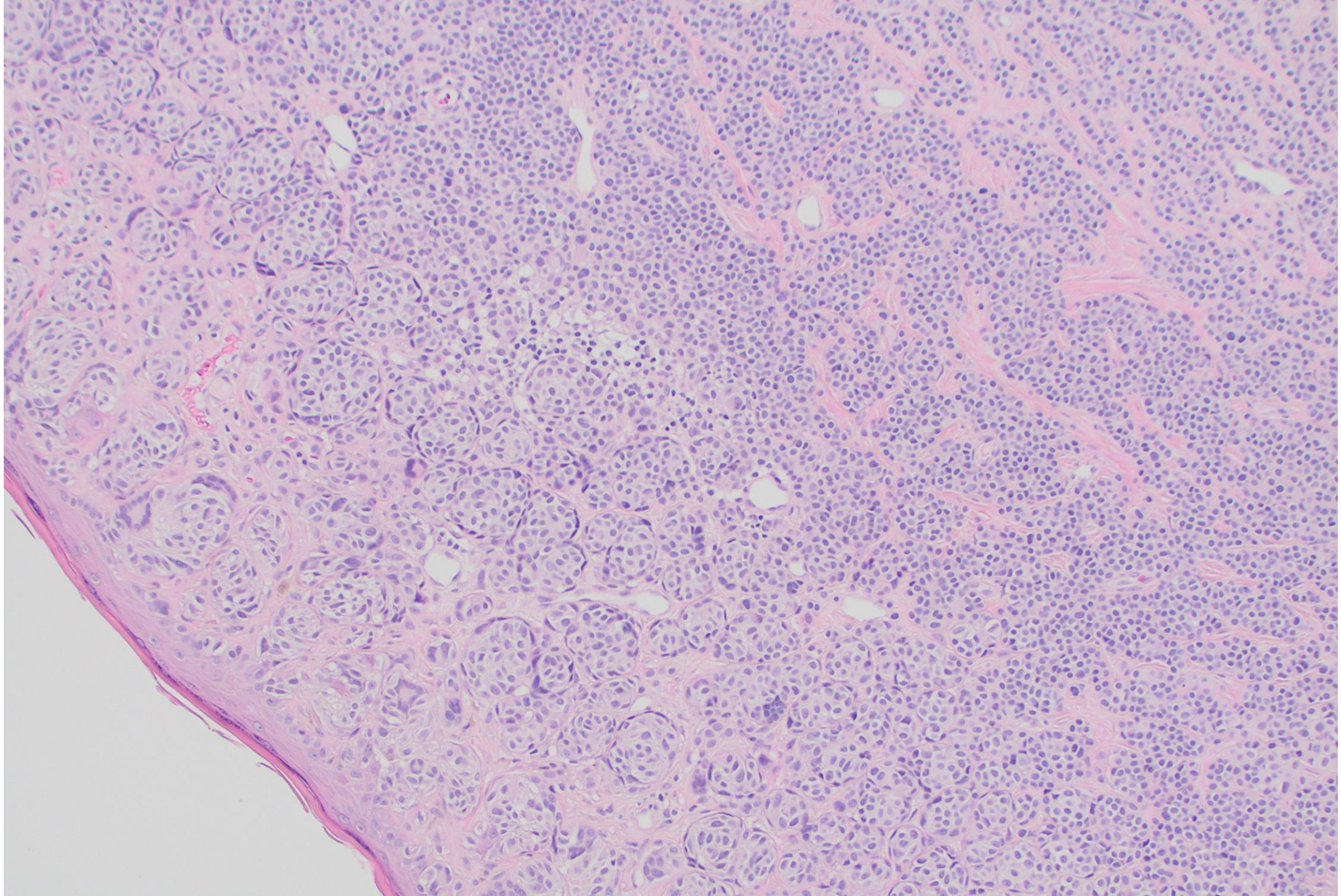

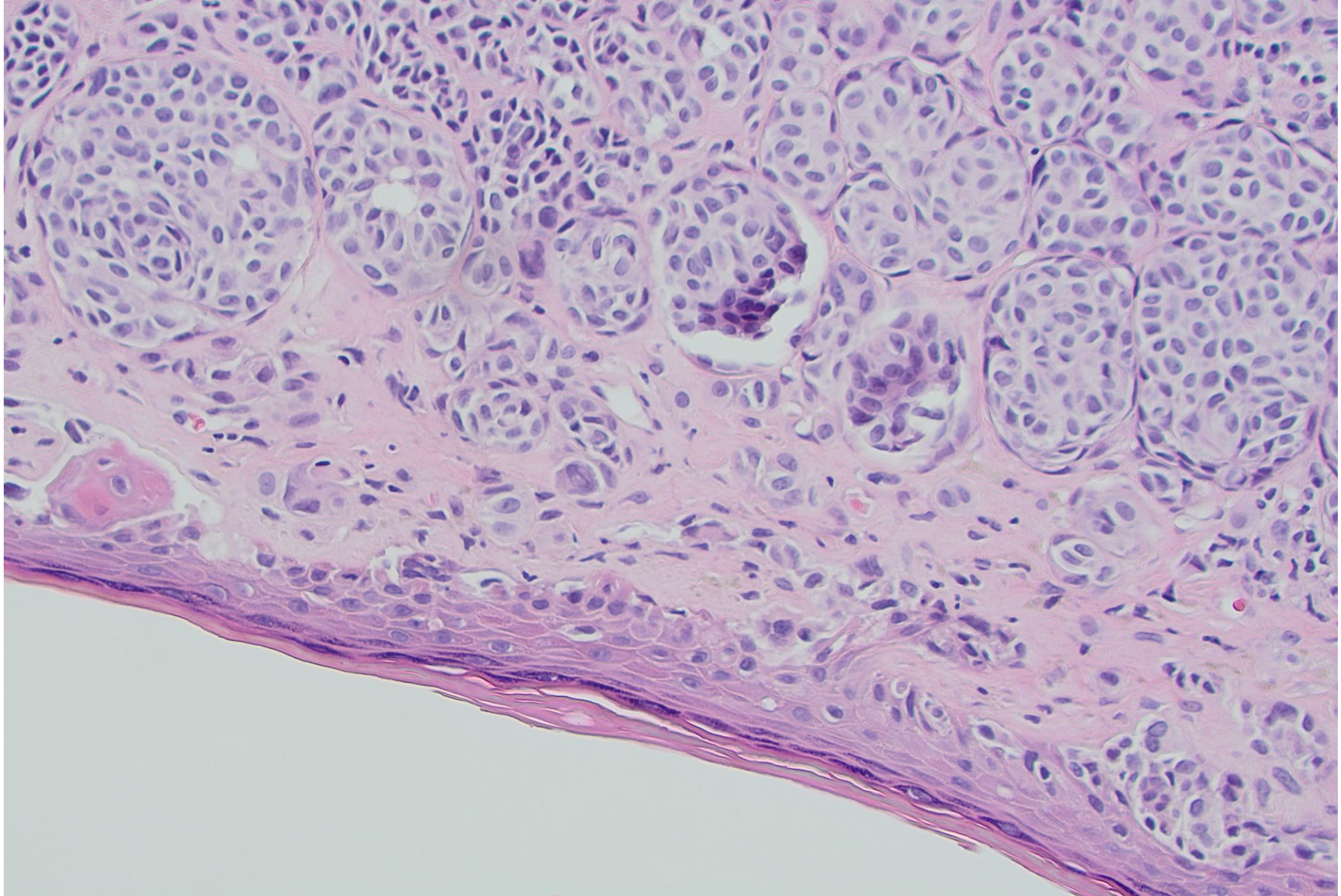

BAP1 Tumor predisposition syndrome

- Inherited disorder
- Atypical Spitz tumors
- Uveal melanoma
- Mesothelioma
- Clear cell renal cell CA
- Tumors tend to arise at a younger age and are more aggressive
- BAP1 negative mesothelioma patients appear to survive longer

Cause=mutations in BAP1 gene

- BAP1 protein = tumor suppressor
- Removes ubiquitin
- BAP1 protein is involved in cell proliferation, cell death, repair of damaged DNA, control of gene activity
- Inherited germline + non-inherited somatic mutation=tumor
- Environmental and lifestyle factors may determine type of tumor

23-1203

Greg Rumore; Kaiser Permanente, Diablo Service Area

Early 30’s female with breast carcinoma and a thyroid mass

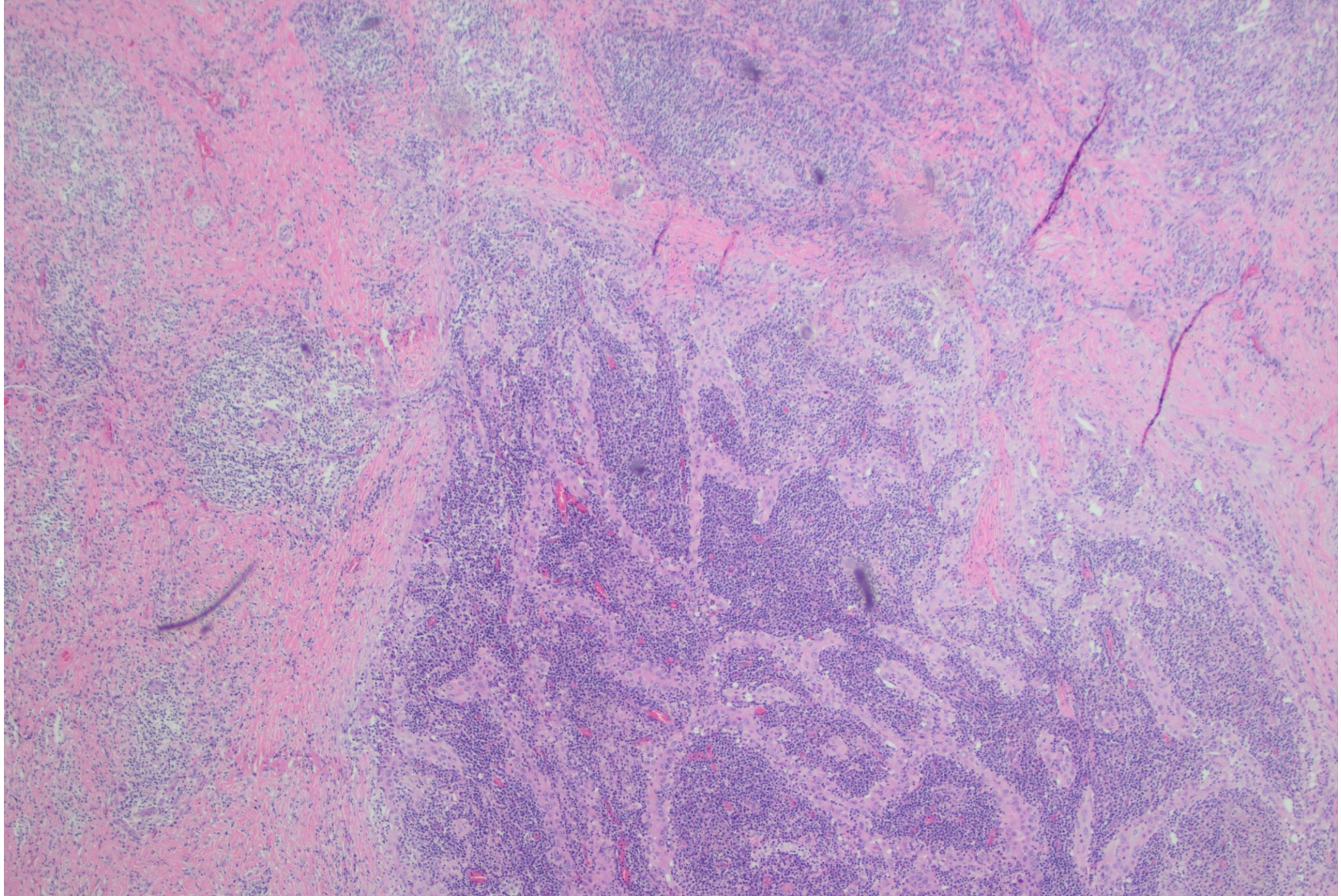

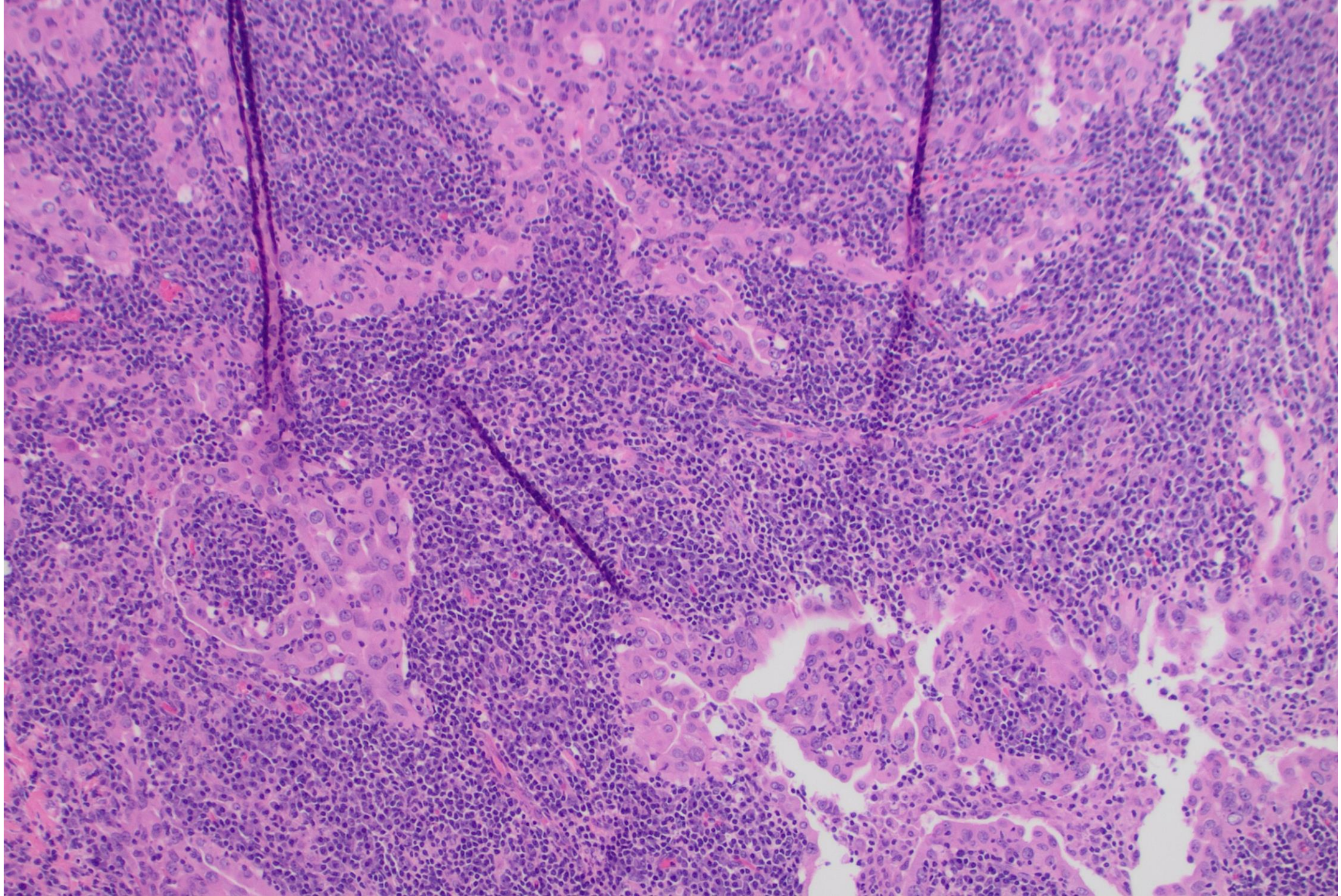

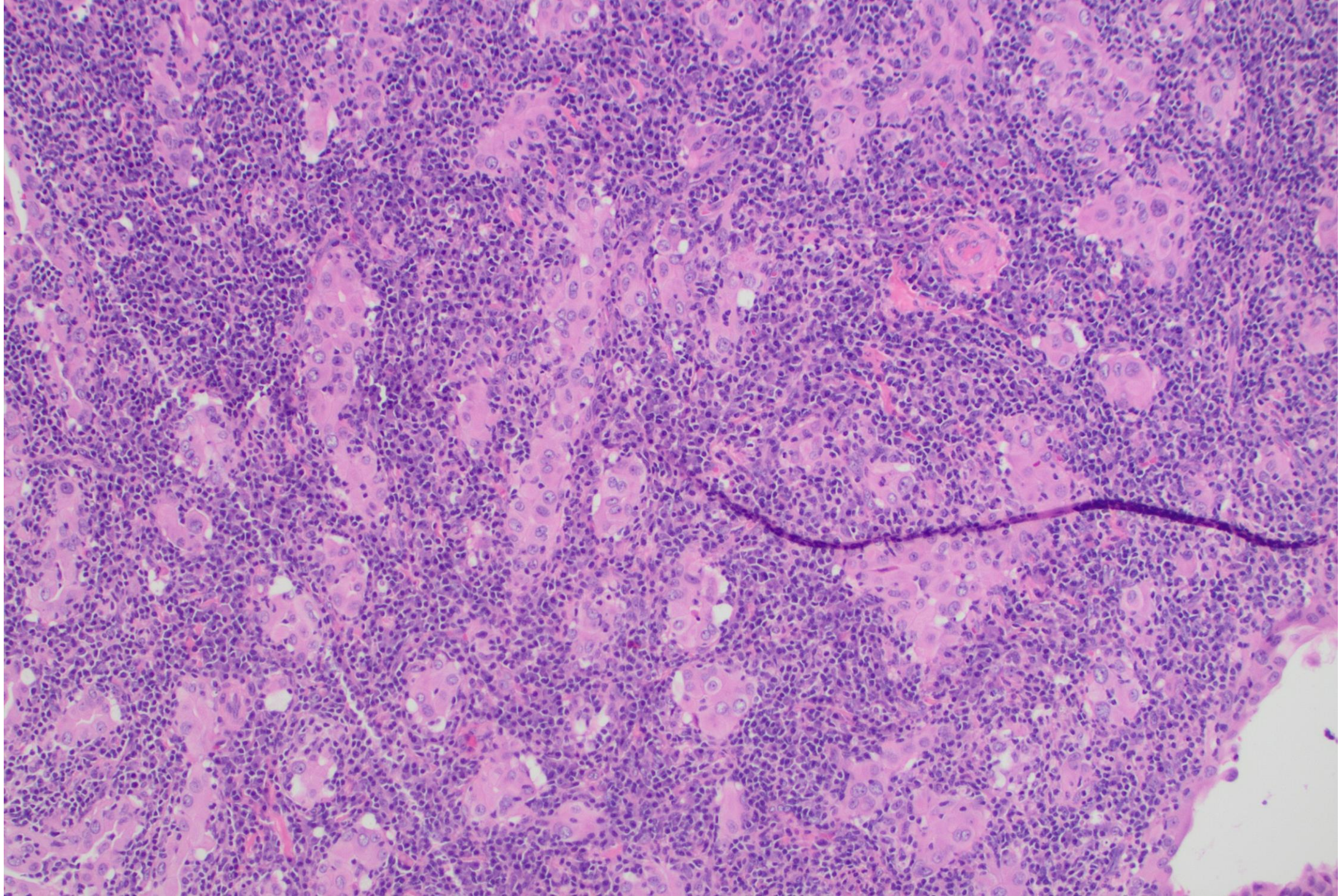

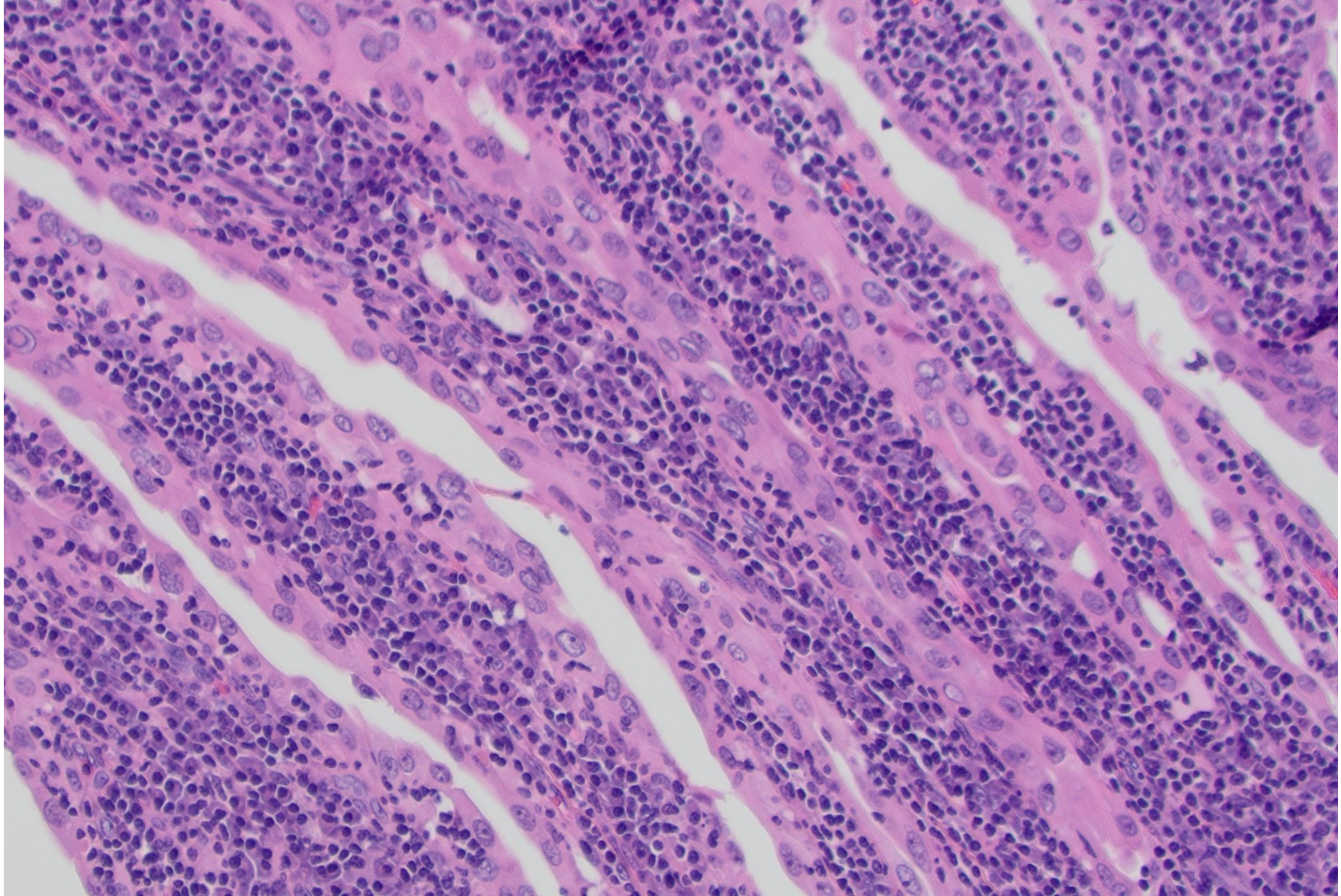

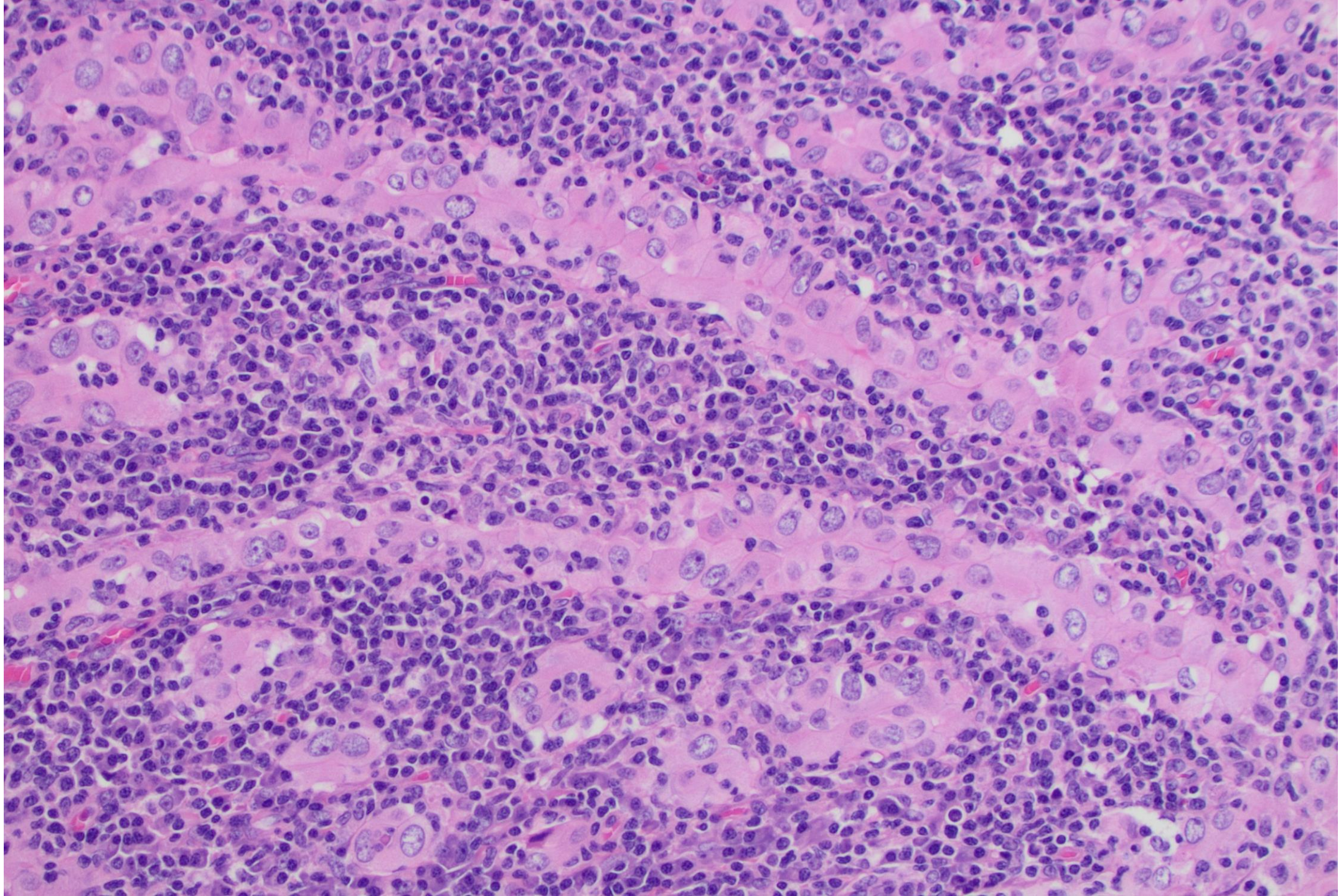

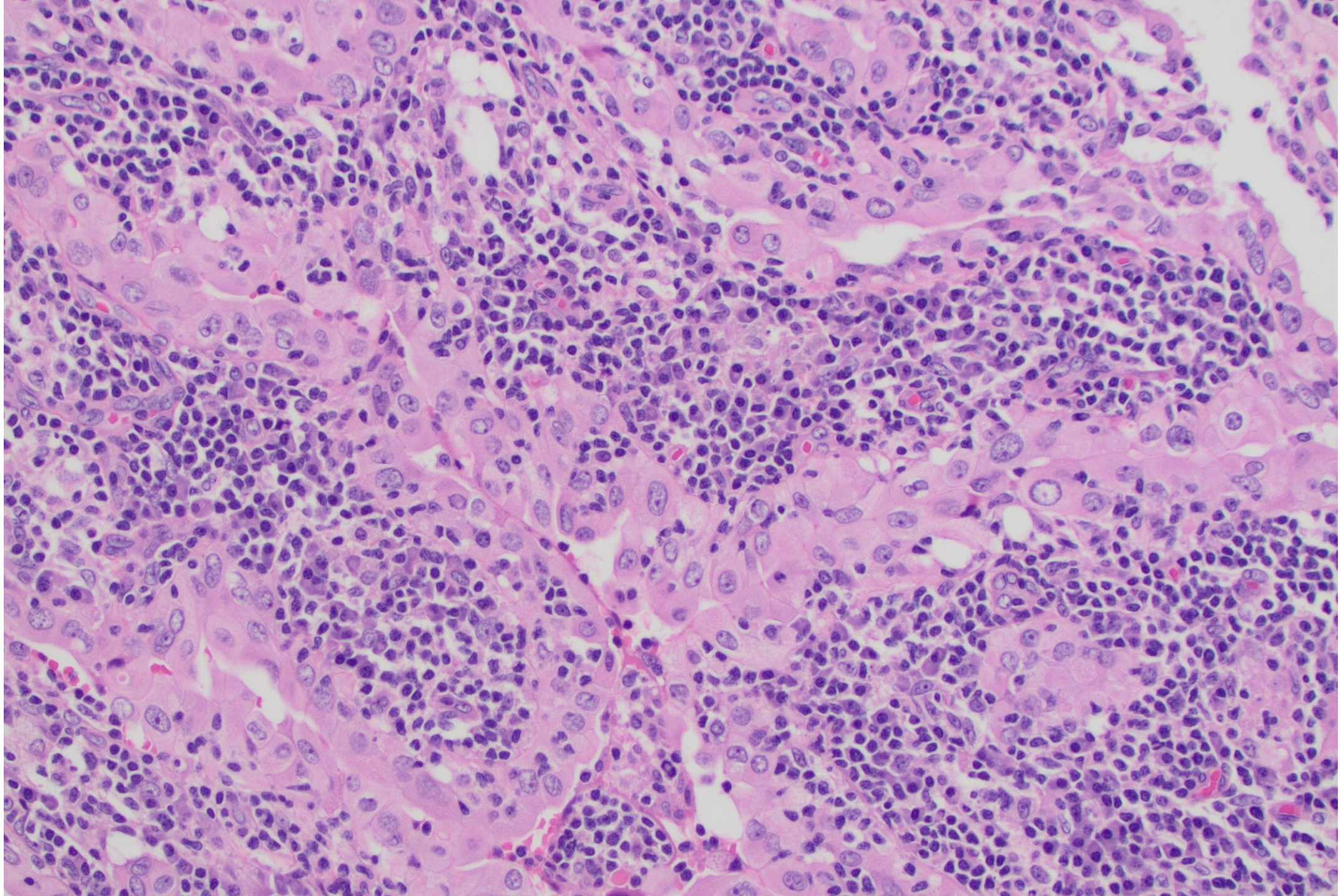

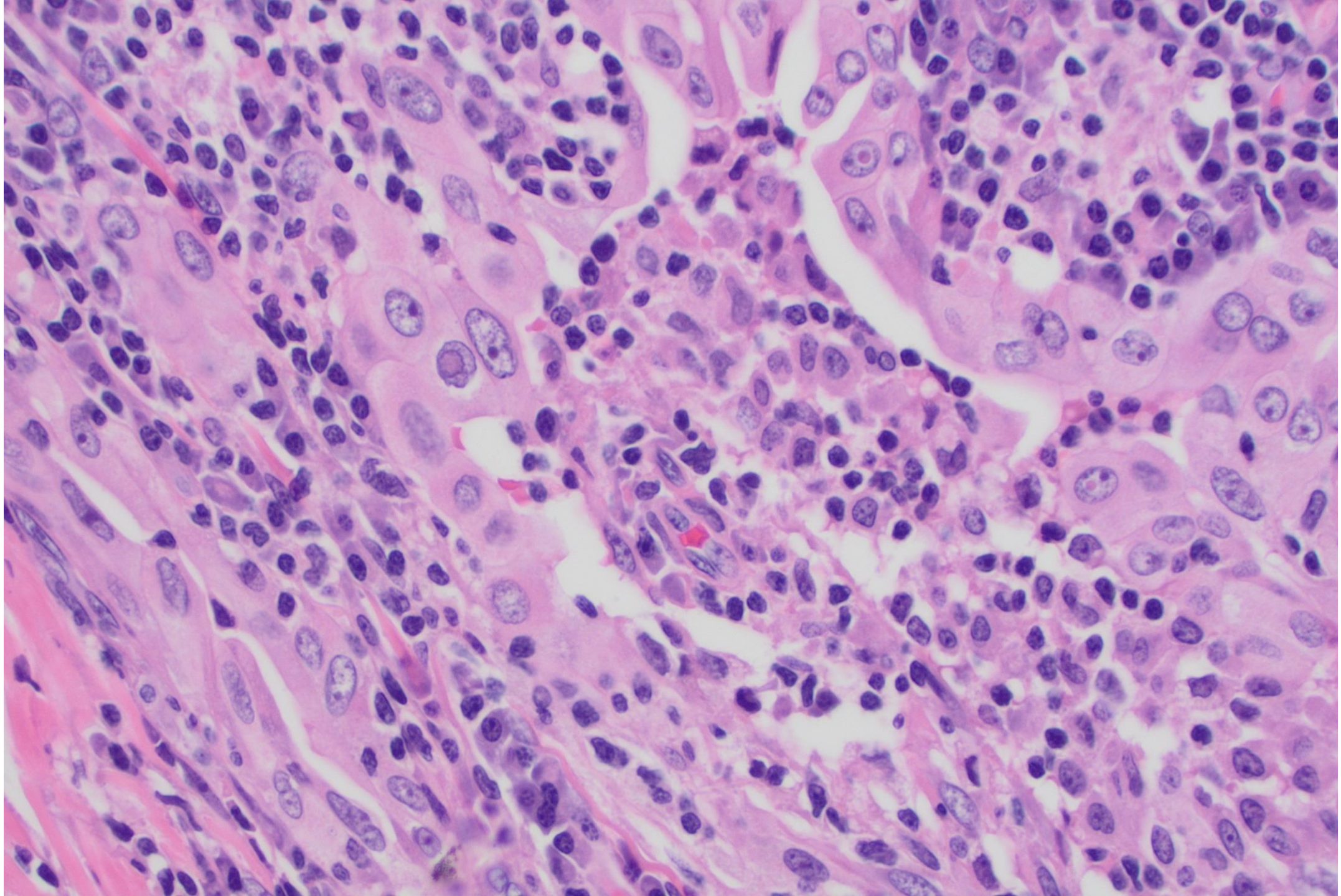

DIAGNOSIS?

Warthin-like variant of Papillary Thyroid CA

- Related to oncocytic variant of PTC
- Nuclear features of PTC
- Granular eosinophilic cytoplasm
- Stroma packed with lymphocytes
- Overall appearance reminiscent of Warthin tumor of salivary gland
- Prognosis good- even better than classic PTC

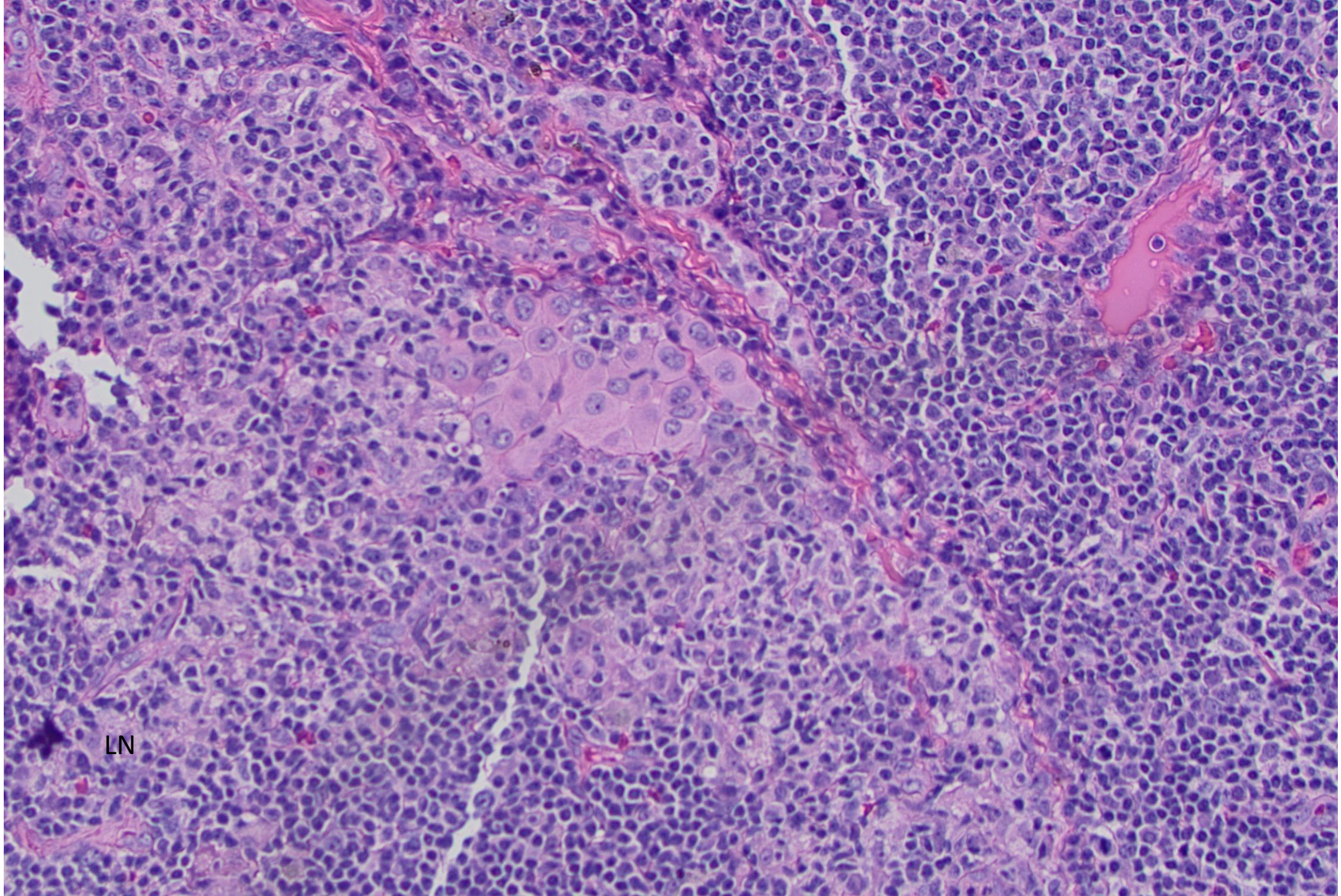
LN

23-1204

Hubert Lau; VA Palo Alto

70-something-year-old man, history of G3 clear cell RCC s/p radical nephrectomy one year prior, rising serum PSA (~100 ng/mL), presenting with progressive fatigue, weight loss, and found to have widely metastatic disease (lymph nodes, bone, lungs, adrenals, mesentery)

Selected PyL scan details:

Multiple scattered foci of uptake in the calvarium for example in the right frontal bone with SUV max 4.9 and right clivus with SUV max 11.8.

Enlarged left level 3 lymph node measuring 3.2 x 2.5 cm without significant PyL uptake.

Large right upper lobe/perihilar mass with low-level heterogeneous uptake measuring approximately 8.8 x 5.9 cm.

Diffuse intense uptake in the right prostate gland as well as focal involvement of the left, with SUV max 25.2.

Innumerable lytic and sclerotic lesions throughout the axial and appendicular skeleton with variable PyL uptake. For example, a T12 vertebral body lytic lesion measuring 2.4 cm without uptake. Intensely PyL uptake in the right T4 lamina associated with a lytic lesion and SUV max 12.2.

Left level 3

lymph node FNA:

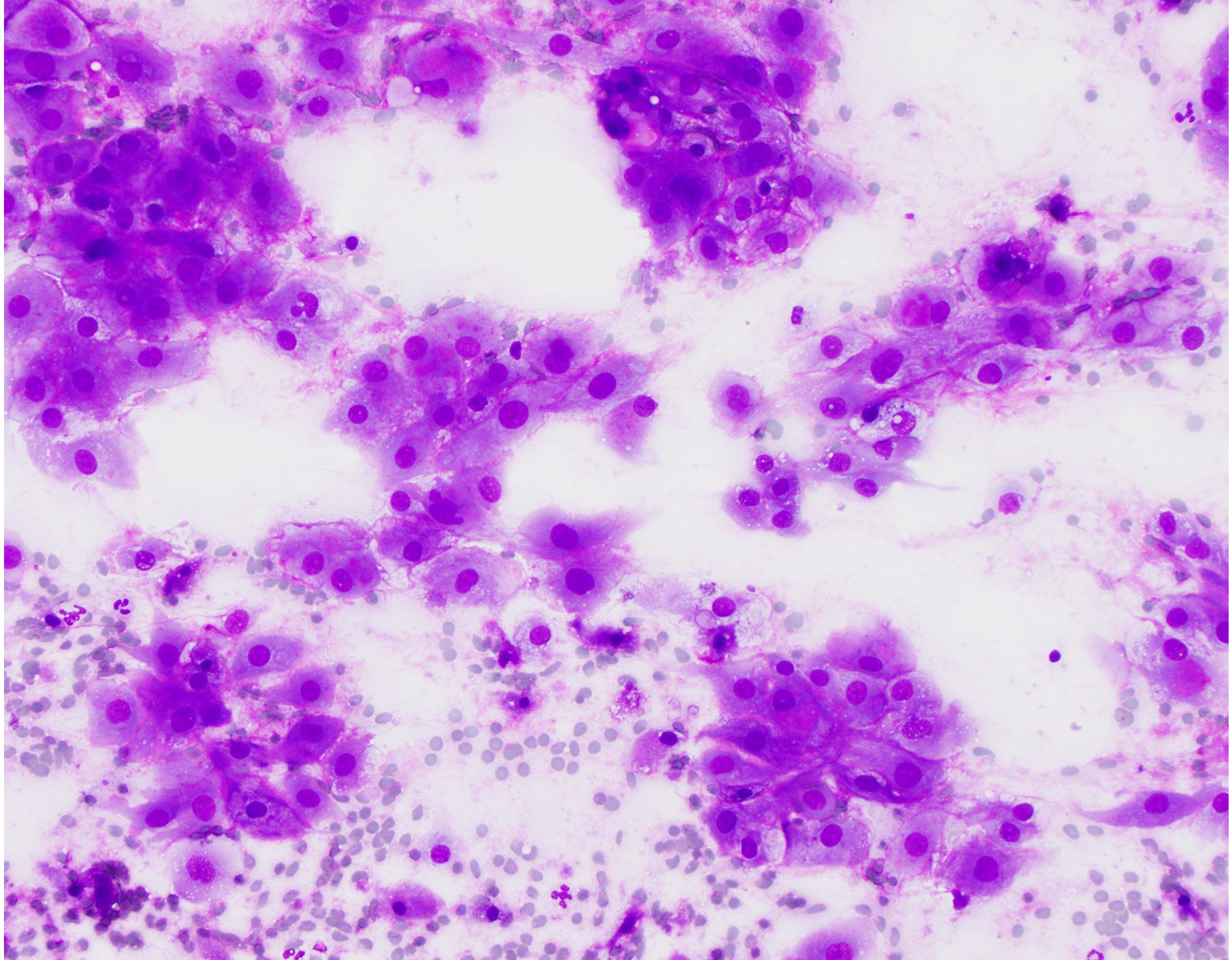

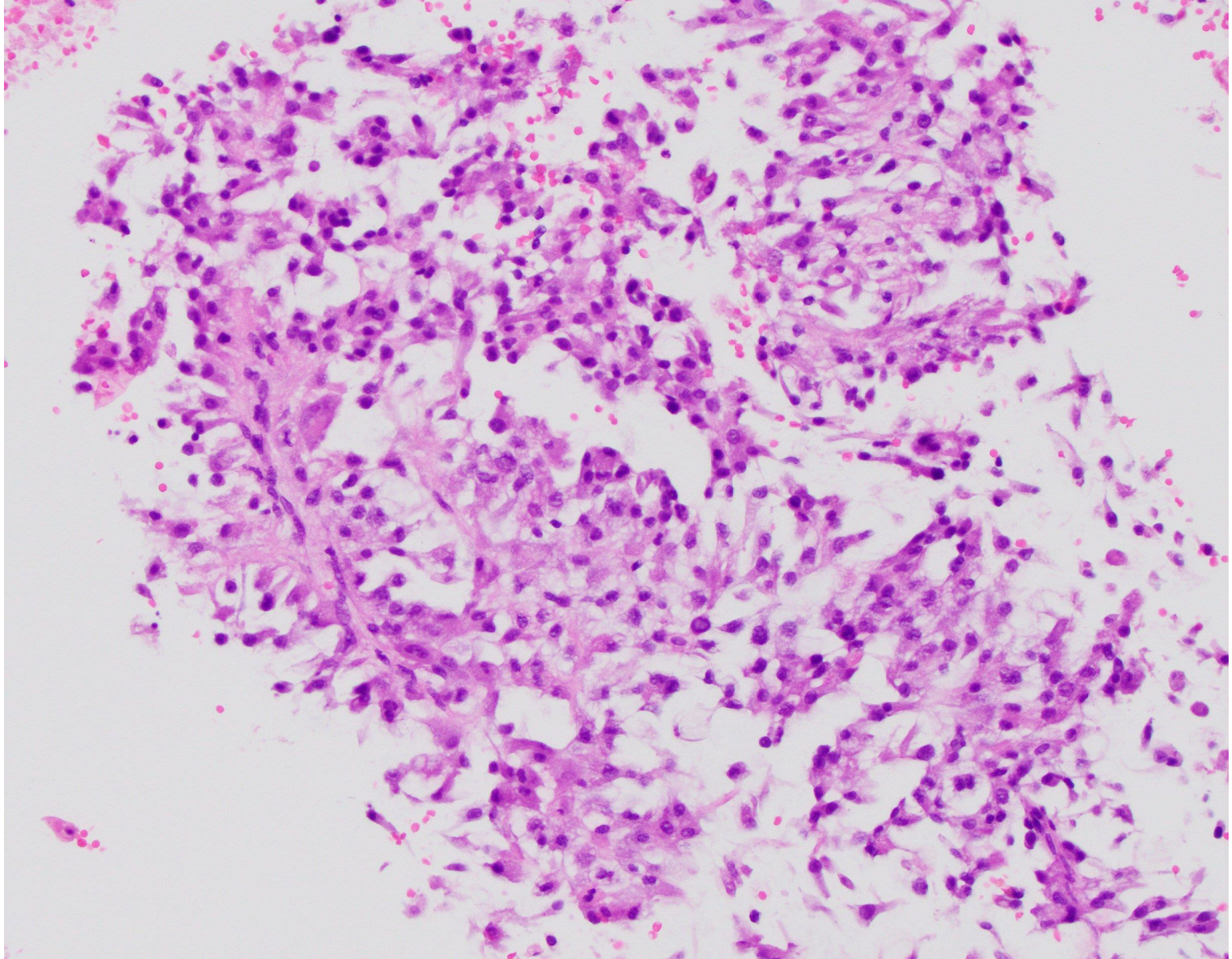

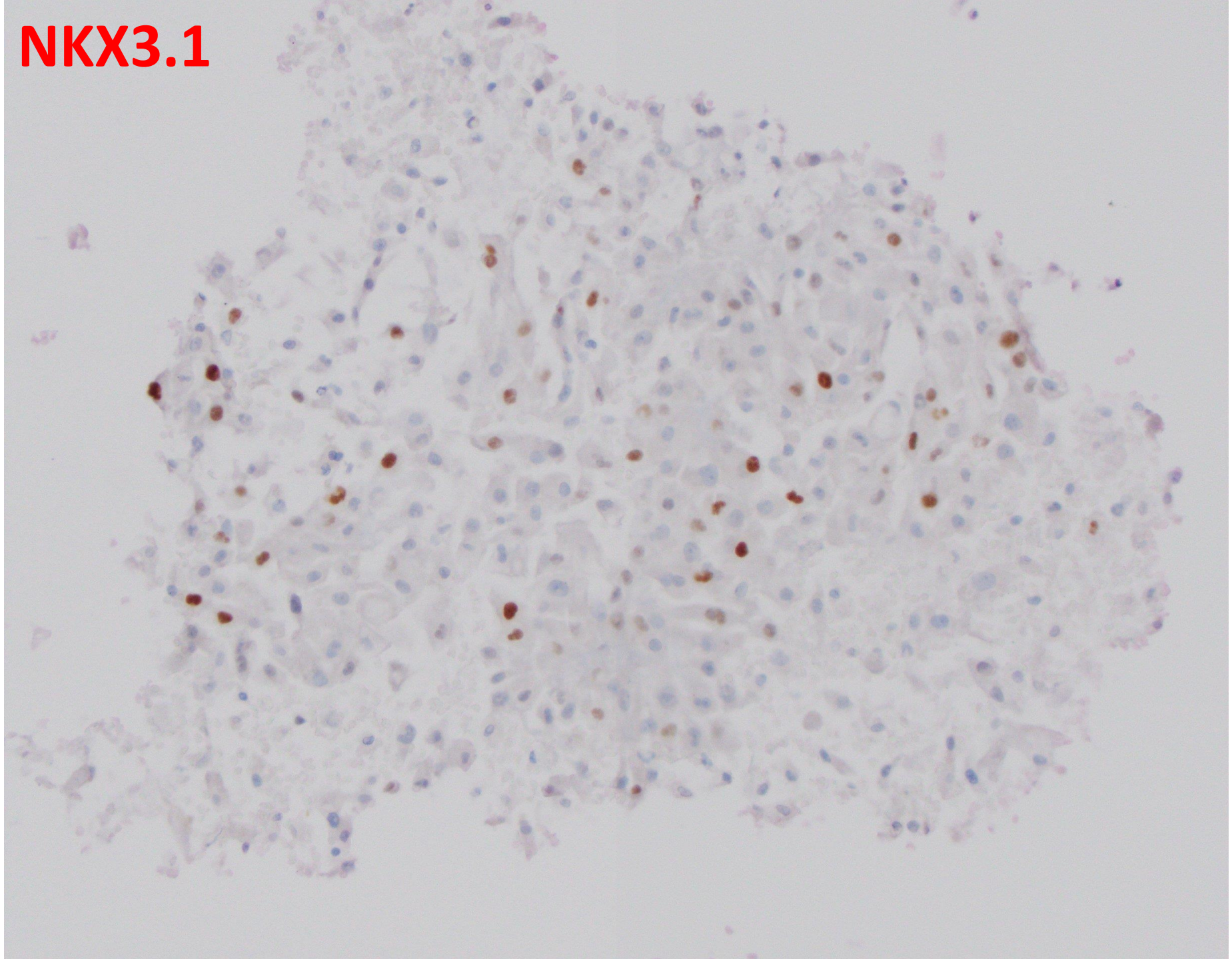
NKX3.1

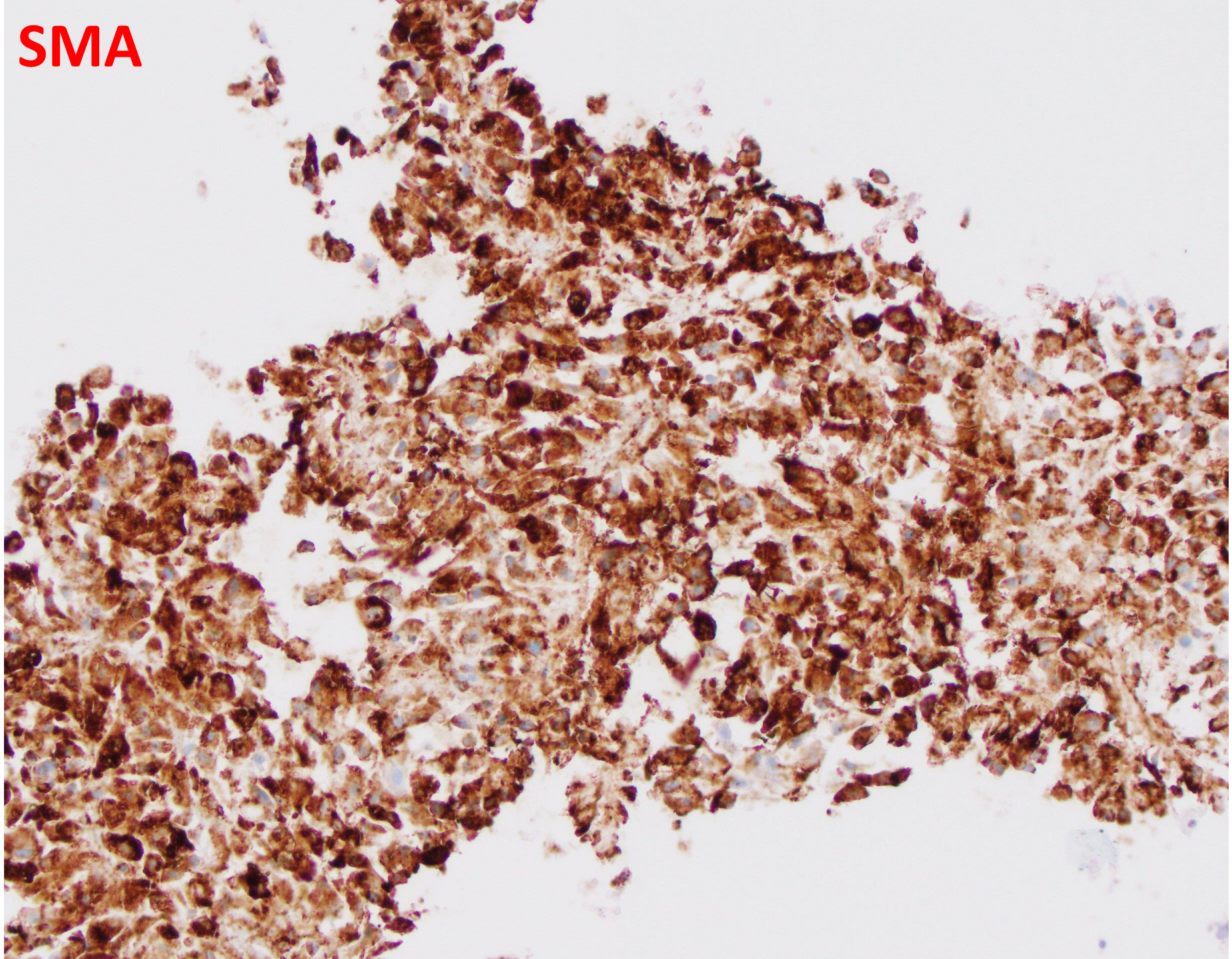
SMA

Completely negative stains:

Pankeratin (AE1/AE3/PCK26)	TTF-1	Melan-A
CK7	p40	HMB-45
CK20	PSA	desmin
PAX8	ERG	ALK
	Sox-10	

DIAGNOSIS?

Metastatic (dedifferentiated) renal cell carcinoma

GENOMIC FINDINGS & BIOMARKERS IDENTIFIED

Results reported in this section are not prescriptive or conclusive for labeled use of any specific therapeutic product. See *professional services* section for additional information.

Microsatellite status MS-Stable §
Tumor Mutational Burden 8 Muts/Mb §

BAP1 V255fs*4
VHL N78_R79del

PATHOLOGIST COMMENTS

This assay is not validated to identify chromosome-level cytogenetic aberrations. However, manual review of the copy-number profile reveals multiple chromosome-level gains and losses, including loss of the short arm of chromosome 3. In conjunction with the VHL and BAP1 alterations identified and the patient's reported history of renal cell carcinoma, these findings raise the possibility of a metastatic renal cell carcinoma. Clinicopathologic and genomic correlation is advised.

Unexpected IHC results in dedifferentiated/undifferentiated RCC

- Poorly differentiated or undifferentiated component frequently shows progressive loss of RCC markers, including cytokeratins, EMA, and PAX8 (~40%)
- Some markers, such as P504S/AMACR and CD10 can be aberrantly expressed
- Genetically-defined RCCs retain their defining genetic features that are detectable using surrogate IHC markers

Agaimy A, Cheng L, Egevad L, et al. *American Journal of Surgical Pathology*. 2017;41(2):253-262.
Agaimy A, Hartmann A, Trpkov K, Hes O. *Seminars in Diagnostic Pathology*. 2021;38(6);152-162.

Strong, diffuse carbonic anhydrase 9 expression tends to be retained in sarcomatoid/dediff ccRCC

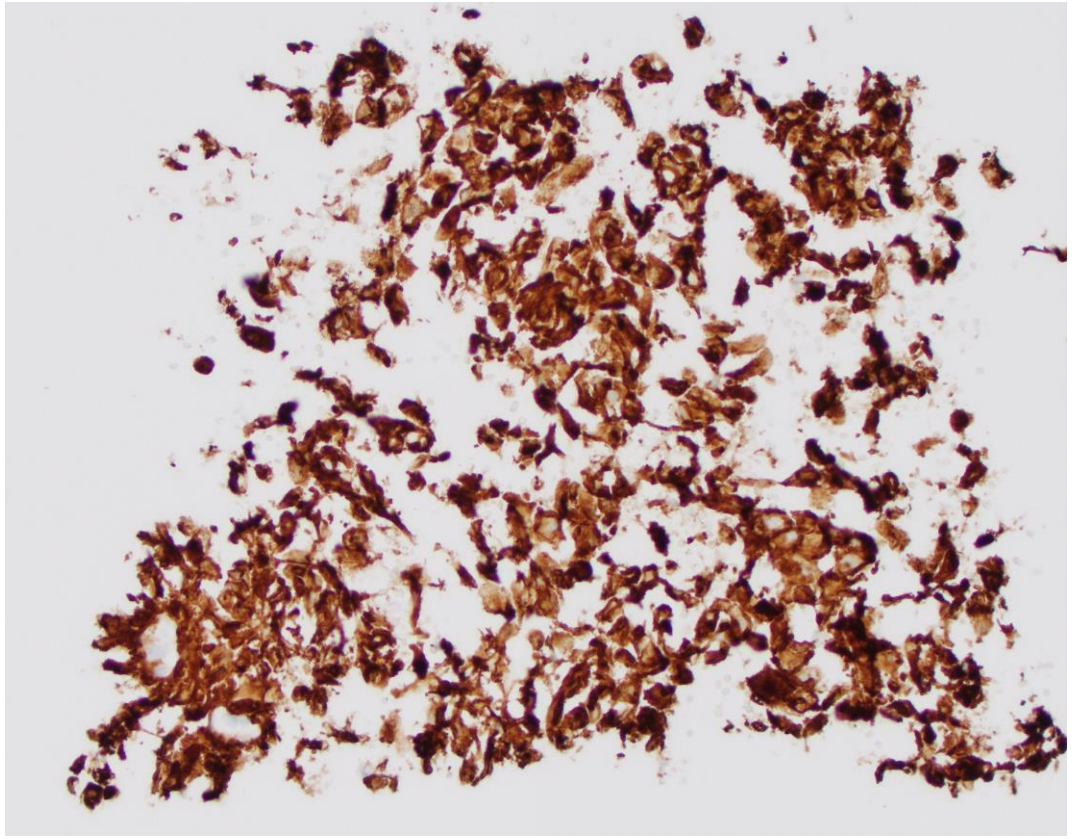

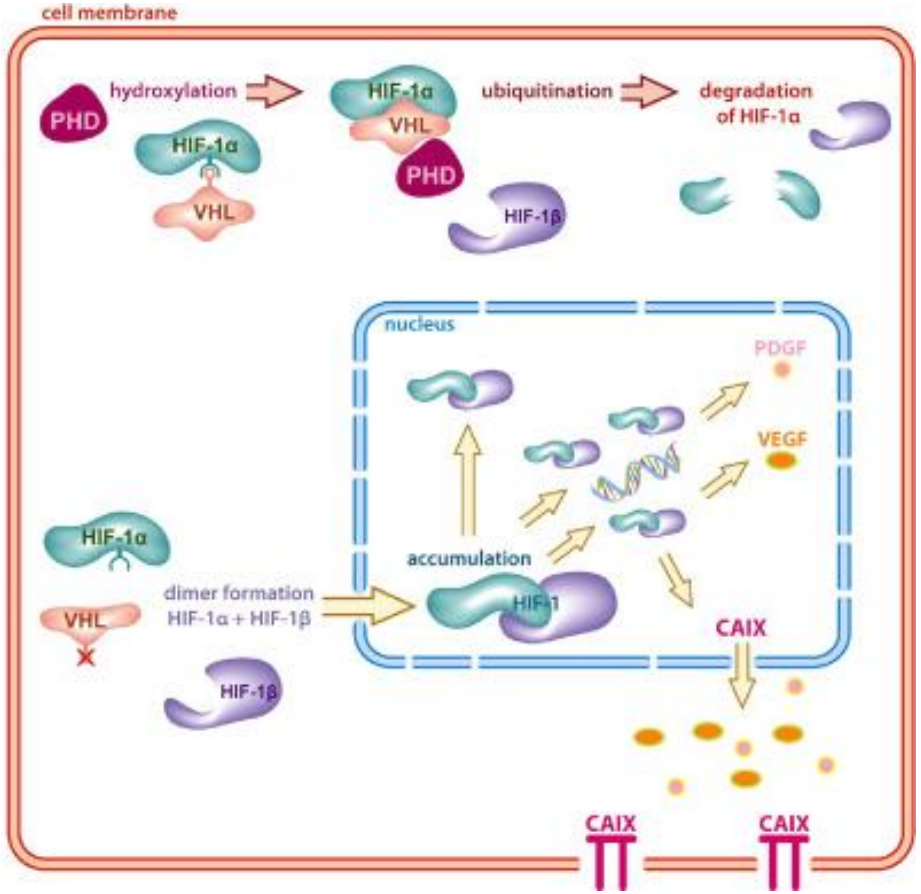

Stillebroer AB, Mulders PFA, Boerman OC, Oyen WJG, Oosterwijk E. *European Urology*. 2010;58(1):75-83.

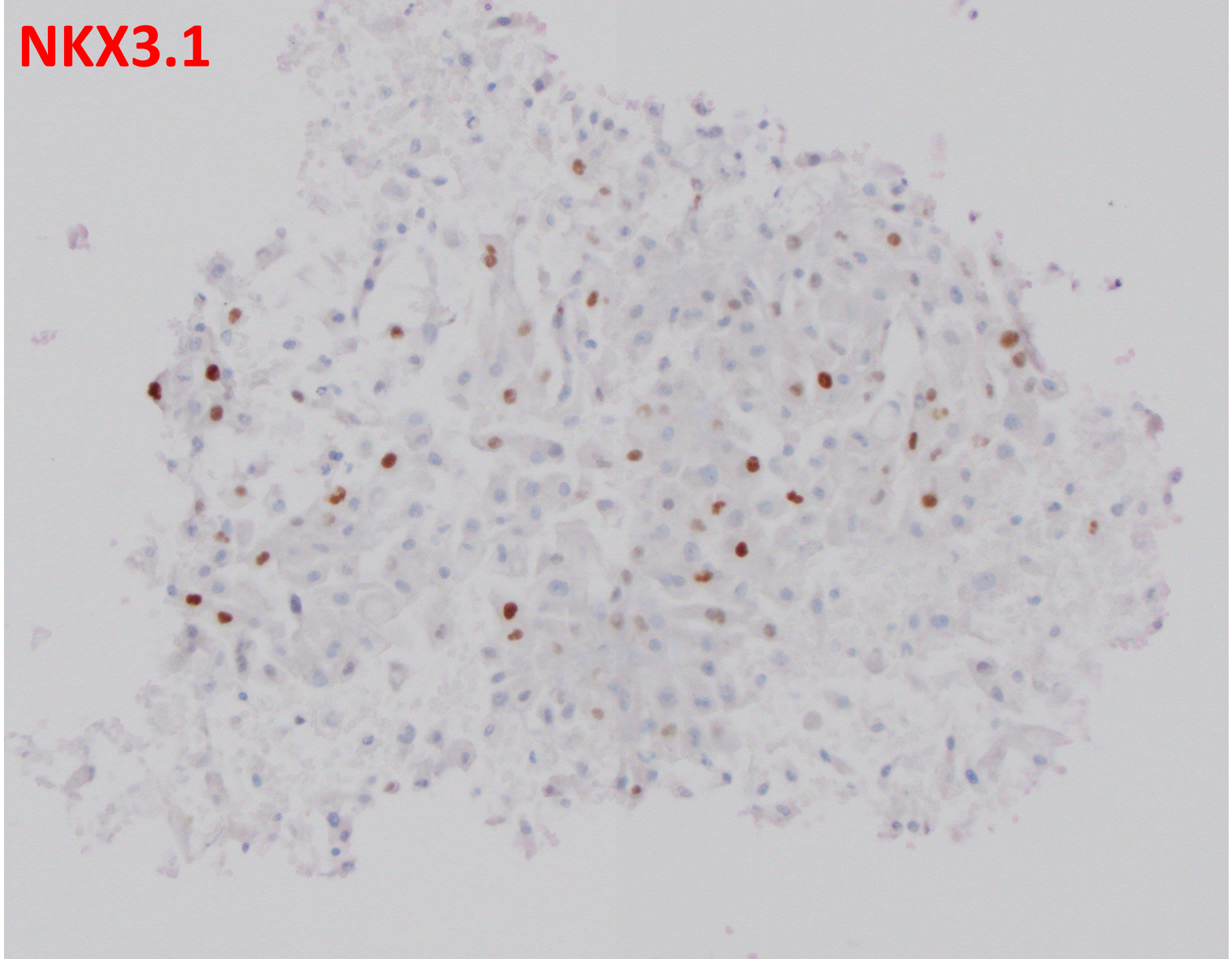
NKX3.1

BAP1-mutated clear cell renal cell carcinoma

- *BAP1* is mutated in ~10% of ccRCC and at much lower frequencies in other RCCs
- Associated with high nuclear grade, tumor necrosis, sarcomatoid differentiation, and advanced stage, including metastasis at presentation

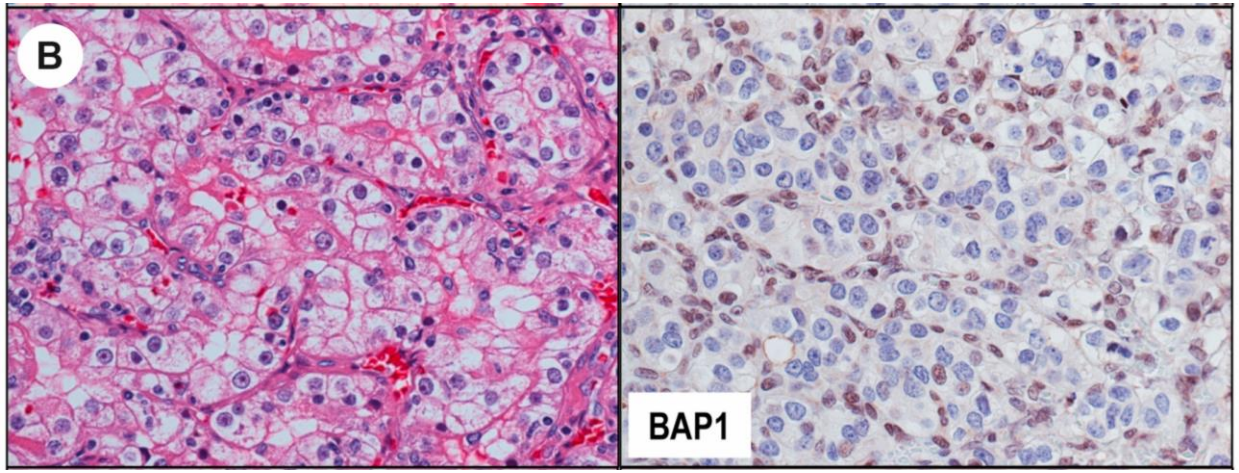

Kapur P, Rajaram S, Brugarolas J. *Human Pathology*. 2023;133:22-31.

BAP1-mutated clear cell renal cell carcinoma

- Frequent biphasic morphology with a component demonstrating papillary/tubulopapillary or expanded nested architecture
- Granular eosinophilic cytoplasm with prominent cytoplasmic globules
- Frequent prominent intratumoral lymphocytic infiltrate
- Strong P504S/AMACR staining in BAP1-deficient areas

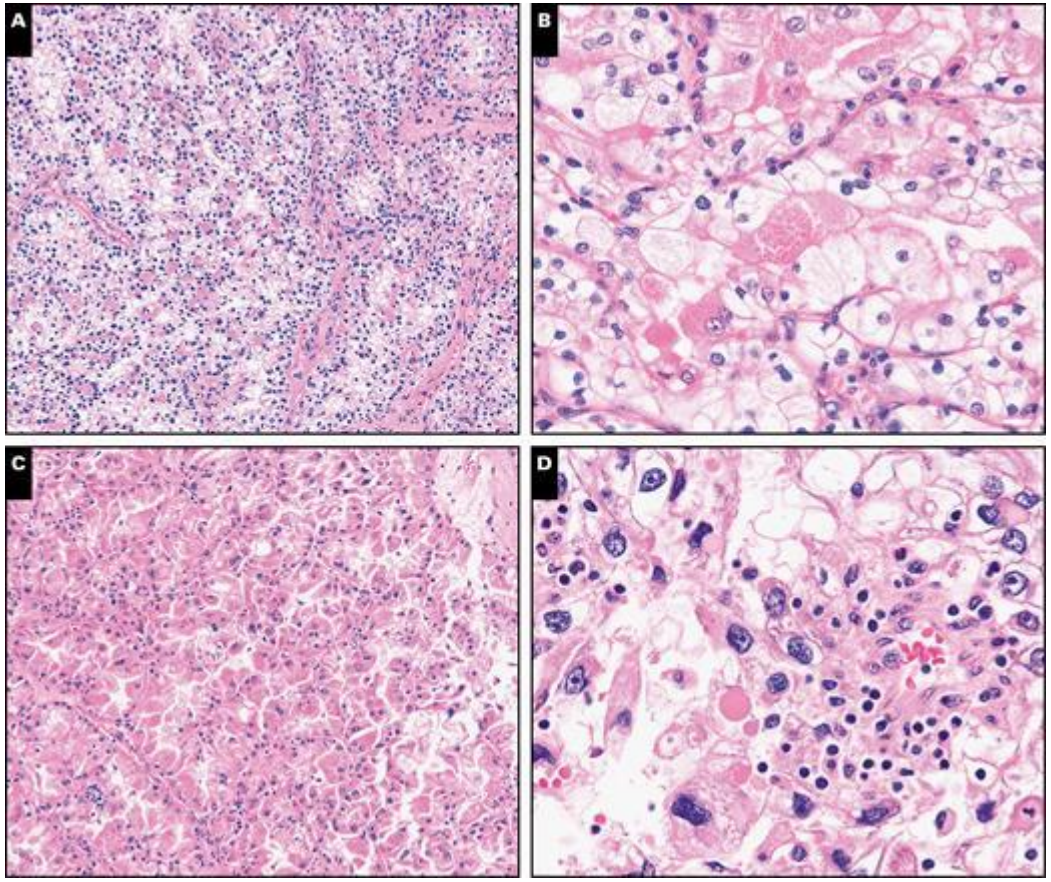

Gallan AJ, Parilla M, Segal J, Ritterhouse L, Antic T. *American Journal of Clinical Pathology*. 2021;155(5):718-728.

23-1205

Margarita Muñoz de Toro/David Bingham; Stanford

56 Y female with history of left LE pyoderma gangrenosum (on prednisone), DM and history of chronic pancreatitis presented with R abdominal pain, nausea, and vomiting

CT showed an infiltrative, heterogeneous and ill-defined mass projecting from the region of the pancreatic uncinate process extending along the right mesenteric root measuring approximately 6 cm with main duct dilatation and suspected nodal and peritoneal metastases, also with a 4.5 cm hypodense L kidney mass and geographic hypoattenuation of the spleen

Clinically thought to have pancreatic mass compressing bowel vasculature, resulting in ischemic bowel, now s/p ex lap, small bowel resection, partial colectomy, and mesenteric tissue biopsy

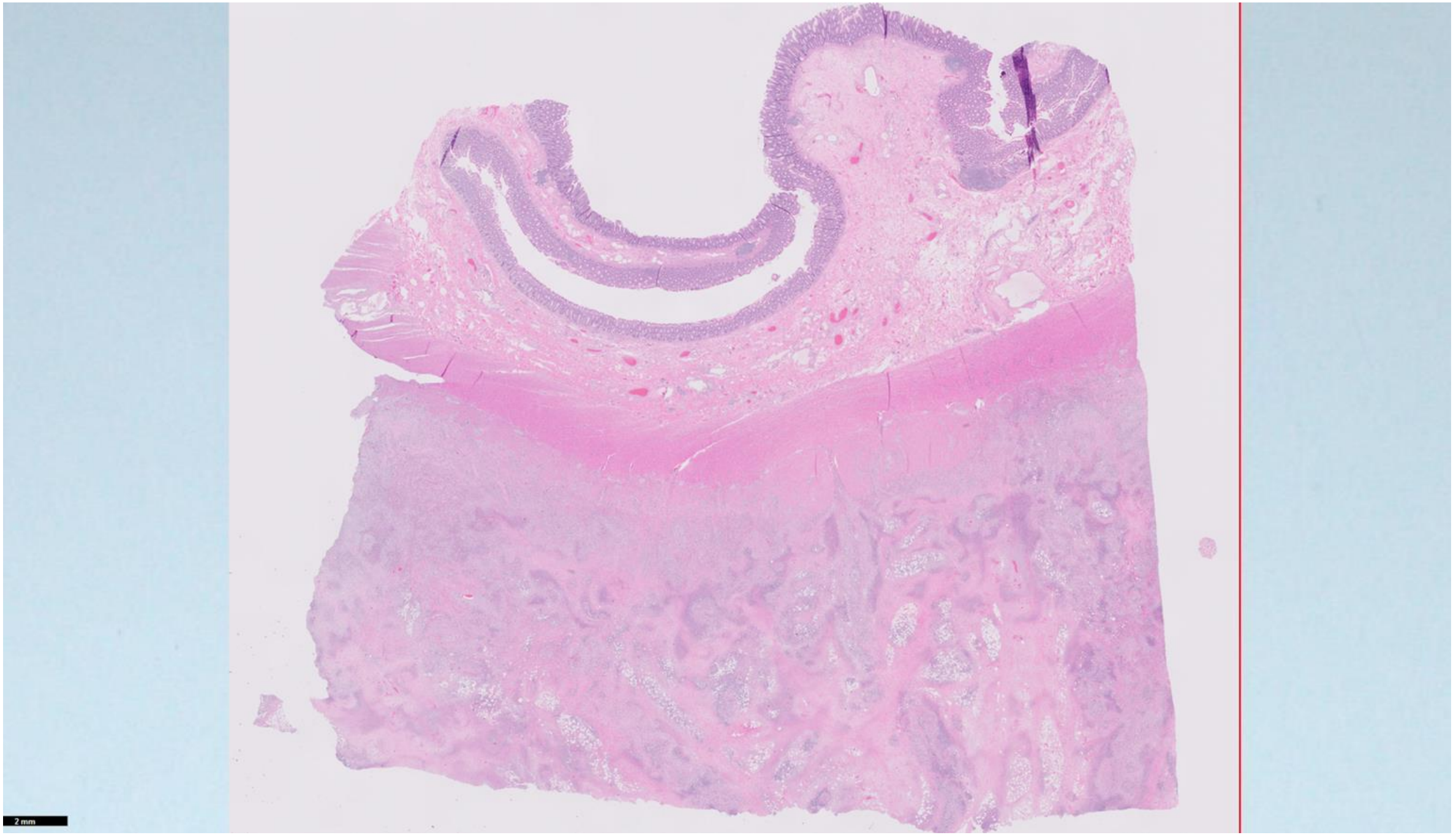
2 mm

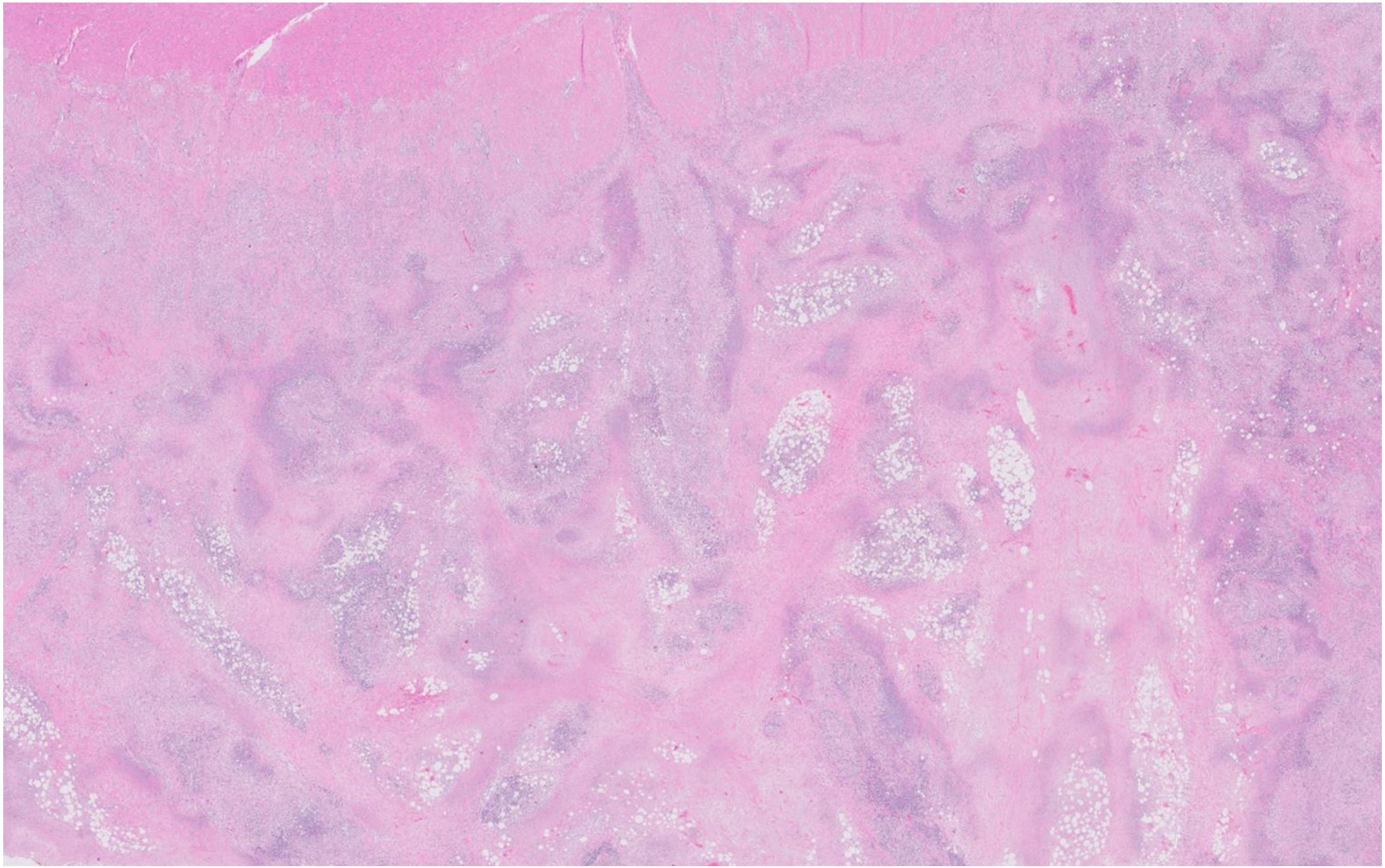

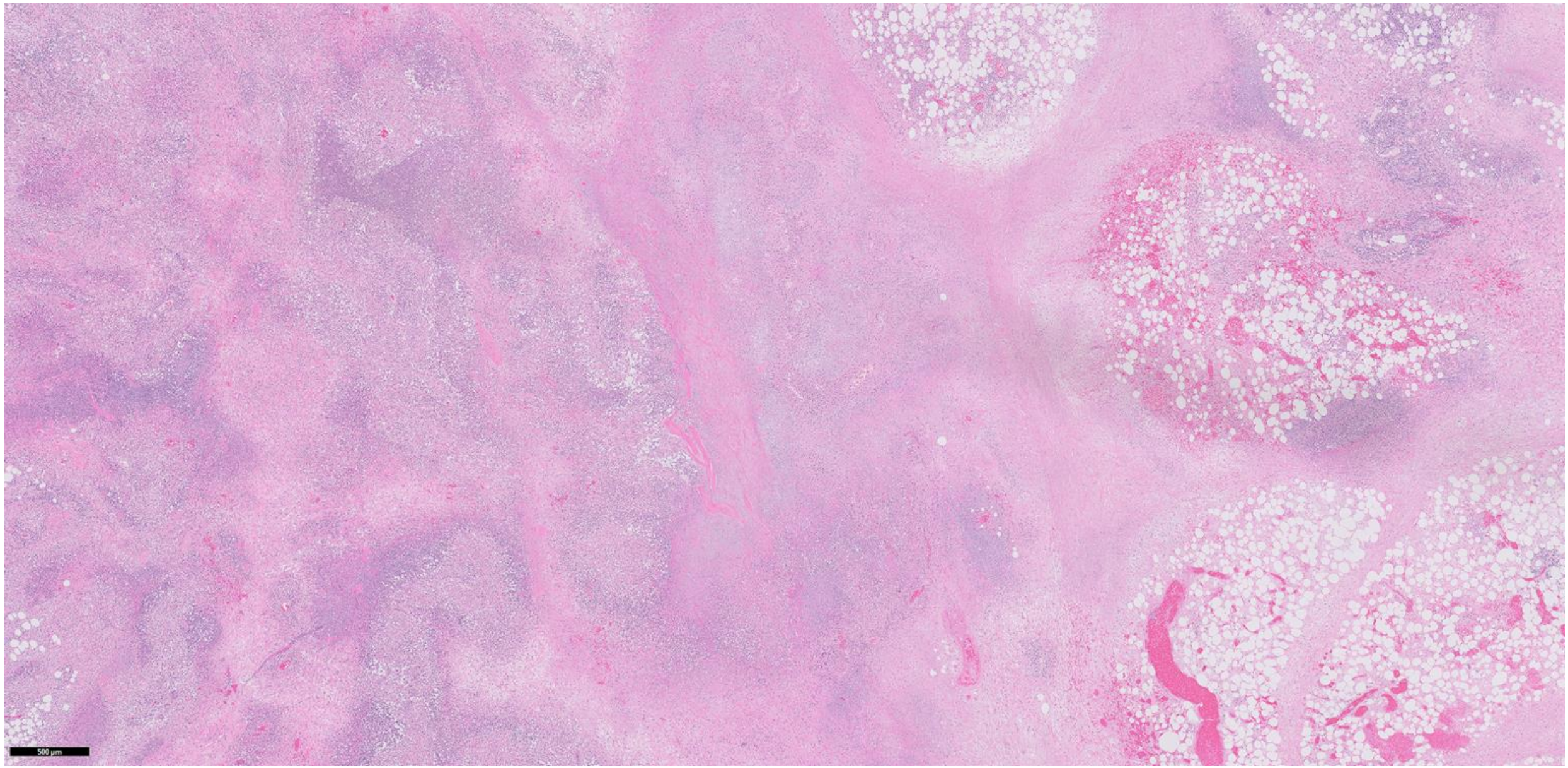
500 µm

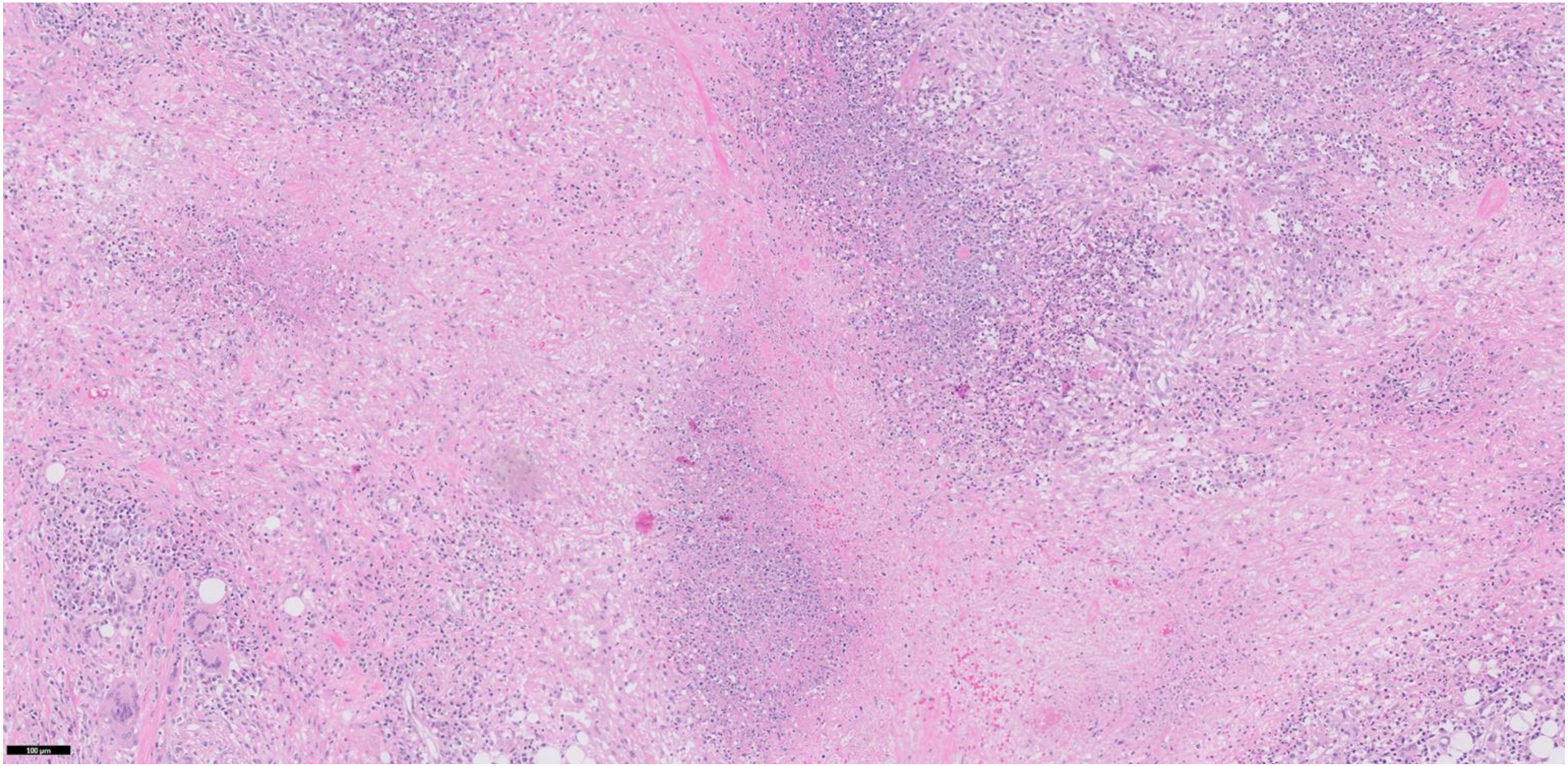
100 µm

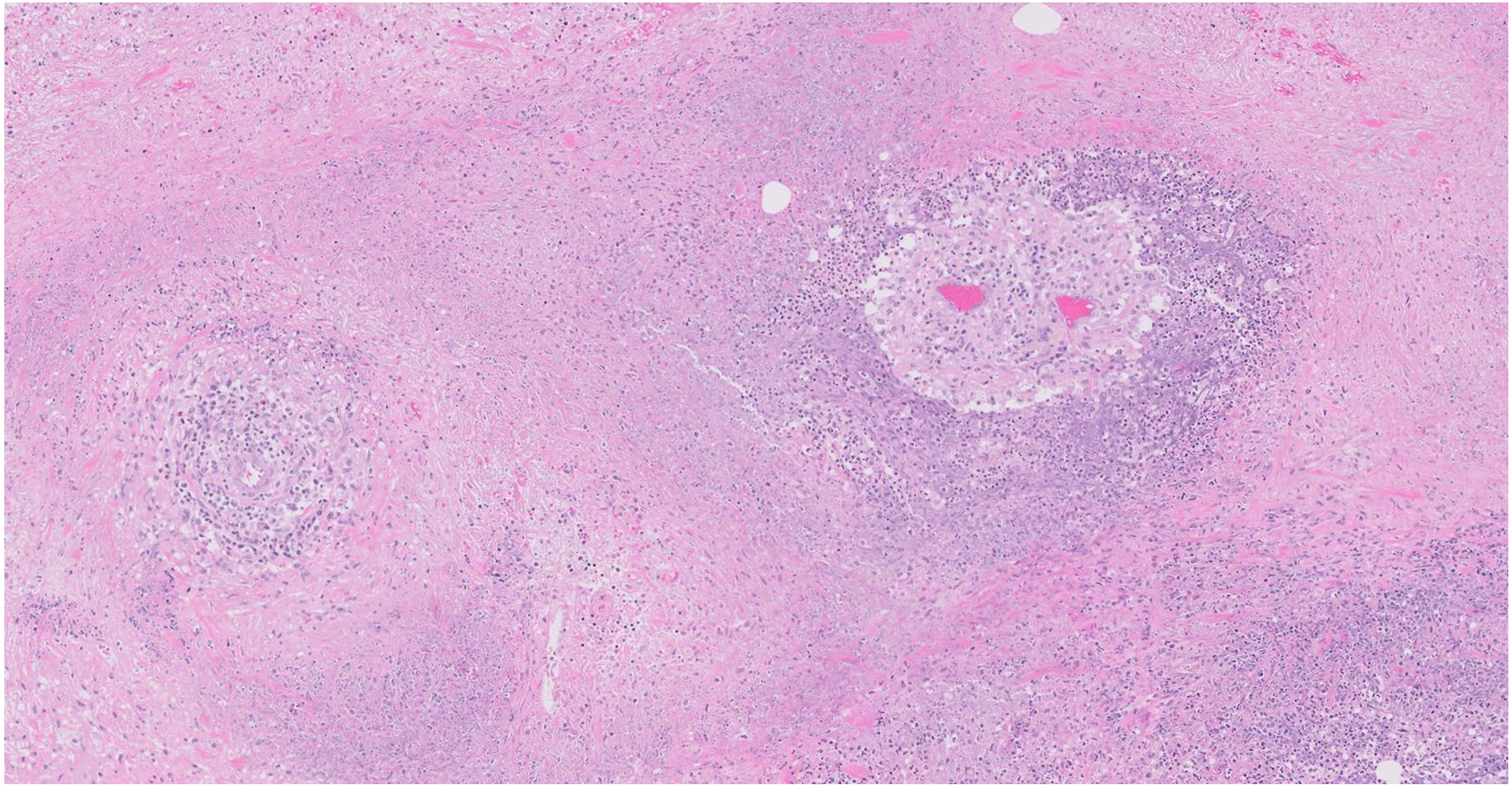

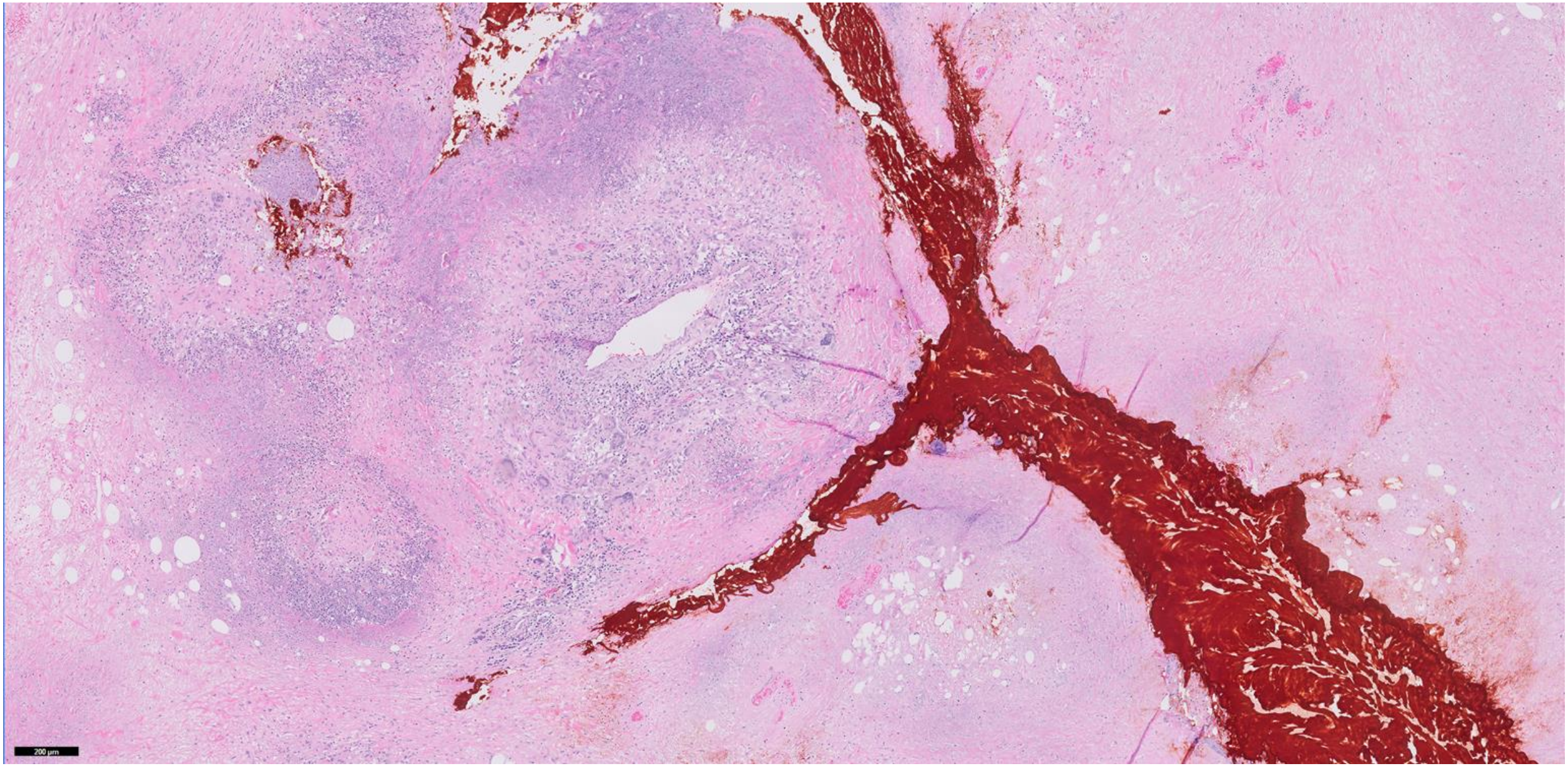
200 µm

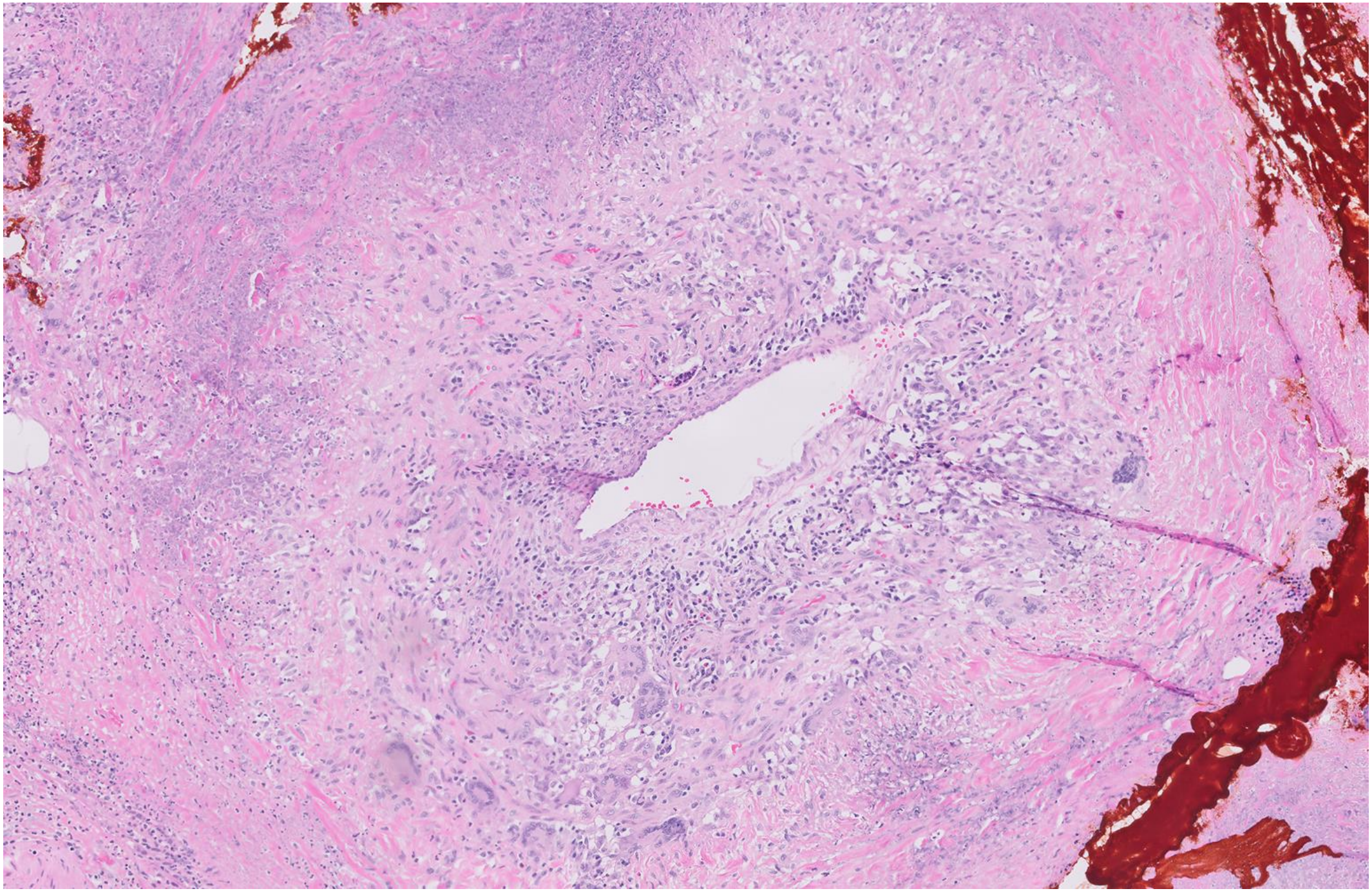

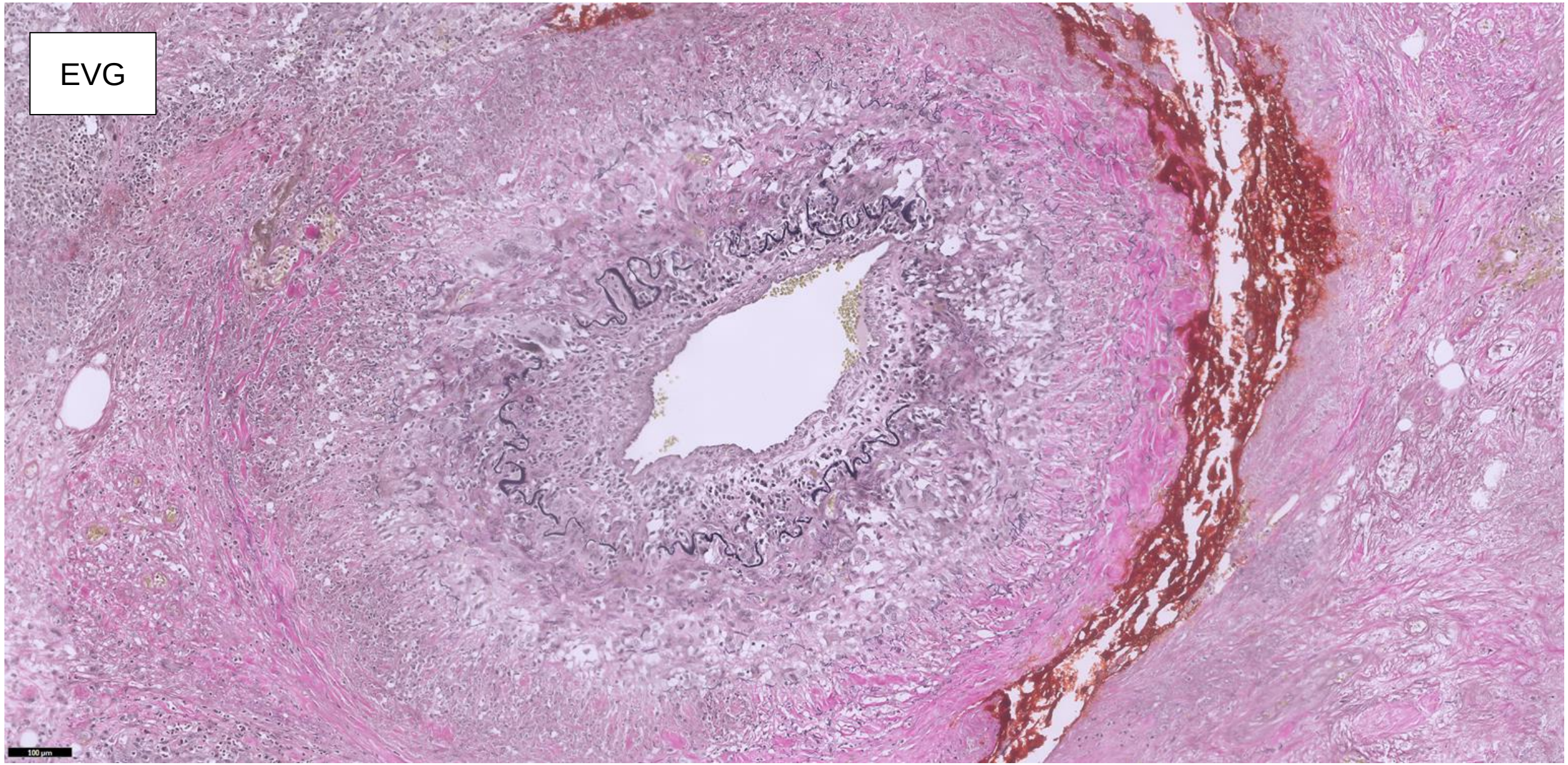
EVG
100 µm

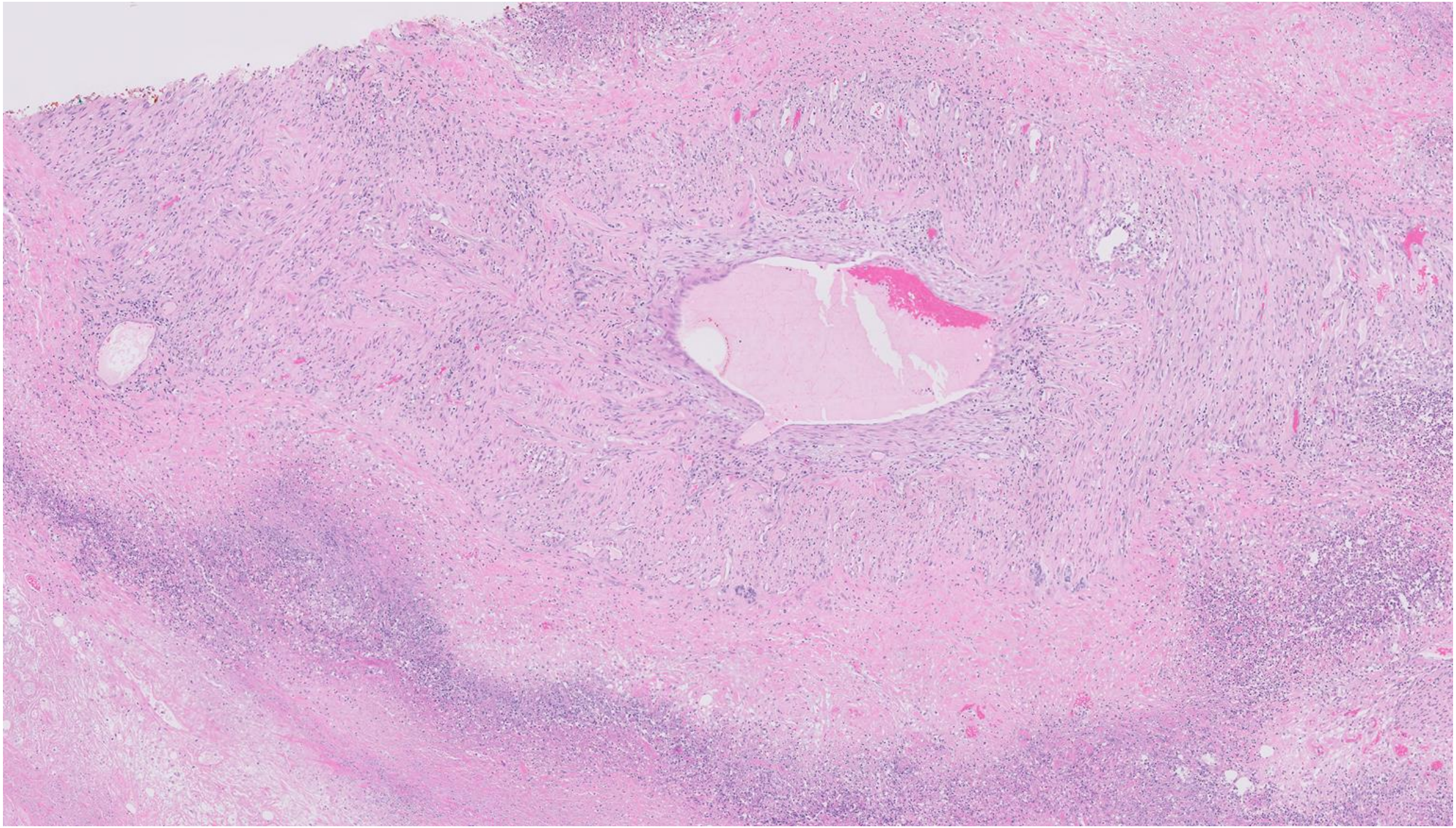

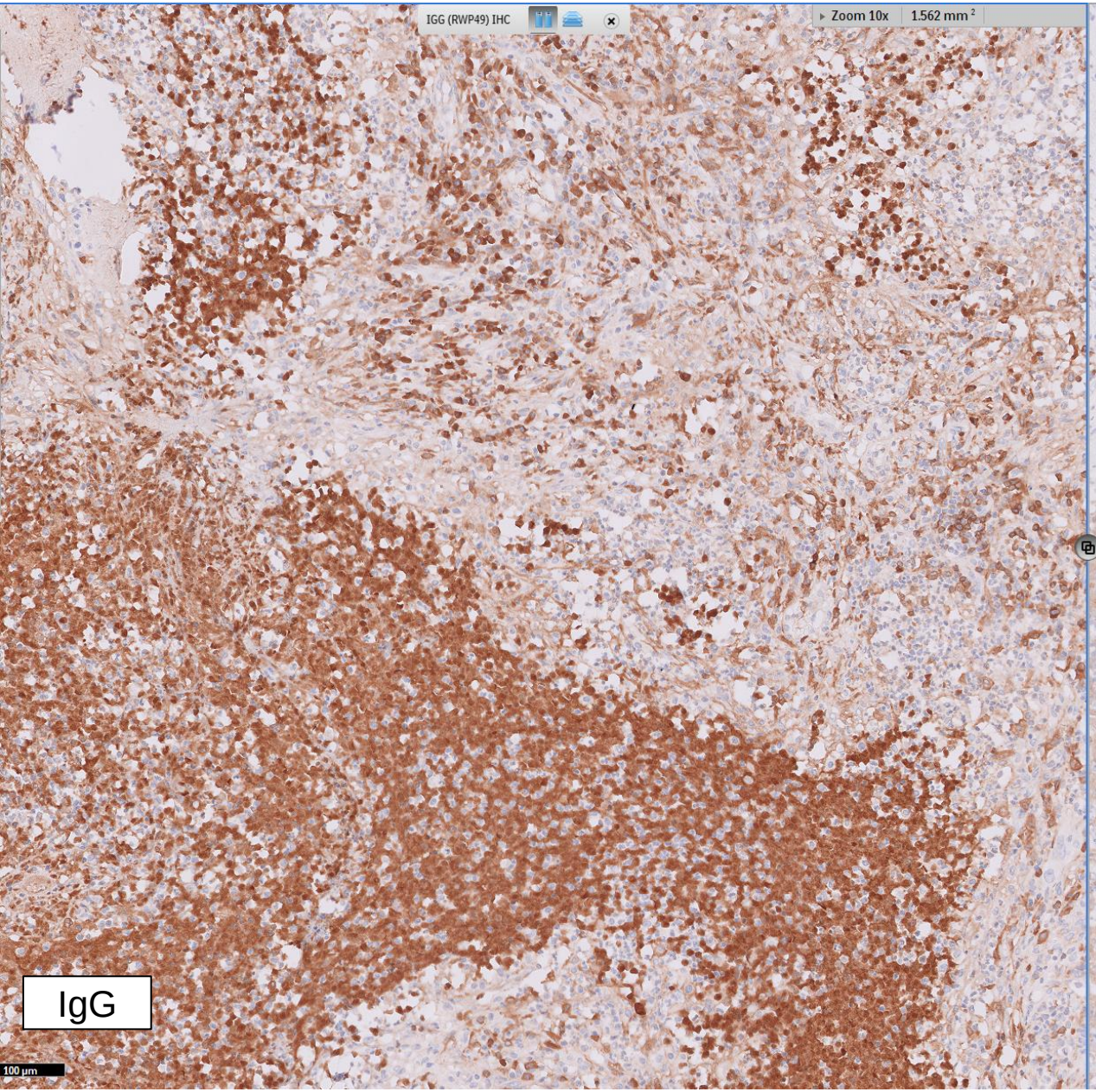
IGG (RWP49) IHC
Zoom 10x
1.562 mm²
IgG
100 µm

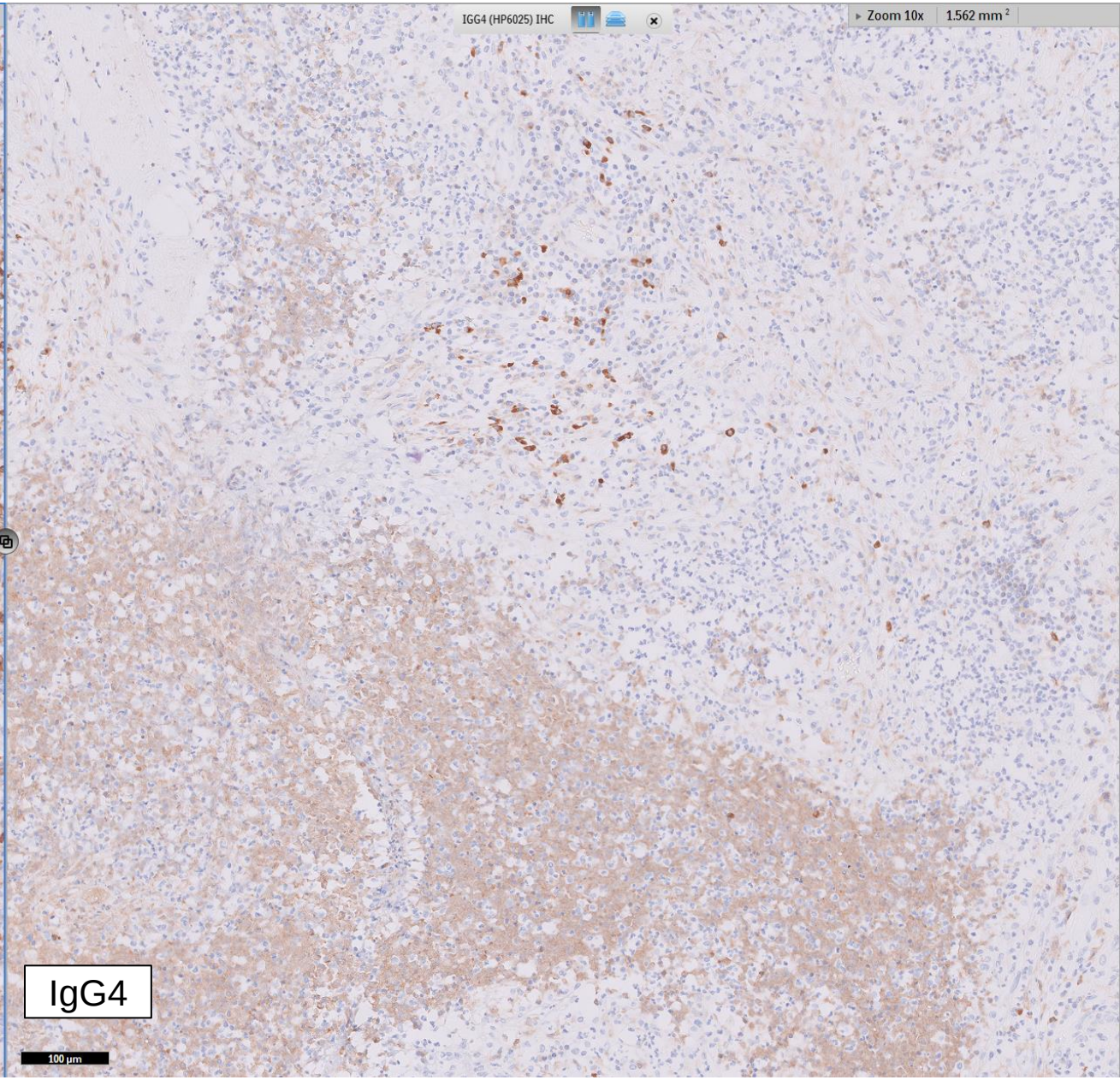
IGG4 (HP6025) IHC
Zoom 10x
1.562 mm²
IgG4
100 µm

DIAGNOSIS?

Diagnosis: Granulomatosis with polyangiitis (GPA)

(formerly called Wegener's granulomatosis)

cANCA (+)

Anti-PR3 Ab (+)

Consistent with GPA

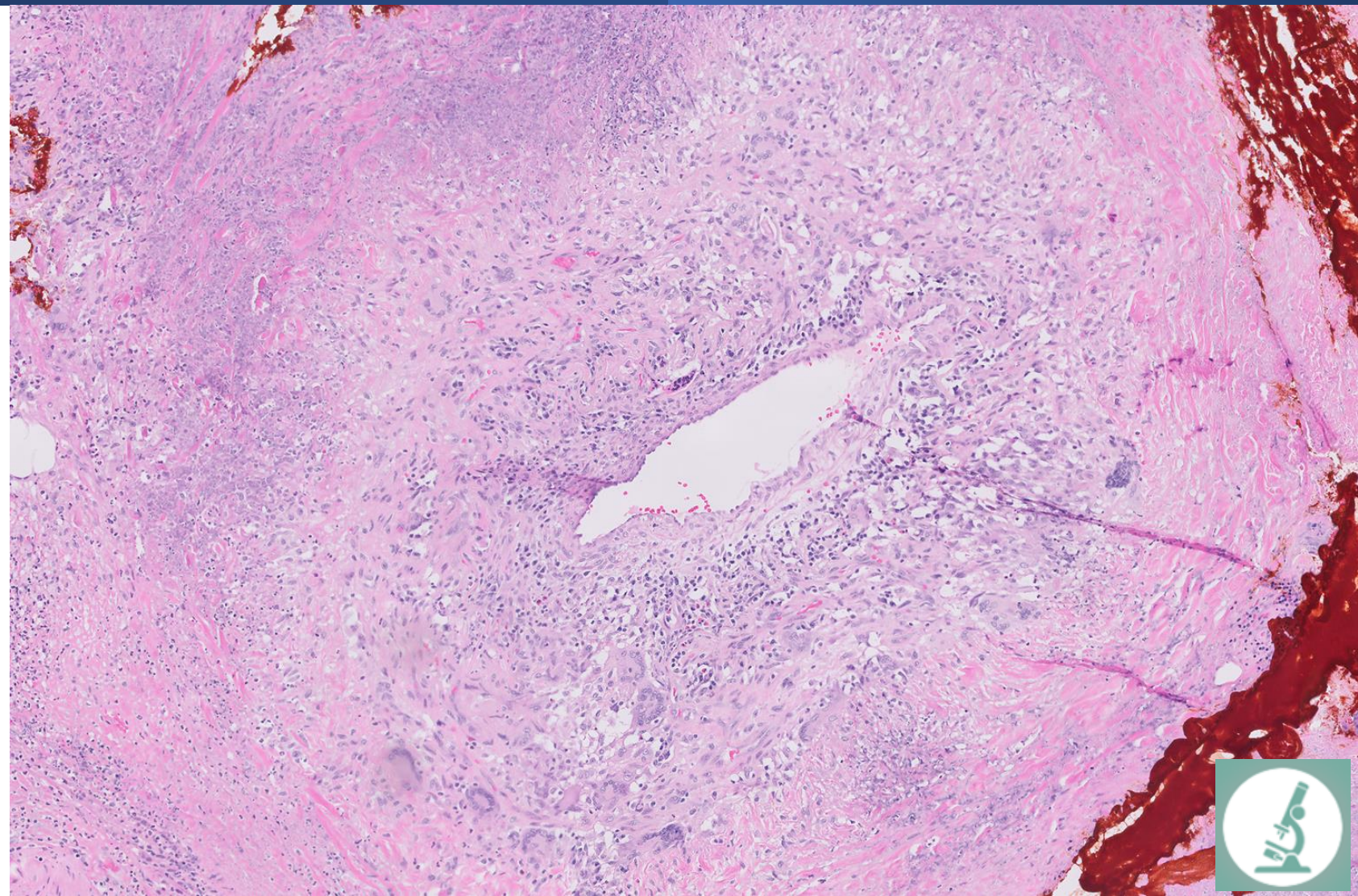

Granulomatosis with polyangiitis (GPA)

- Anti-neutrophil cytoplasmic antibodies (ANCA) associated vasculitis
- Necrotizing vasculitis
- Small-sized or medium-sized vessels
- Incidence: 8–10 cases per million
- 50 - 60 years - wide distribution
- Between 8-15% cases occur in younger people (< 19 y/o)
- No sex predilection

Granulomatosis with polyangiitis (GPA)

- Systemic manifestations:
  - Upper and lower respiratory tract involvement (90%)
  - Kidneys (70-85%)
  - Skin (50%) → **Pyoderma gangrenosum-like ulcerations**
  - GI tract (5-11%)
  - Systemic symptoms: Arthralgia and myalgia
  - Nervous system: peripheral neuropathies

Pancreatic involvement	Small and large intestine involvement
Acute pancreatitis New pancreatic mass Pancreatic exocrine insufficiency	Ulcerations Ischemic bowel disease with intestinal wall necrosis Perforations

Granulomatosis with polyangiitis (GPA)

Diagnosis:

Clinical findings:

- Nasal involvement
- Cartilaginous involvement
- Conductive or sensorineural hearing loss
- Others

Imaging findings:

- Inflammation, consolidation, or effusion of nasal/paranasal sinuses
- Pulmonary nodules, mass, or cavitation on imaging

Histopathological findings:

- Vasculitis
- Necrosis
- Granulomatous inflammation, giant multinucleated cells on bx
- Pauci-immune glomerulonephritis on bx

Serological findings:

- cANCA (+) or Anti-PR3-ANCA (+)
- pANCA (+) or Anti-MPO-ANCA (+)

Granulomatosis with polyangiitis (GPA)

Table 1 Demographic and disease features of cases of GPA and comparators*

	GPA (n=724)	Comparators (n=813)*	P value
Age, mean±SD years	53.6±16.2	56.4±17.1	0.001
Sex, no. (%) female	340 (47.0)	424 (52.2)	0.048
Maximum serum creatinine, mean			0.077
μmoles/L	168.3	185.2	
mg/dL	1.9	2.1	
cANCA positive, no. (%)	531 (73.3)	40 (4.9)	<0.001
pANCA positive, no. (%)	71 (9.8)	342 (42.1)	<0.001
Anti-PR3-ANCA positive, no. (%)	595 (82.2)	21 (2.6)	<0.001
Anti-MPO-ANCA positive, no. (%)	59 (8.1)	399 (49.1)	<0.001
Maximum eosinophil count ≥1×10^9/L, no. (%)	196 (27)	366 (45)	<0.001

- 10% ANCA negative GPA:
  - Limited disease
  - Confined to the upper and lower respiratory tracts
  - Tissue diagnosis of active sites plays a crucial role in the confirmation of GPA.

Granulomatosis with polyangiitis (GPA)

Treatment:

- Immunosuppressive agents: cyclophosphamide, glucocorticoids, rituximab, azathioprine, methotrexate, and plasmapheresis
- Induction phase (3-6 months):
  - Life or organ-threatening disease: cyclophosphamide/Rituximab (RAVE trial) + GC
  - Limited disease: methotrexate + GC
- Maintenance phase (12-36 months):
  - Methotrexate, azathioprine, or Rituximab
  - High risk of relapse, maintenance therapy is continued indefinitely

Prognosis:

- >50% rate of relapse within 5 years of initial remission
- 5-year survival rate □ ~80%
- Mortality is 2.6 times higher in patients with GPA than in an age and sex matched population.

Our patient: differential diagnosis

- Autoimmune pancreatitis with pancreatic panniculitis
- IgG4-related disease

Autoimmune pancreatitis

- Frequent obstructive jaundice with or without a pancreatic mass (can mimic a pancreatic malignancy)
- Encompasses 2 distinct entities

Type I - AIP	Type II - AIP
- **Lymphoplasmacytic sclerosing pancreatitis** - Pancreatic manifestation of IgG4-RD - Older men - Asian descent - Increased serum gamma-globulin, IgG and/or IgG4 - Other organ involvement - HP: LPSP, abundant infiltration of lymphocytes and plasma cells, fibrosis, obliterative phlebitis - Usually responds to steroids	- **Idiopathic duct centric pancreatitis with granulocytic epithelial lesions** - Caucasian - < 40-year-old - No sex predilection - No serum IgG4 elevation - 30% associated with IBD - HP: GEL (intraluminal and intraepithelial neutrophils in medium-sized and small ducts and in acini) + destruction and obliteration of the pancreatic duct

IgG4-related disease

- Immune-mediated fibro-inflammatory disorder
- Middle-aged and elderly, Asian descent men (3:1)
- Characterized by:
  - Diffuse of focal organ enlargement and mass-forming, nodular or thickened lesions in various organs
  - Multi-organ involvement (20% single organ)
  - Synchronous or metachronous lesions
- Elevation serum IgG4 concentration (>135mg/dL)
- Histology:
  - Marked lymphocytes and plasma cell infiltration and fibrosis (storiform fibrosis)
  - Infiltration of IgG4 positive plasma cells: ration of IgG4/IgG >40% and >10% IgG4 (+) plasma cells/hpf.
- Good response to steroids

Organs:
CNS
Thyroid gland
Lacrimal glands
Salivary glands
Breast
Lung
Liver
Bile duct
Pancreas → IgG4-related pancreatitis
Type I - AIP
GI tract
Kidney
Prostate
Retroperitoneum
Arteries
LN
Skin

Our patient

Hearing loss

Breast inflammatory lesion

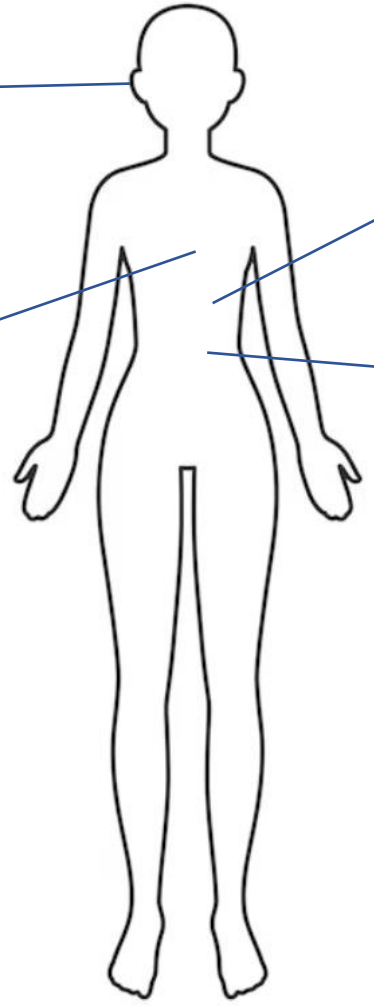

Geographic hypoattenuation of the spleen

4.5 cm hypodense mass in the left kidney

All which may be part of GPA

Treated with Rituximab and prednisone taper with improvement

Summary

- Although rare, GPA can present with pancreatic and gastrointestinal tract involvement
- A negative ANCA does not exclude the diagnosis of GPA
- Tissue diagnosis of active sites plays a crucial role in the confirmation of GPA

References

- Tao JJ, Agarwal A, Cuperfain AB, Pagnoux C. Granulomatosis with polyangiitis presenting as pancreatic disease. *BMJ* Case Rep. 2021;14(3):e241033. Published 2021 Mar 2. doi:10.1136/bcr-2020-241033
- Robson JC, Grayson PC, Ponte C, et al. 2022 American College of Rheumatology/European Alliance of Associations for Rheumatology classification criteria for granulomatosis with polyangiitis. *Ann Rheum Dis*. 2022;81(3):315-320. doi:10.1136/annrheumdis-2021-221795
- Jennette JC, Falk RJ, Bacon PA, et al. 2012 revised International Chapel Hill Consensus Conference Nomenclature of Vasculitides. *Arthritis Rheum*. 2013;65(1):1-11. doi:10.1002/art.37715
- Wallace ZS, Naden RP, Chari S, et al. The 2019 American College of Rheumatology/European League Against Rheumatism classification criteria for IgG4-related disease. *Ann Rheum Dis*. 2020;79(1):77-87. doi:10.1136/annrheumdis-2019-216561
- Masiak A, Zdrojewski Ł, Zdrojewski Z, Bułło-Piontecka B, Rutkowski B. Gastrointestinal tract involvement in granulomatosis with polyangiitis. *Prz Gastroenterol*. 2016;11(4):270-275. doi:10.5114/pg.2016.57887
- Youssef M, Sedarous M, Grin A, Chung A, Hookey L. Acute Pancreatitis as a First Presentation of Granulomatosis With Polyangiitis. ACG Case Rep J. 2023;10(2):e00986. Published 2023 Feb 10. doi:10.14309/crj.0000000000000986
- Tao JJ, Agarwal A, Cuperfain AB, Pagnoux C. Granulomatosis with polyangiitis presenting as pancreatic disease. BMJ Case Rep. 2021;14(3):e241033. Published 2021 Mar 2. doi:10.1136/bcr-2020-241033
- Kubaisi B, Abu Samra K, Foster CS. Granulomatosis with polyangiitis (Wegener's disease): An updated review of ocular disease manifestations. Intractable Rare Dis Res. 2016;5(2):61-69. doi:10.5582/irdr.2016.01014
- Wallace ZS, Lu N, Unizony S, Stone JH, Choi HK. Improved survival in granulomatosis with polyangiitis: A general population-based study. Semin Arthritis Rheum. 2016;45(4):483-489. doi:10.1016/j.semarthrit.2015.07.009

23-1206

Susan Potterveld/Ankur Sangoi; Stanford

40-year-old male patient presents with left hydronephrosis and undergoes robotic assisted laparoscopic pyeloplasty

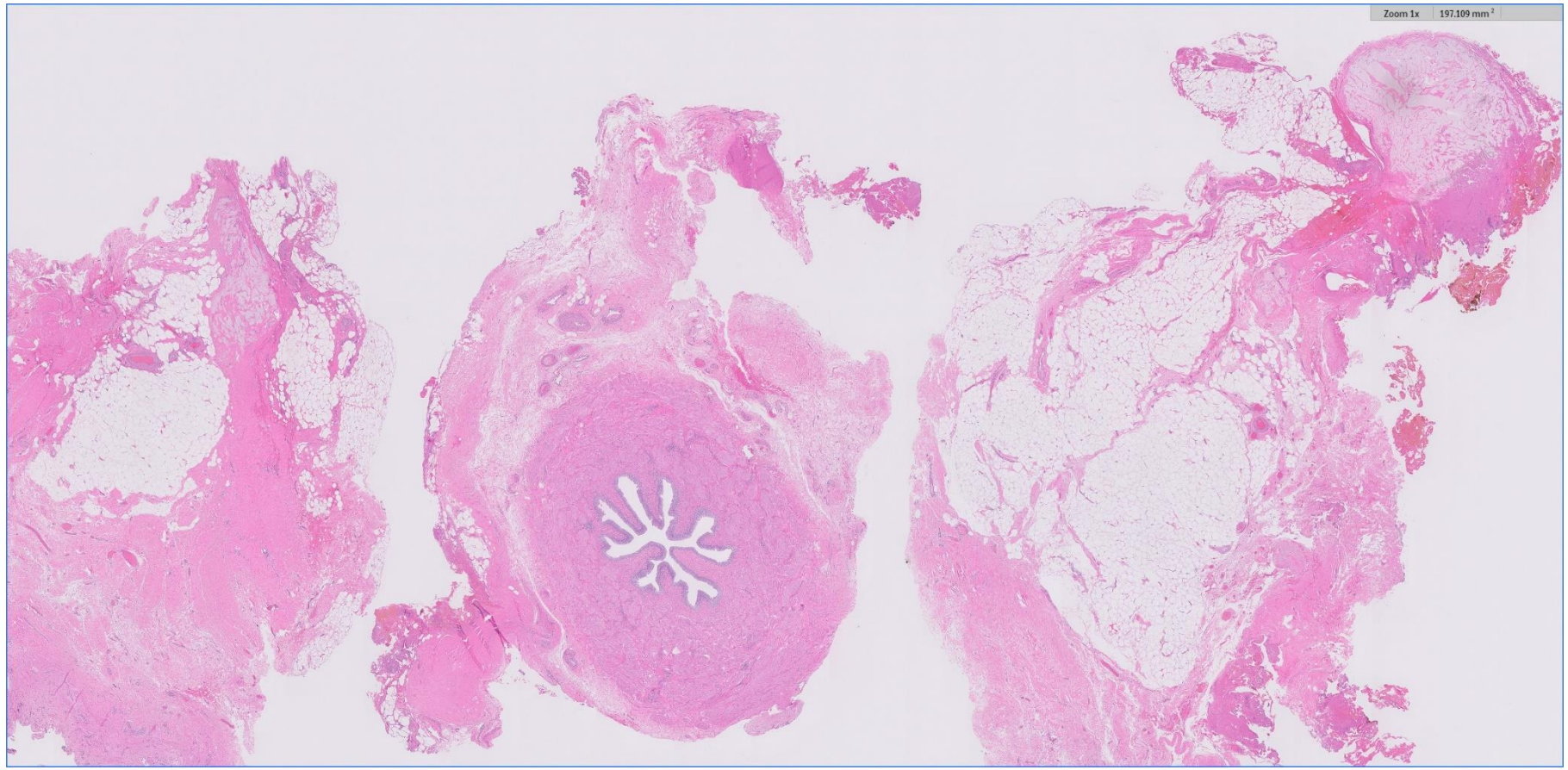
Zoom 1x
197.109 mm²

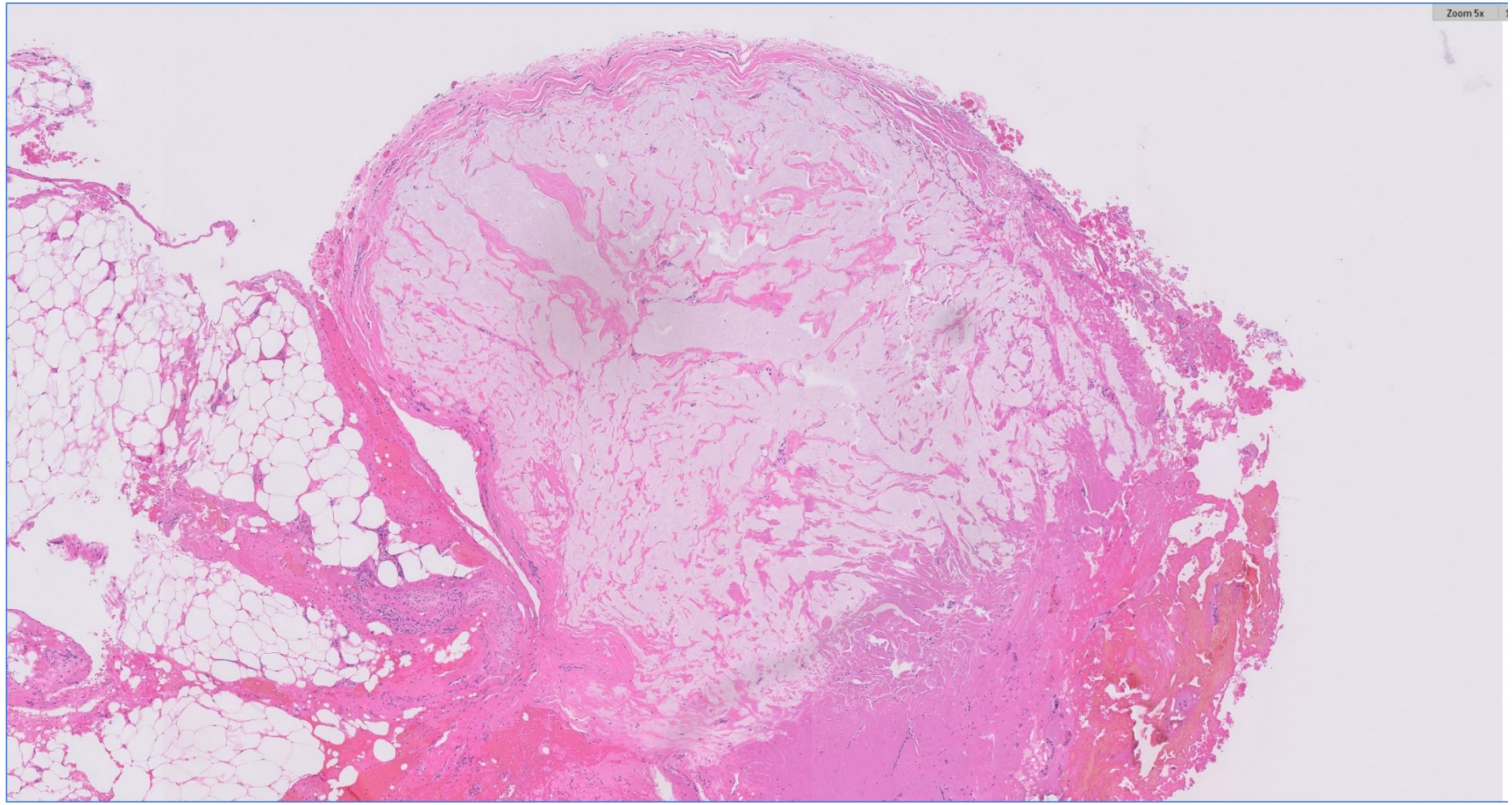
Zoom 5x

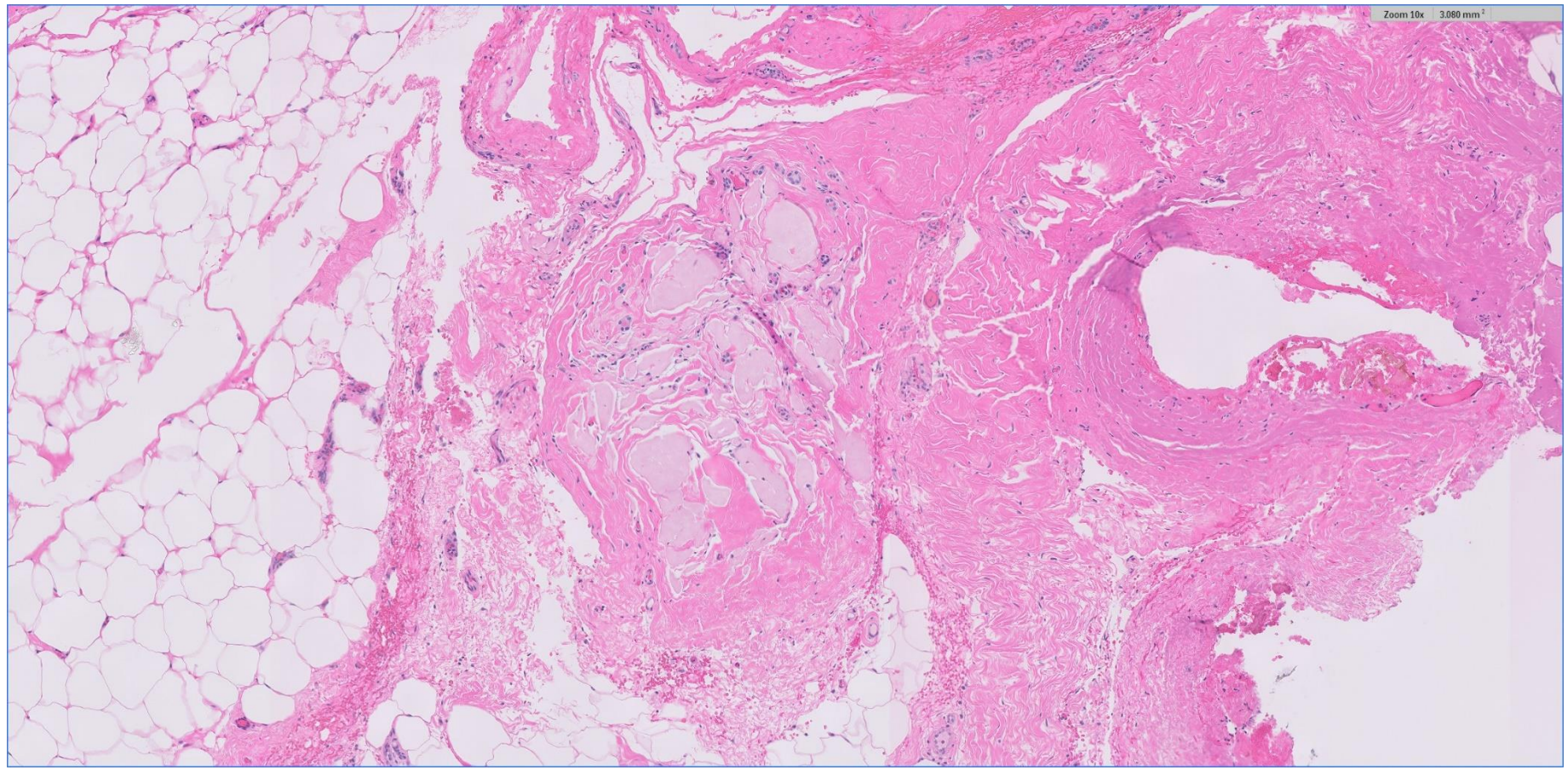
Zoom 10x
3.080 mm²

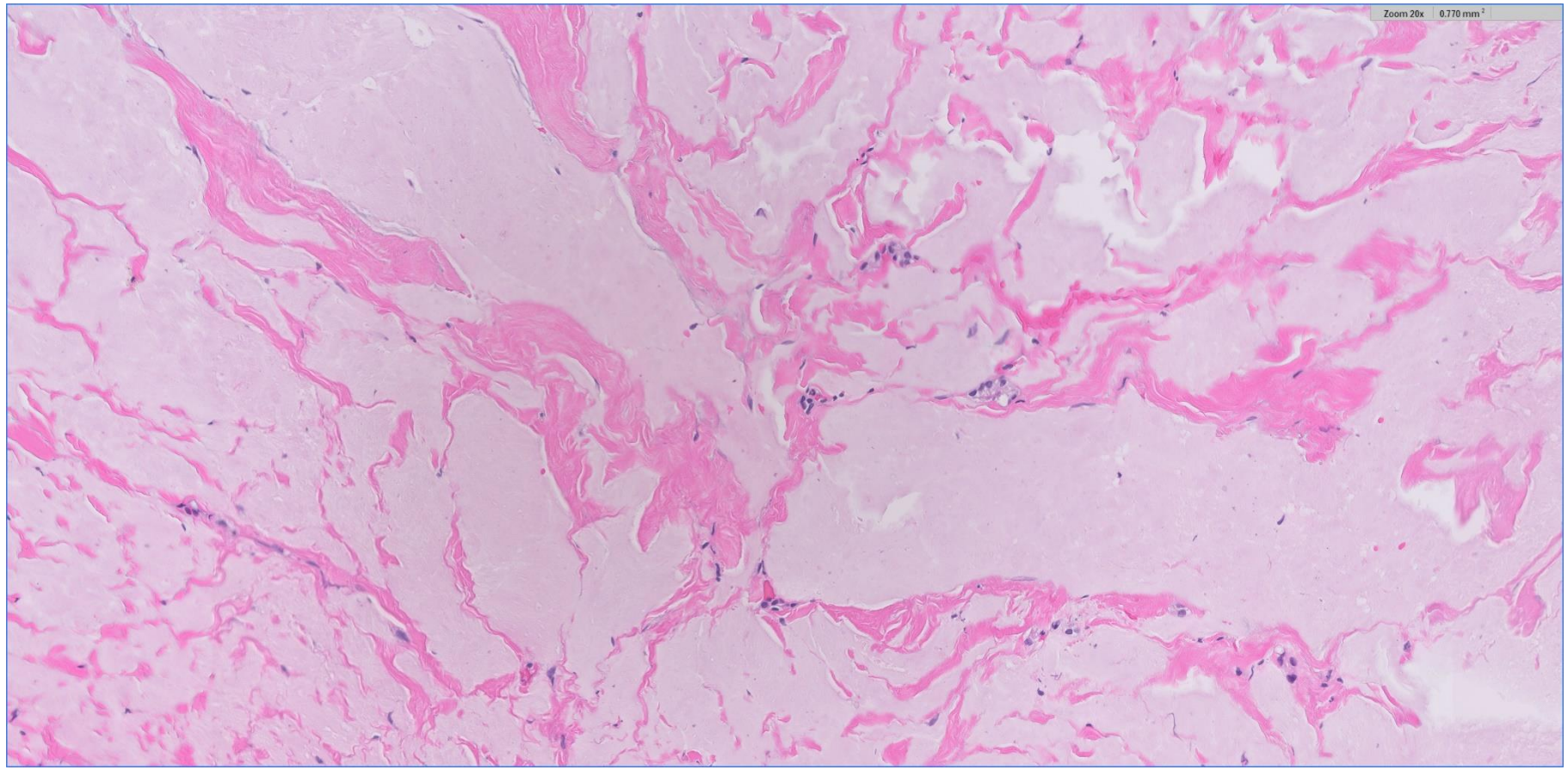
Zoom 20x
0.770 mm²

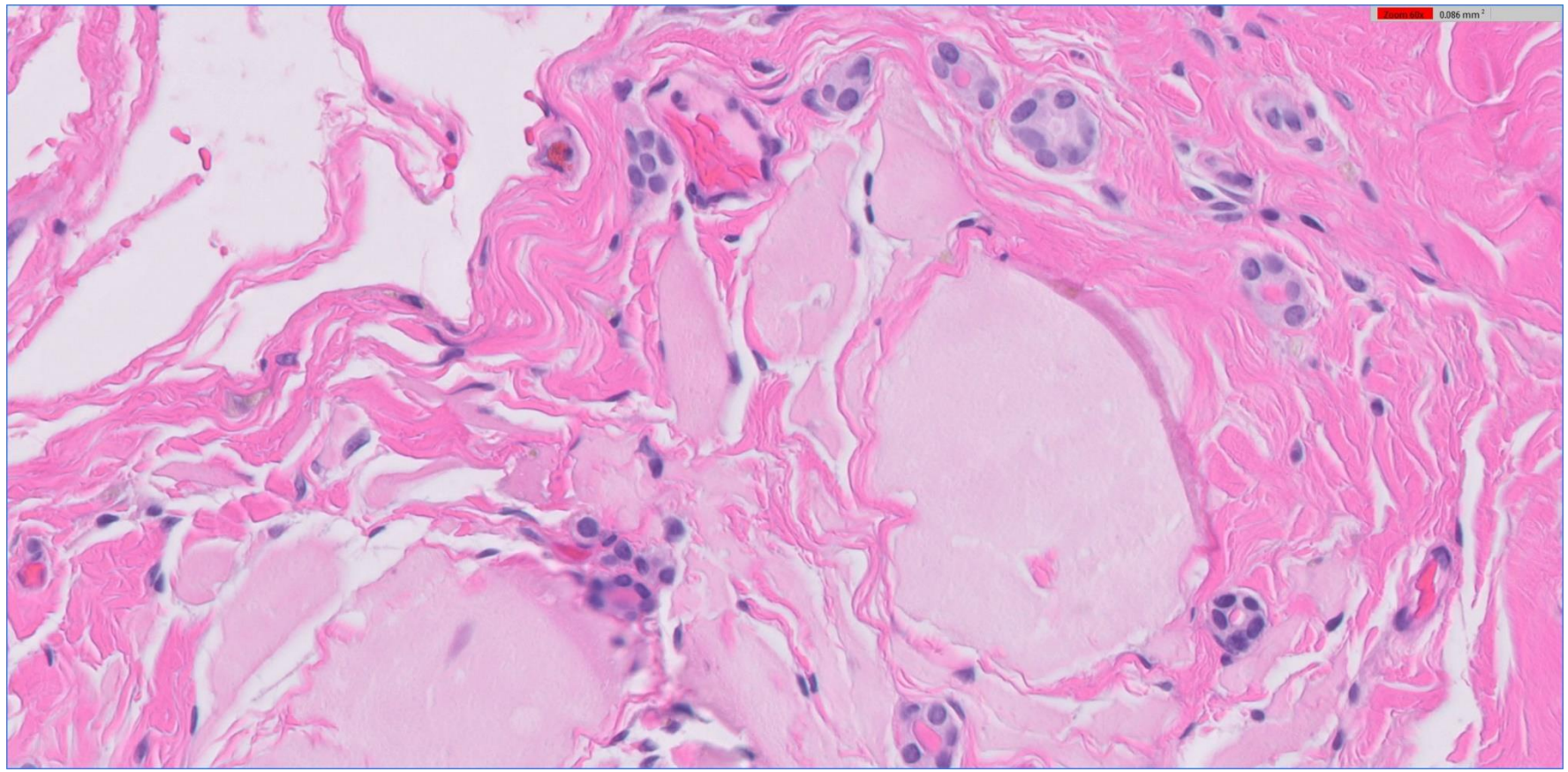
Zoom 60x
0.086 mm²

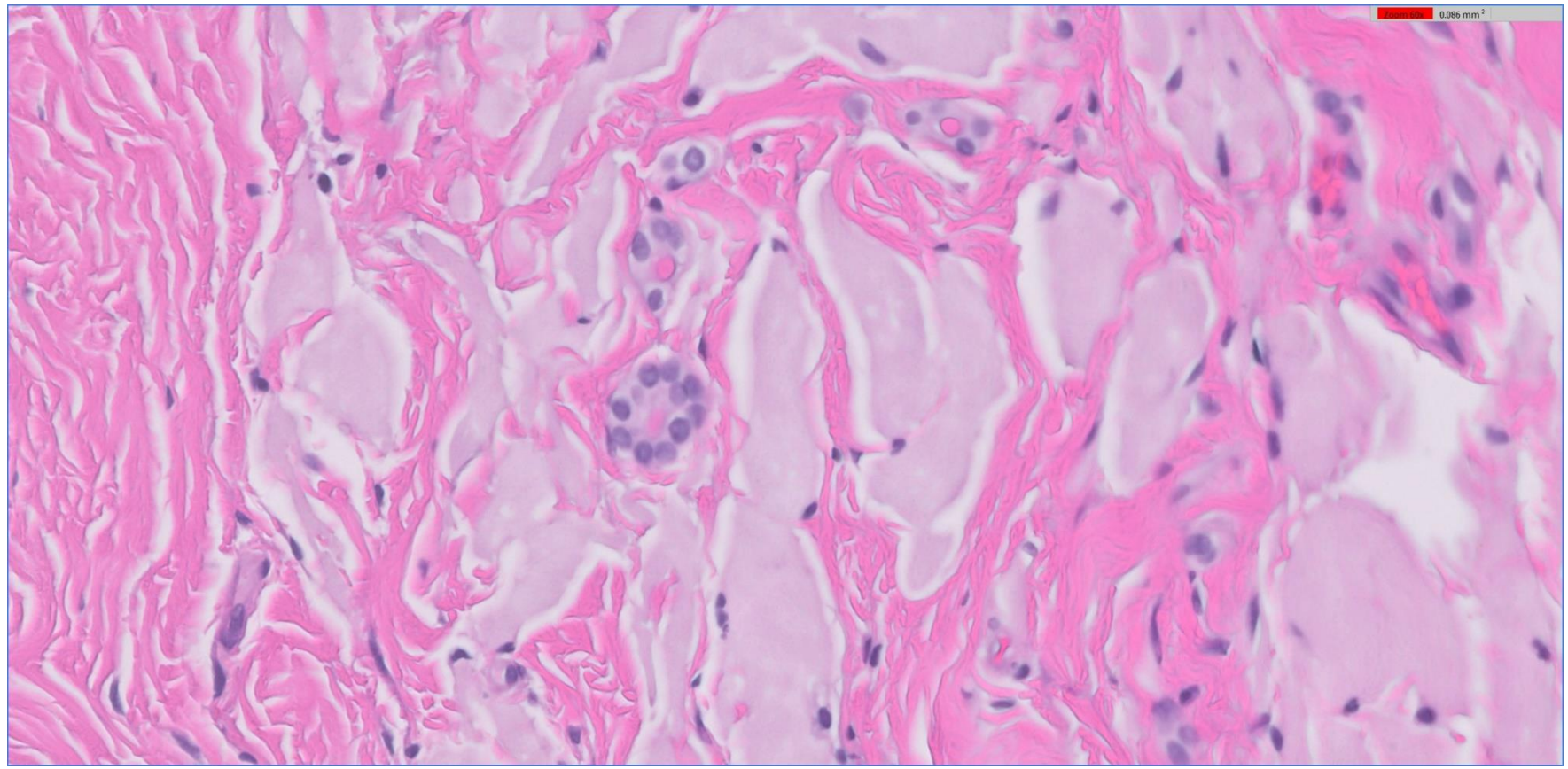
Zoom: 60x
0.086 mm²

DIAGNOSIS?

PAX8

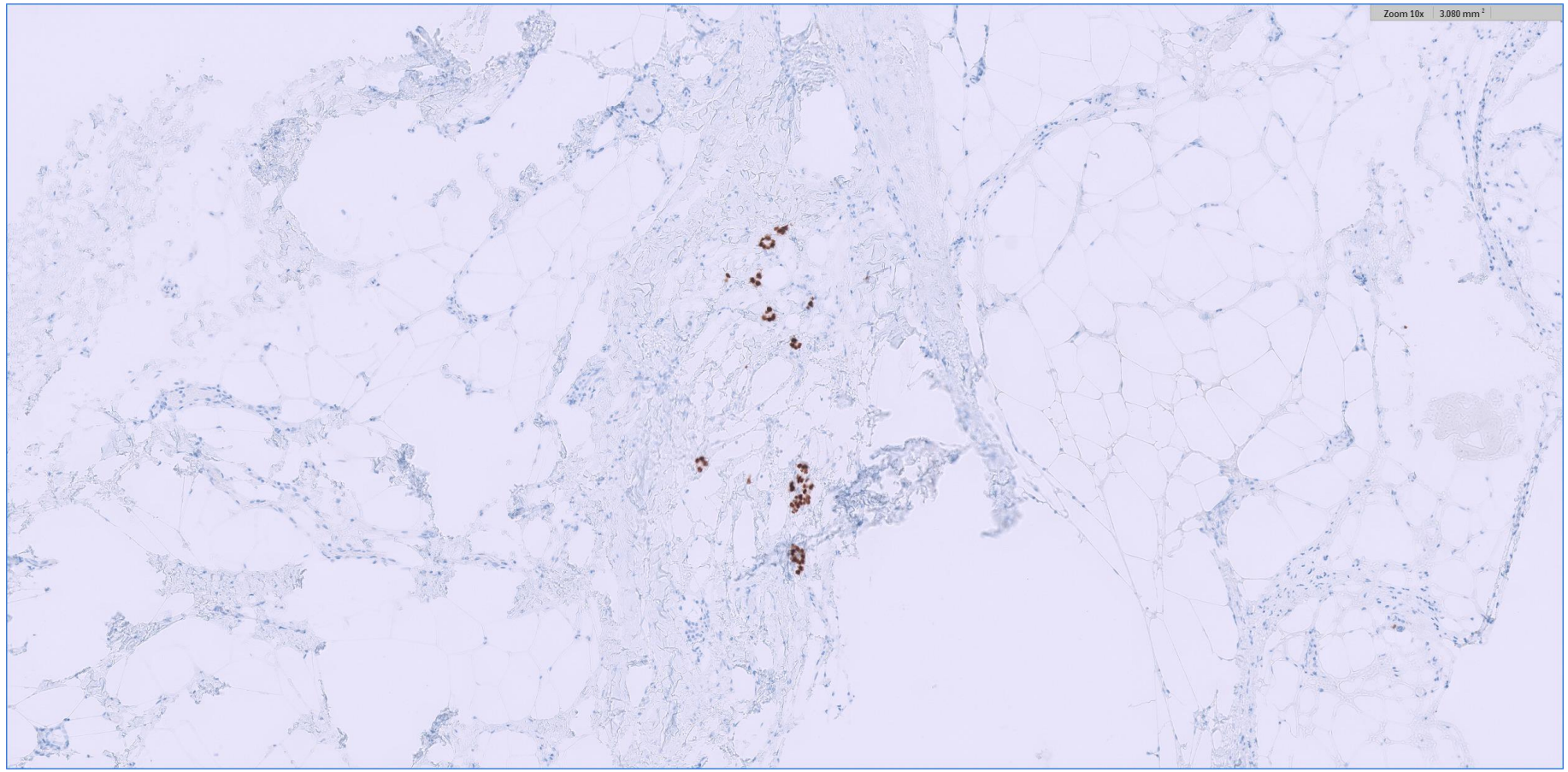

PAX8

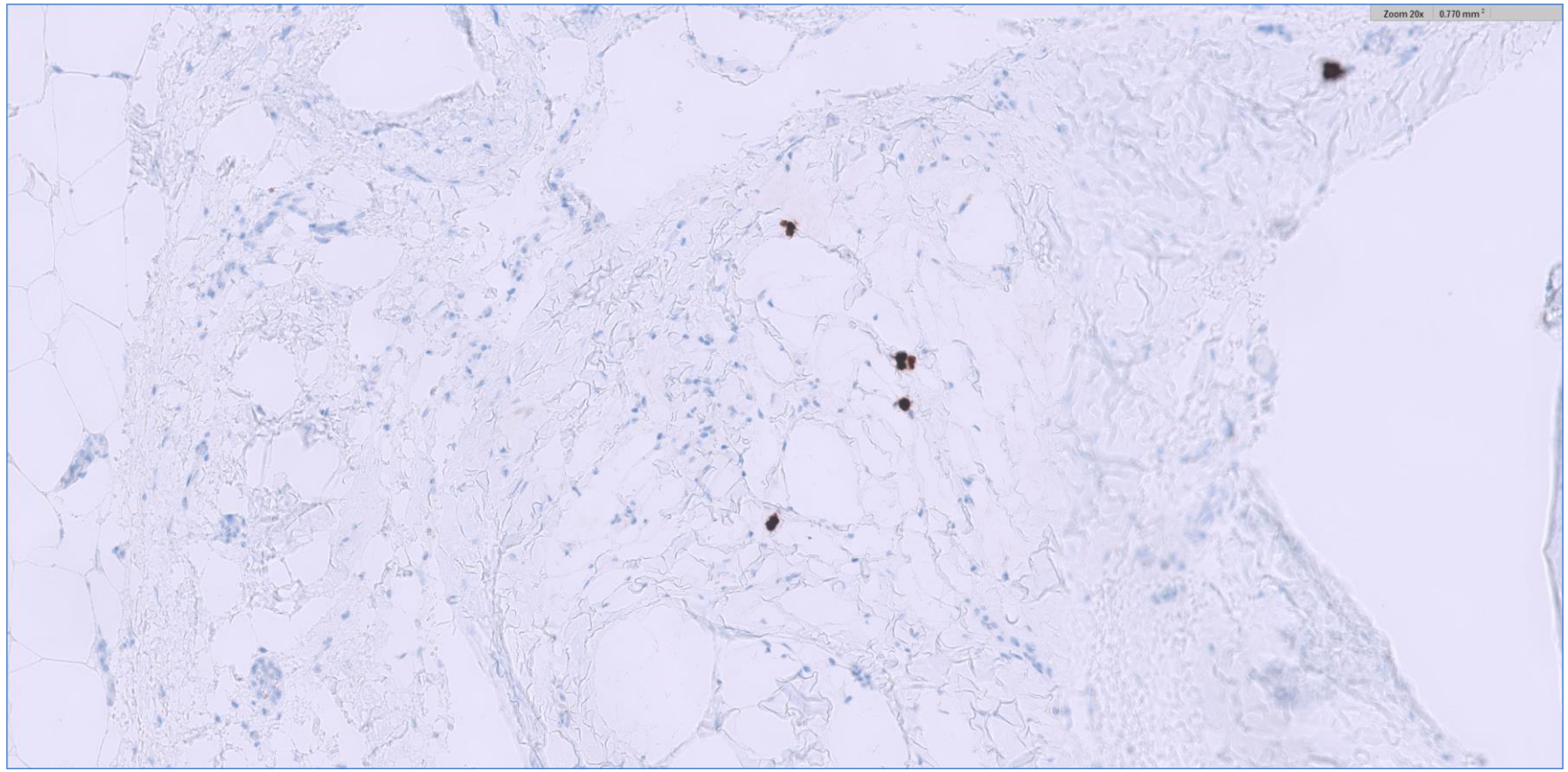

Diagnosis: Nephrogenic Adenoma – Fibromyxoid Subtype

Nephrogenic Adenoma

- General
  - Benign lesion
  - Found following urothelial injury
  - Believed to be derived from shed renal tubular cells
  - May present anywhere along the urothelial tract
- Histology
  - Classic patterns: tubular, papillary, flat, cystic, and microcystic
  - Fibromyxoid pattern (rare):
    - Compressed spindle cells in a prominent fibromyxoid extracellular matrix
    - No nuclear atypia and no mitotic figures
- Immunohistochemistry:
  - PAX8 positive
  - Subset are GATA3 positive

PMIDs: 36395466, 24921643, 17667548

Fibromyxoid Nephrogenic Adenoma: A Newly Recognized Variant Mimicking Mucinous Adenocarcinoma

Donna Elizabeth Hansel, MD, PhD, Tibor Nadasdy, MD,† and Jonathan I. Epstein, MD‡§‖*

Fibromyxoid Nephrogenic Adenoma

A Series of 43 Cases Reassessing Predisposing Conditions, Clinical Presentation, and Morphology

Lin Li, MD, PhD, Sean R. Williamson, MD,† Rosa P. Castillo, MD,‡§ Katiana S. Delma, HT,* Mark L. Gonzalgo, MD, PhD,§‖ Jonathan I. Epstein, MD,¶#** and Oleksandr N. Kryvenko, MD*§‖††*

Nephrogenic Adenoma – Fibromyxoid Subtype

- Predisposing factors: prior instrumentations and injuries of the urothelial mucosa
- Increased predilection to involve tissues beyond the lamina propria
- Differential diagnoses:
  - Amyloid
  - Infiltrative myxoid/mucinous adenocarcinoma
  - Perinephric myxoid pseudotumor of fat

Take Home Points

- Recognize the distinctive histologic appearance of fibromyxoid pattern nephrogenic adenoma to avoid confusion with other entities
- PAX8 IHC is very useful in confirming the diagnosis
- GATA3 IHC can be a potential pitfall

23-1207

Susan Potterveld/Greg Charville; Stanford

71-year-old female patient with a 5.7 cm heterogeneously enhancing mass centered within the proximal right sartorius muscle discovered on work-up for high-grade serous carcinoma

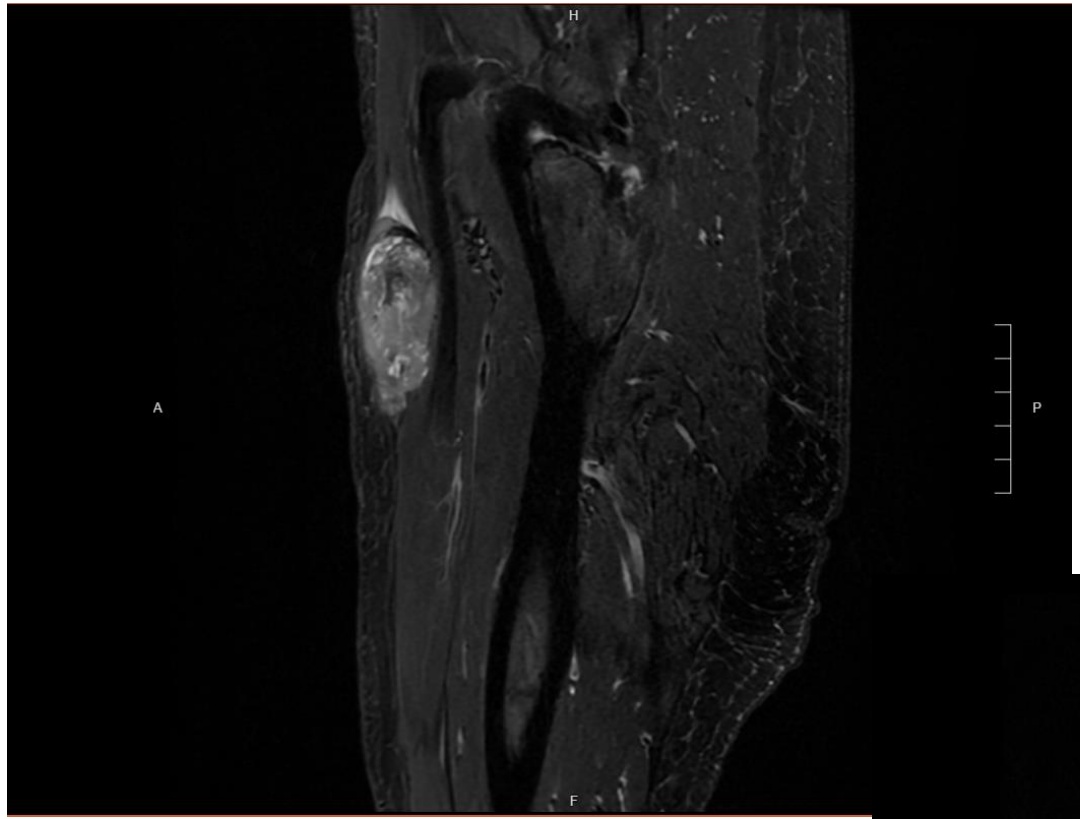

SAG STIR

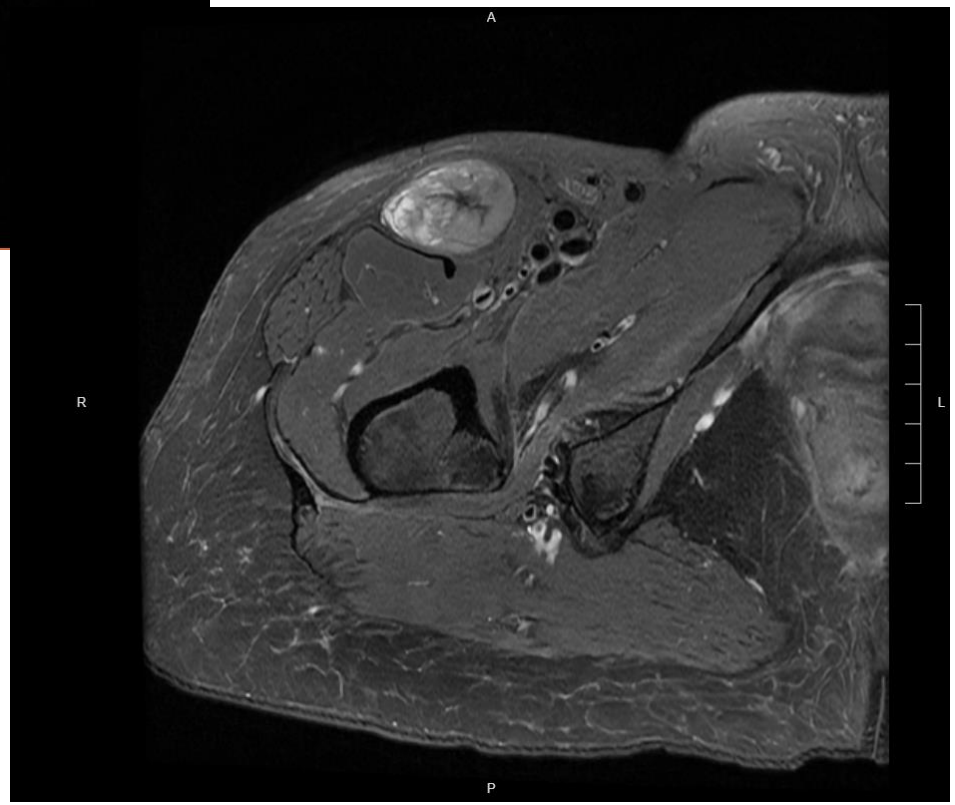

AX T2 FS

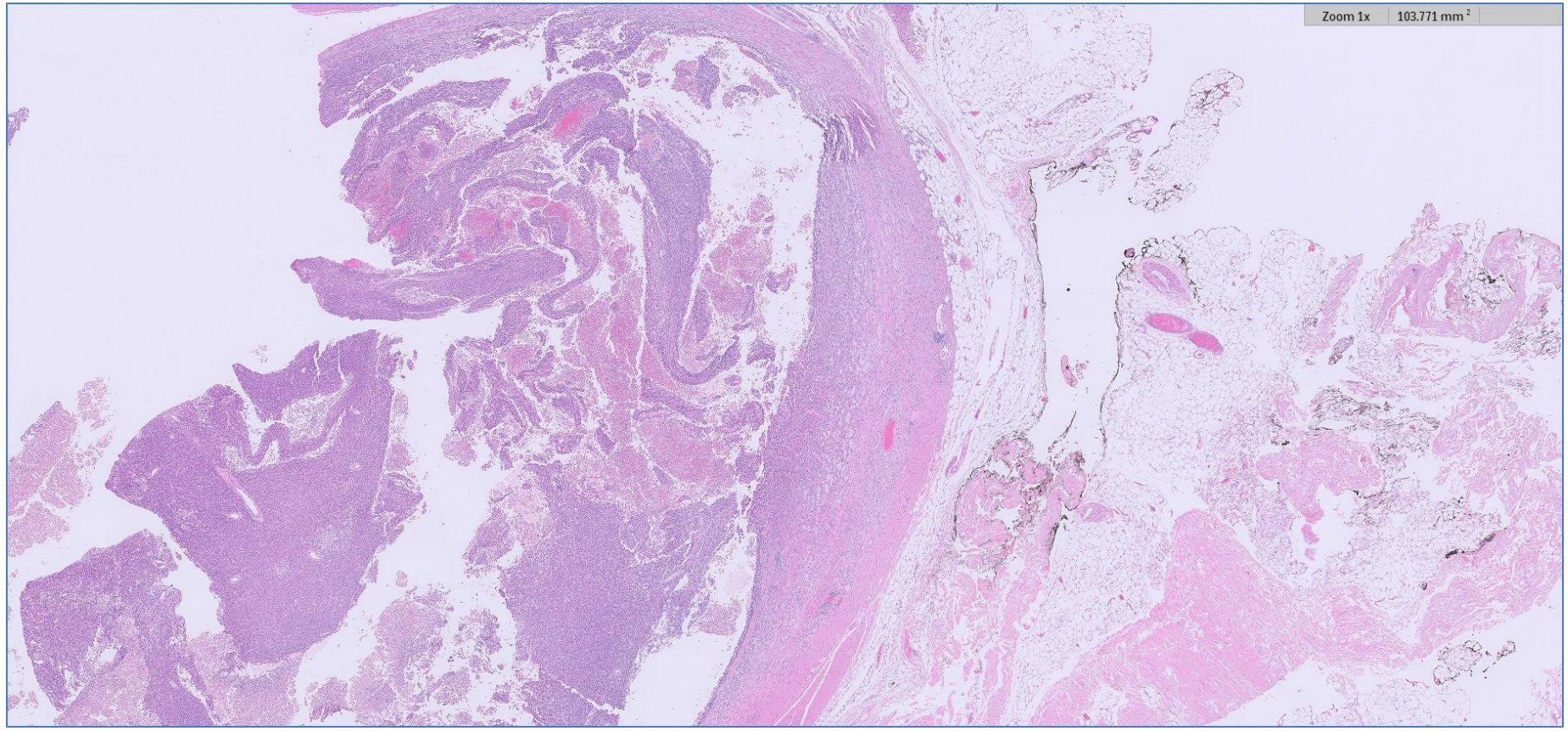
Zoom 1x
103.771 mm²

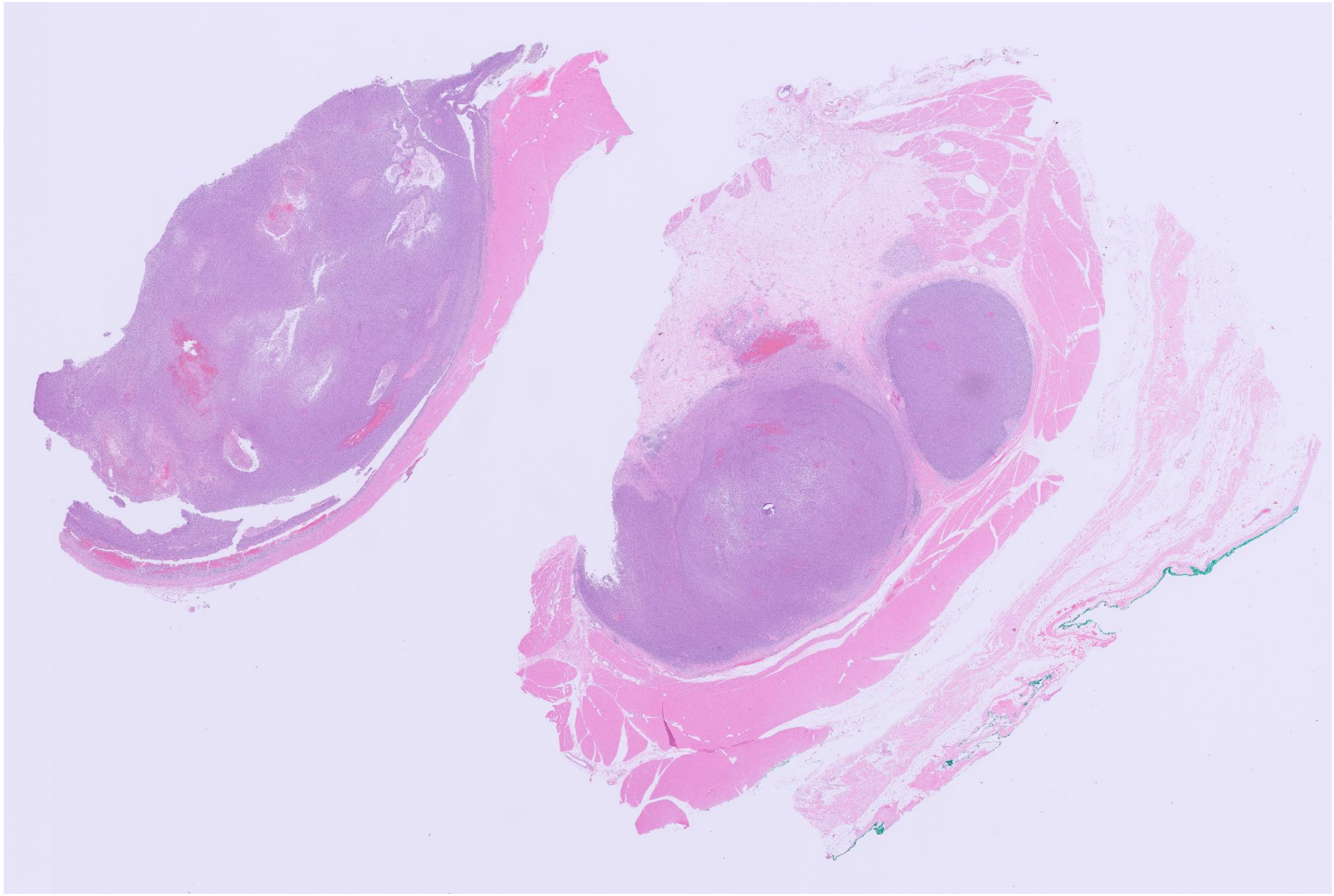

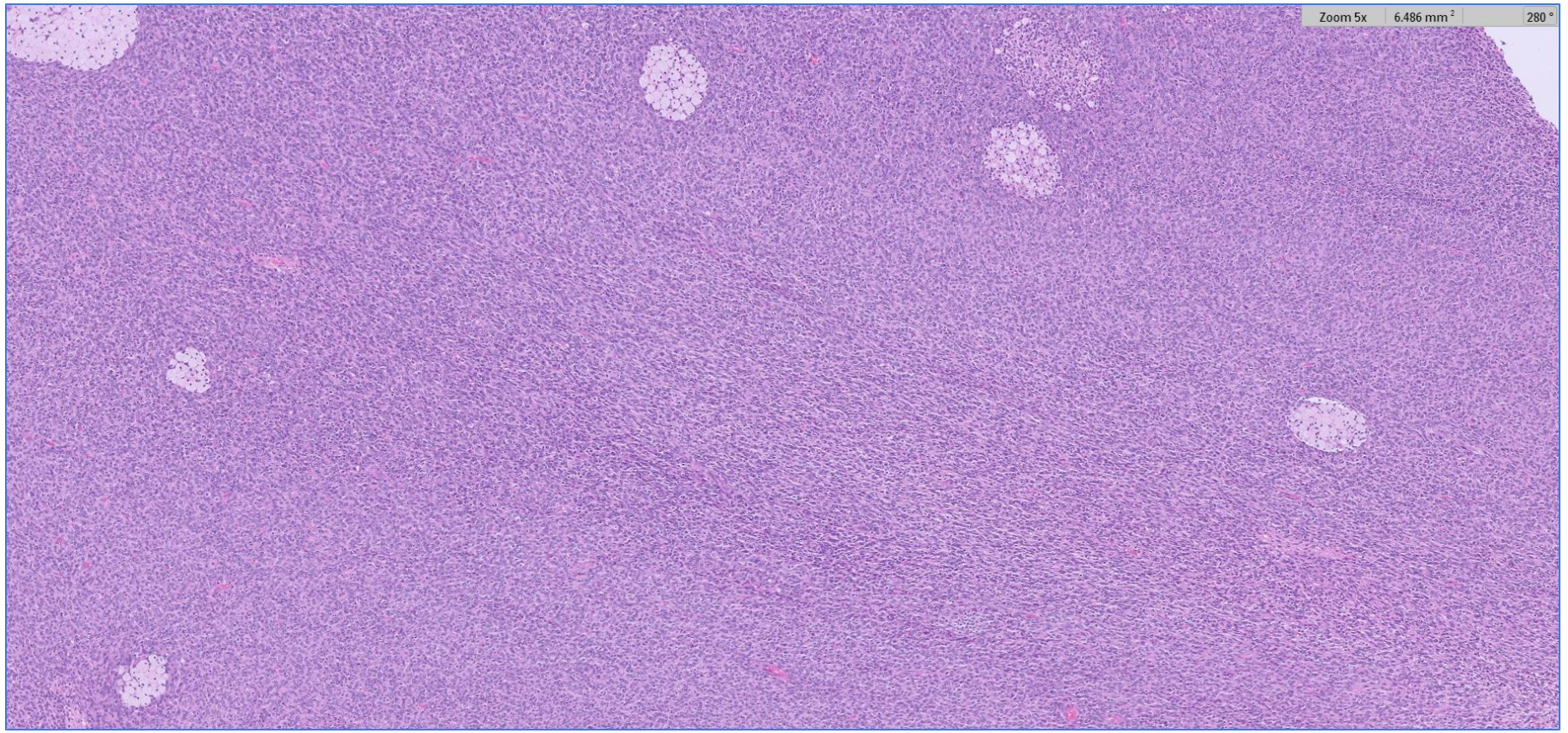
Zoom 5x
6.486 mm²
280 °

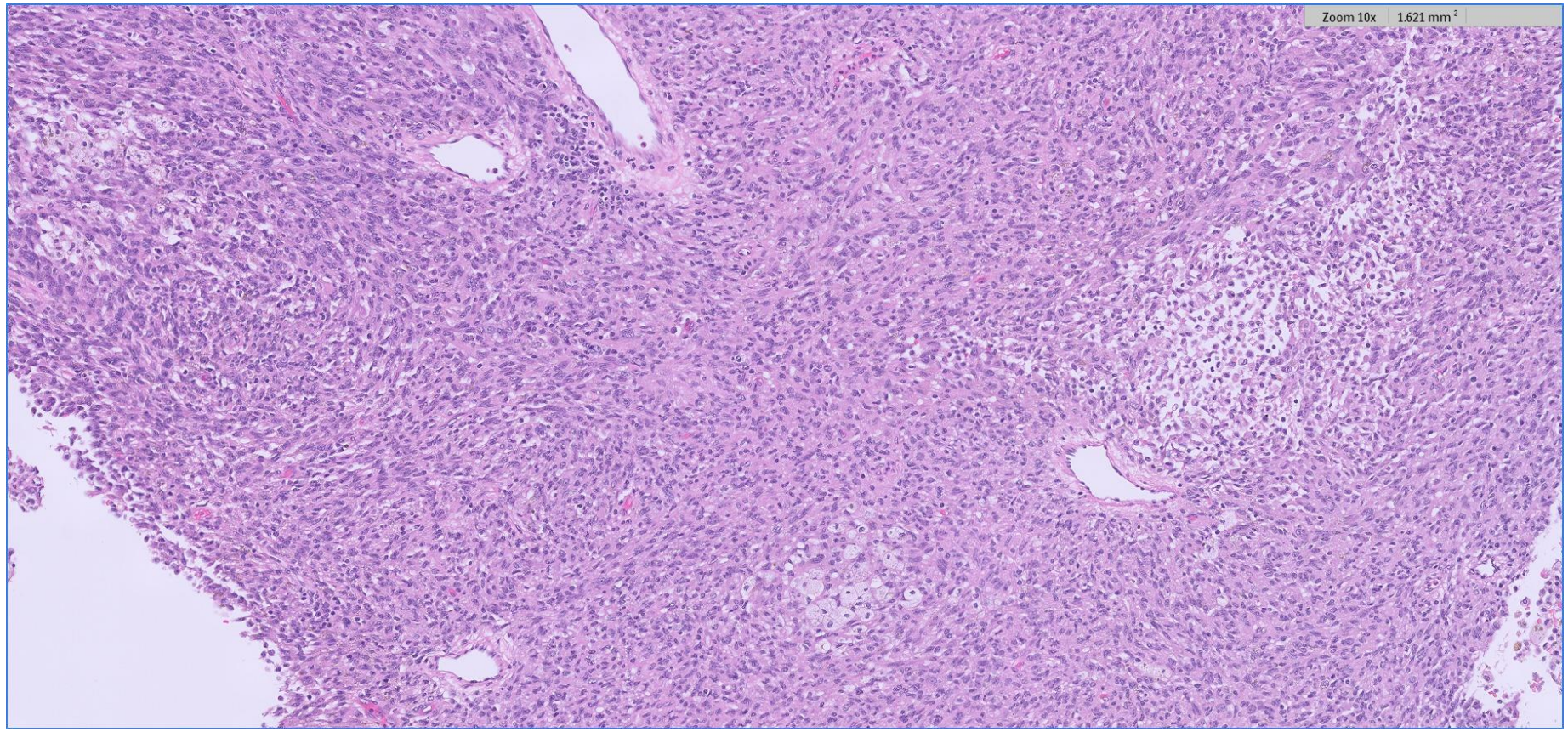
Zoom 10x
1.621 mm ²

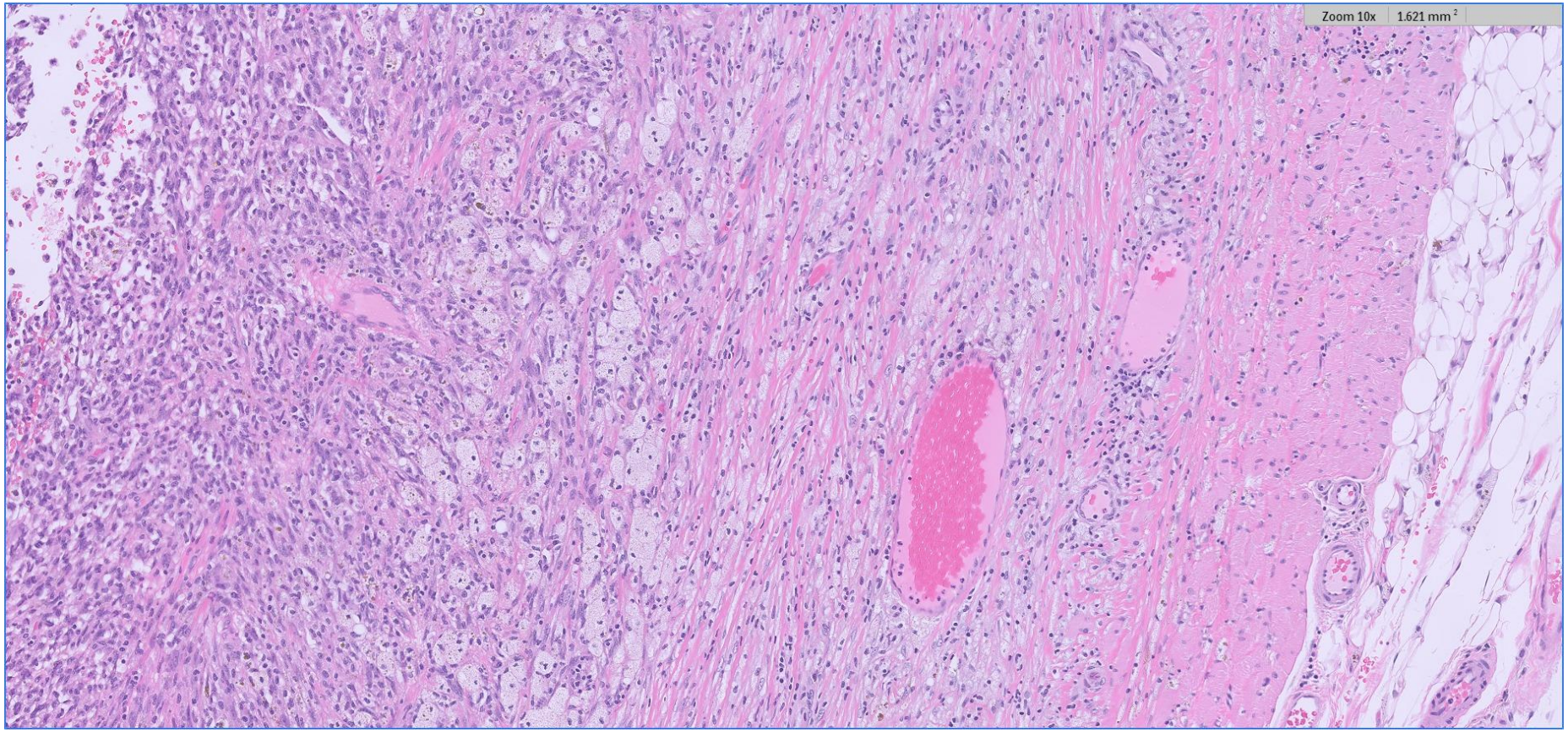
Zoom 10x
1.621 mm 2

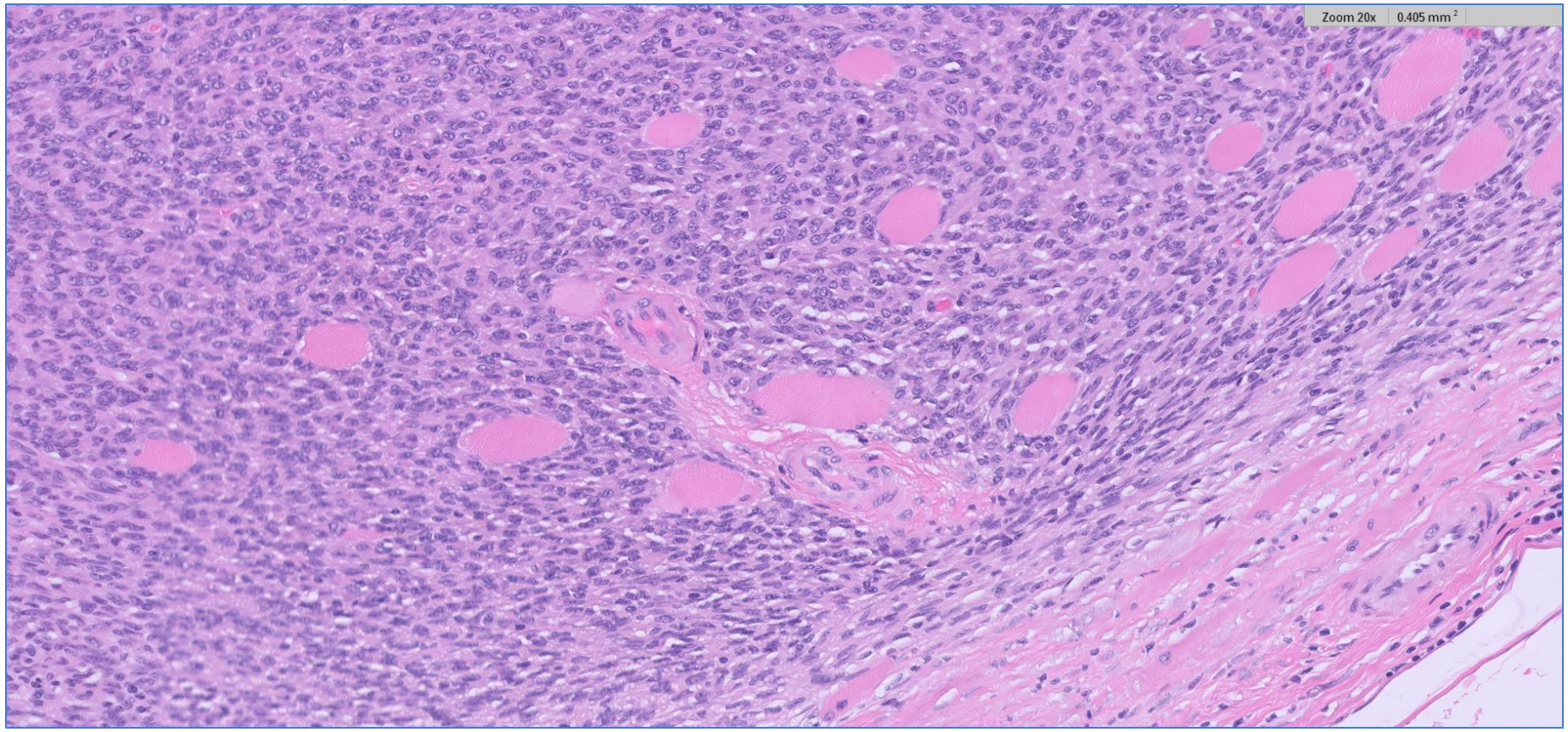
Zoom 20x
0.405 mm ²

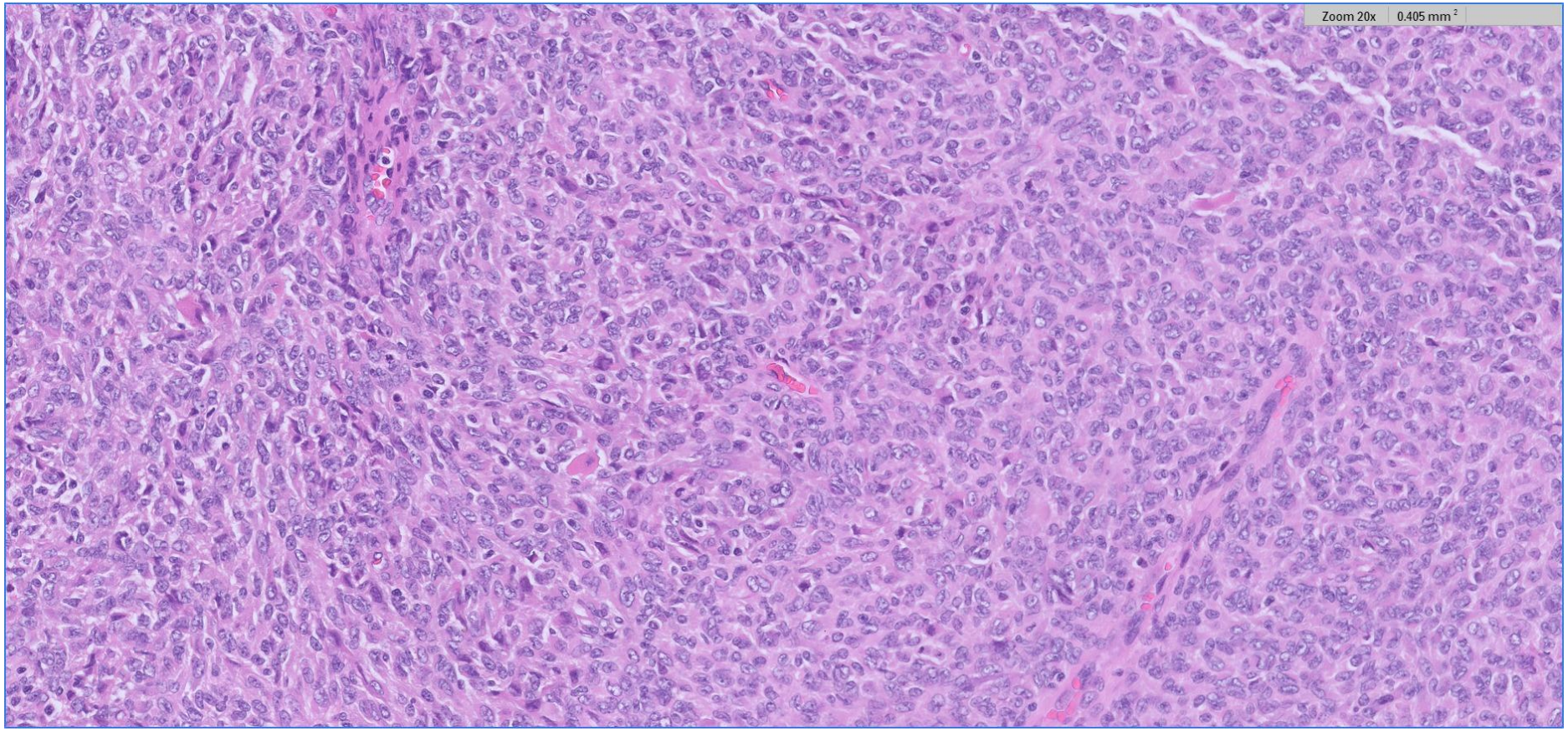
Zoom 20x
0.405 mm ²

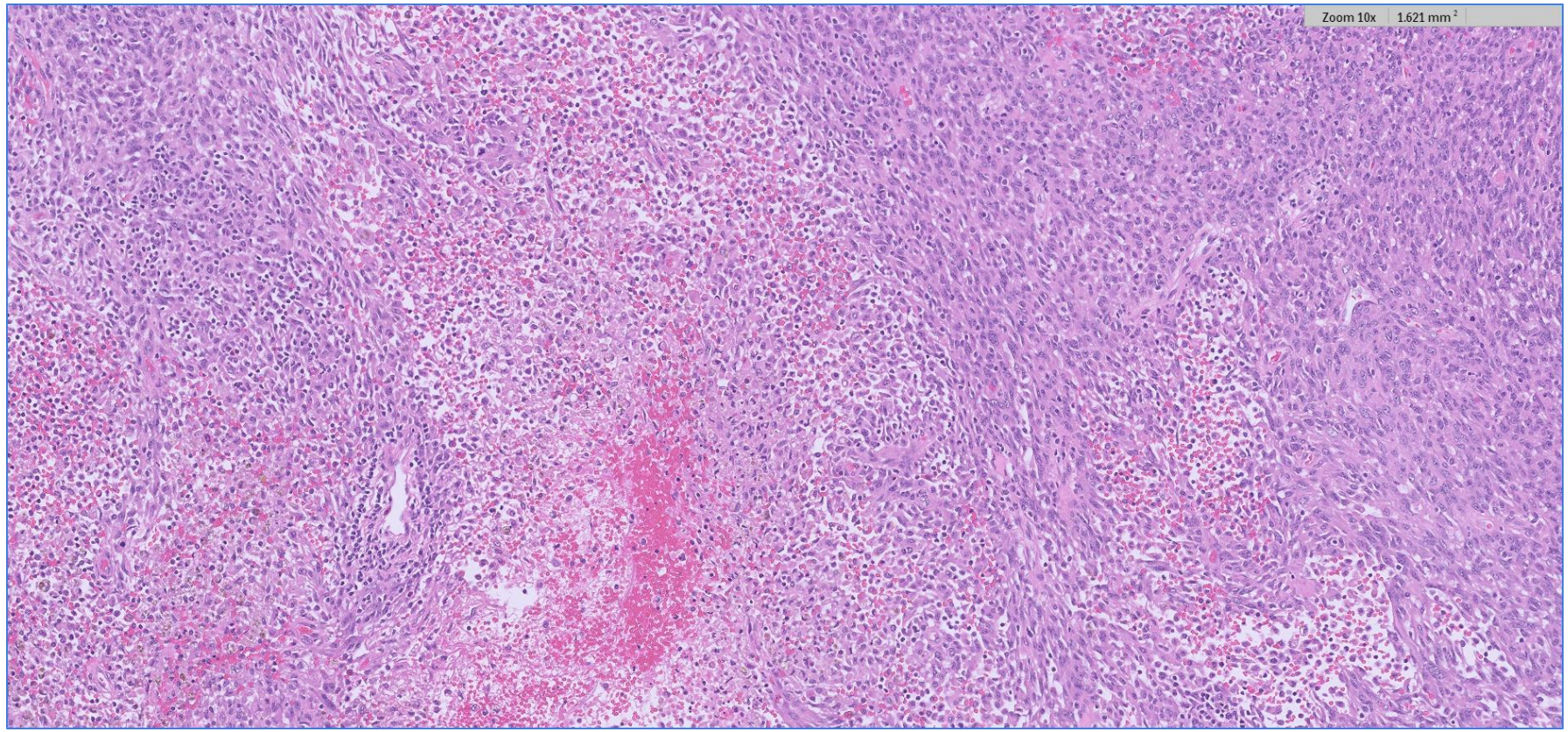
Zoom 10x
1.621 mm 2

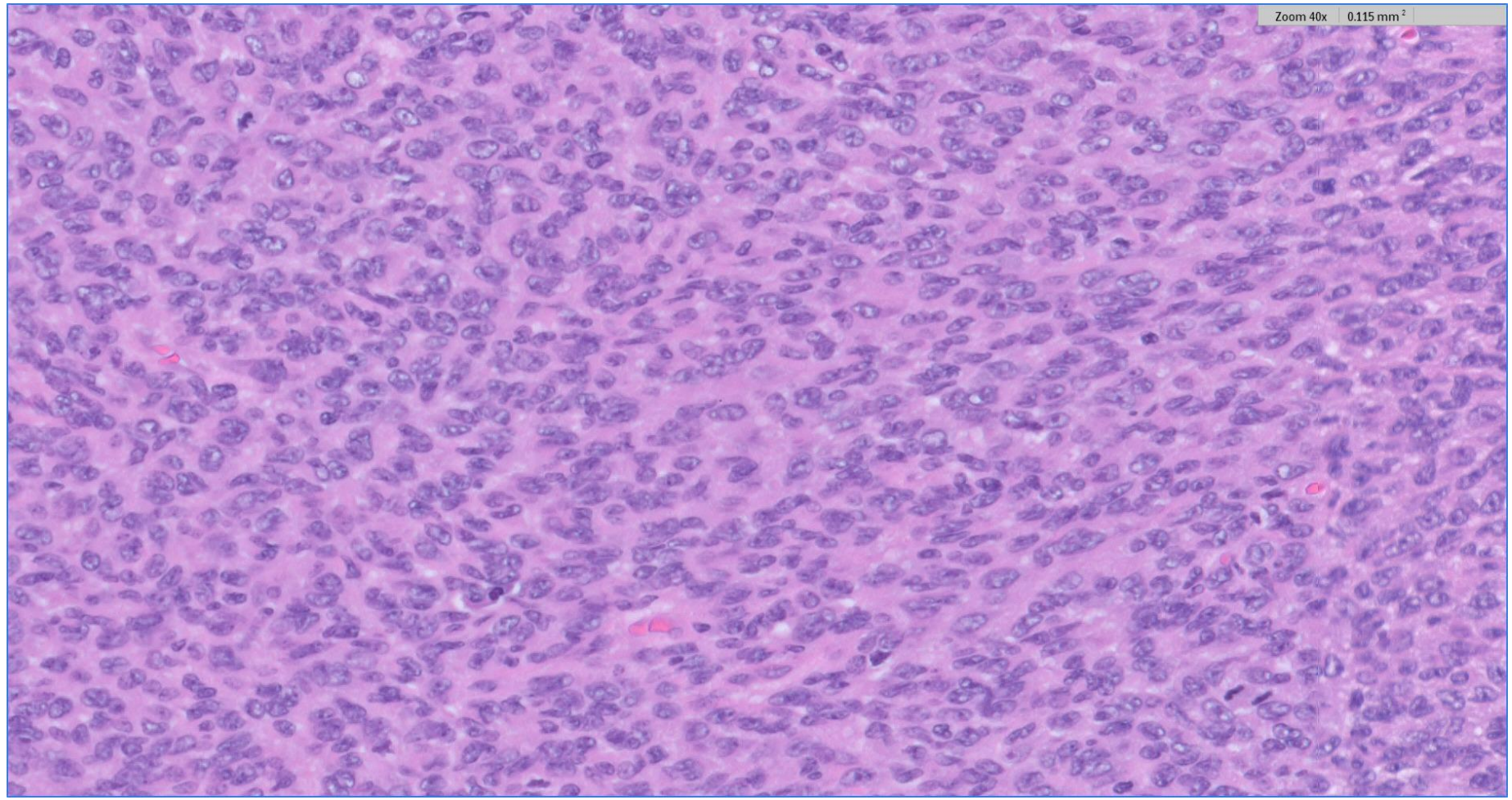
Zoom 40x
0.115 mm ²

Desmin

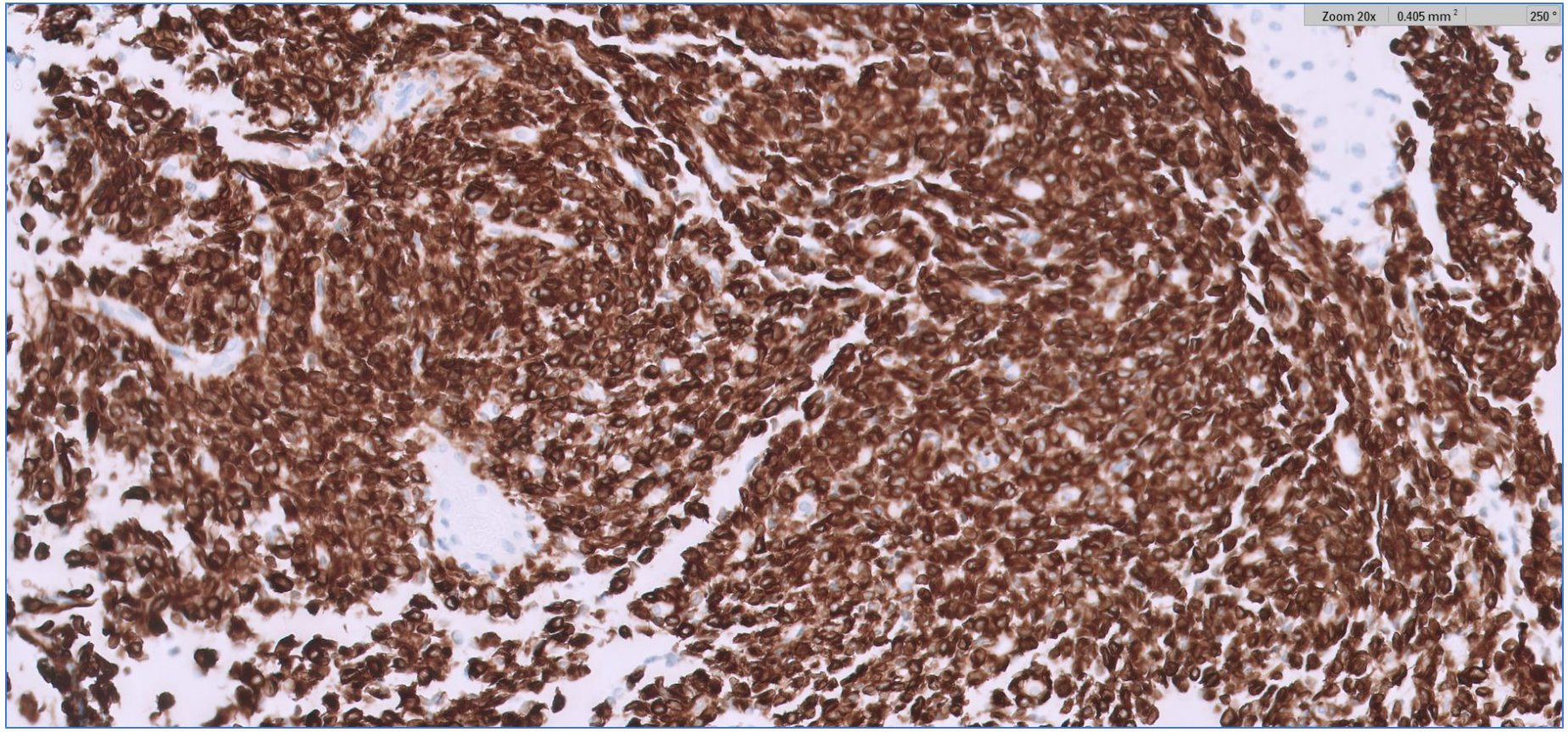

DIAGNOSIS?

PAX7

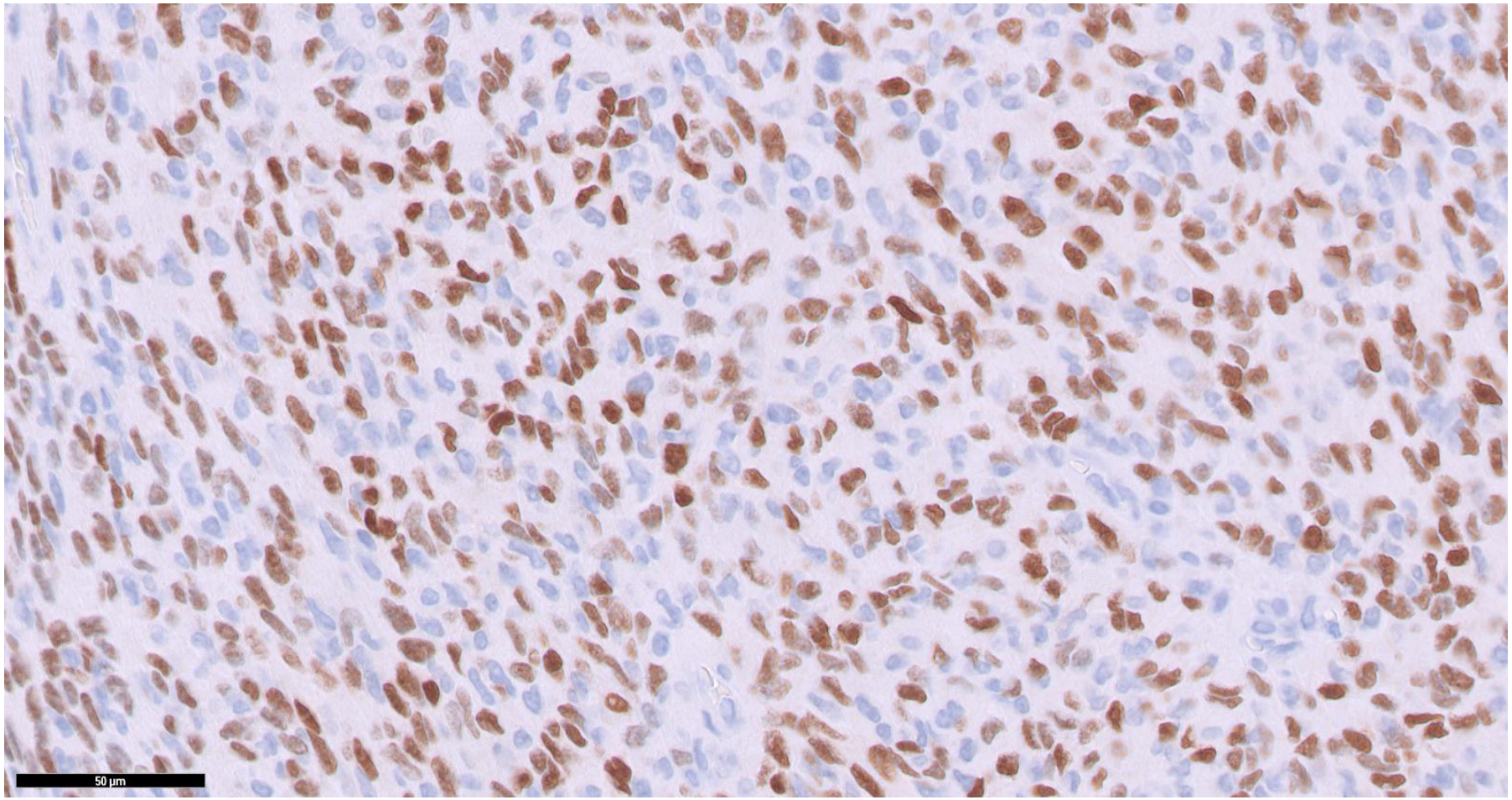

MyoD1

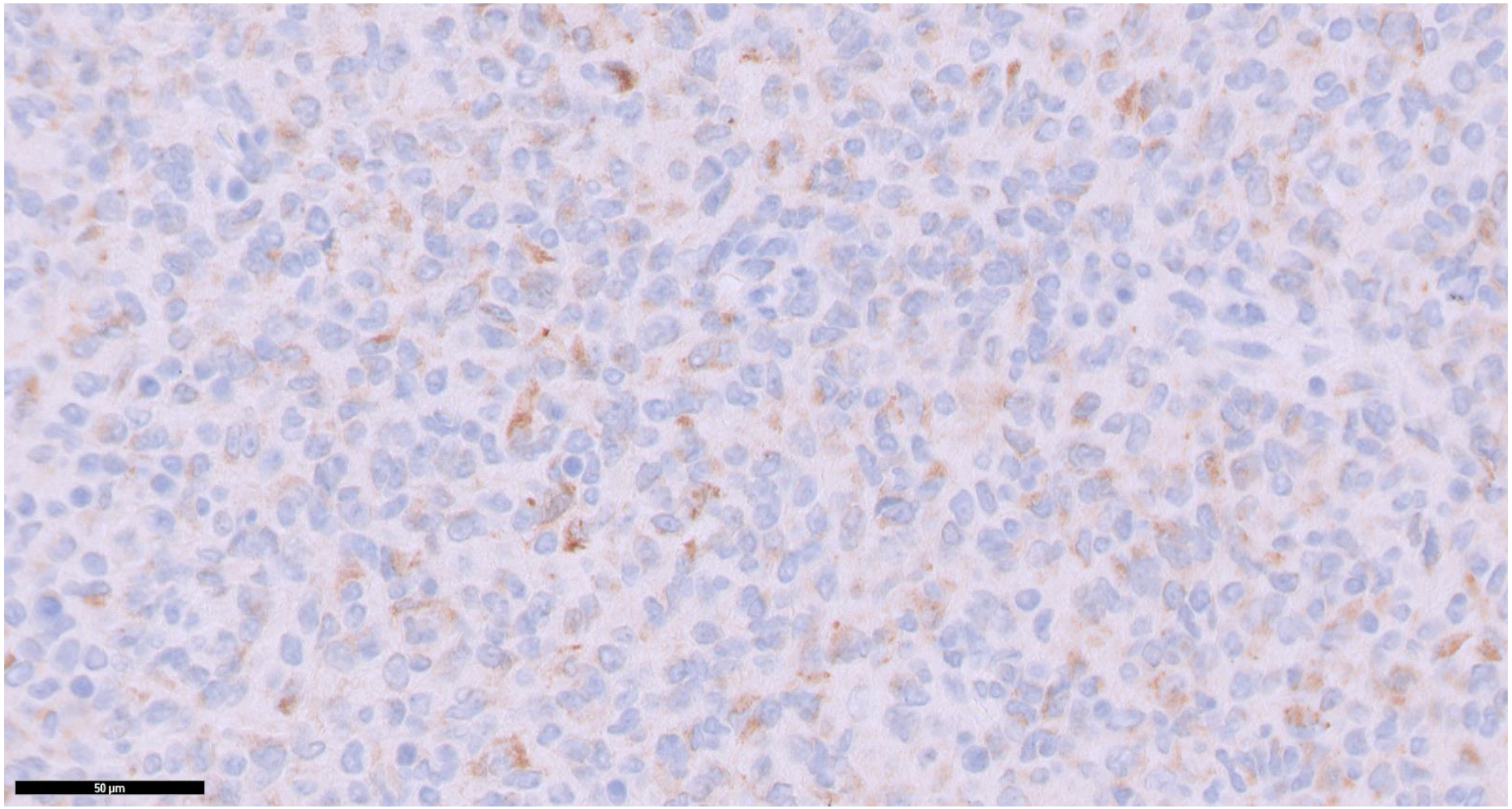

Myogenin

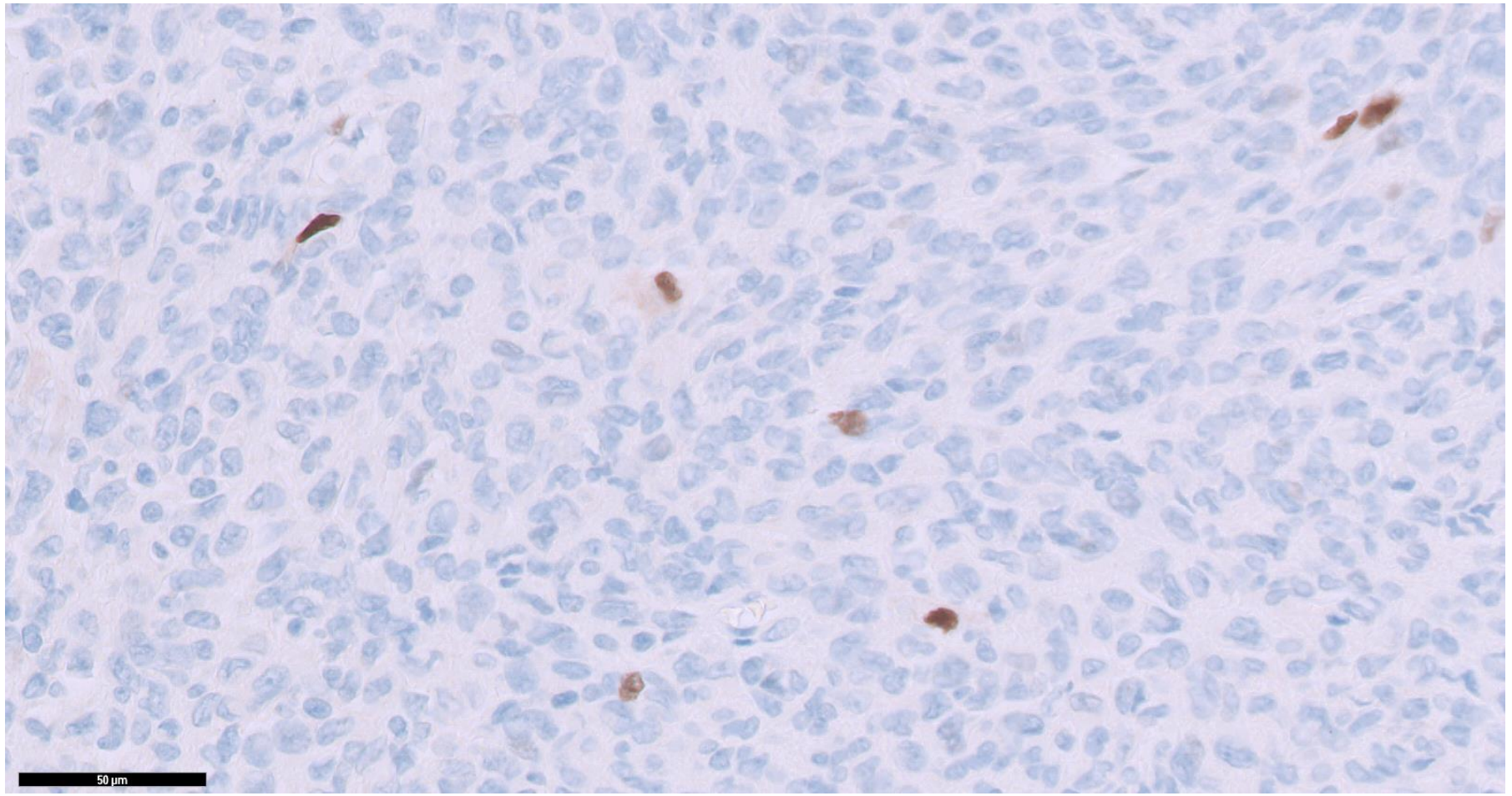

p53

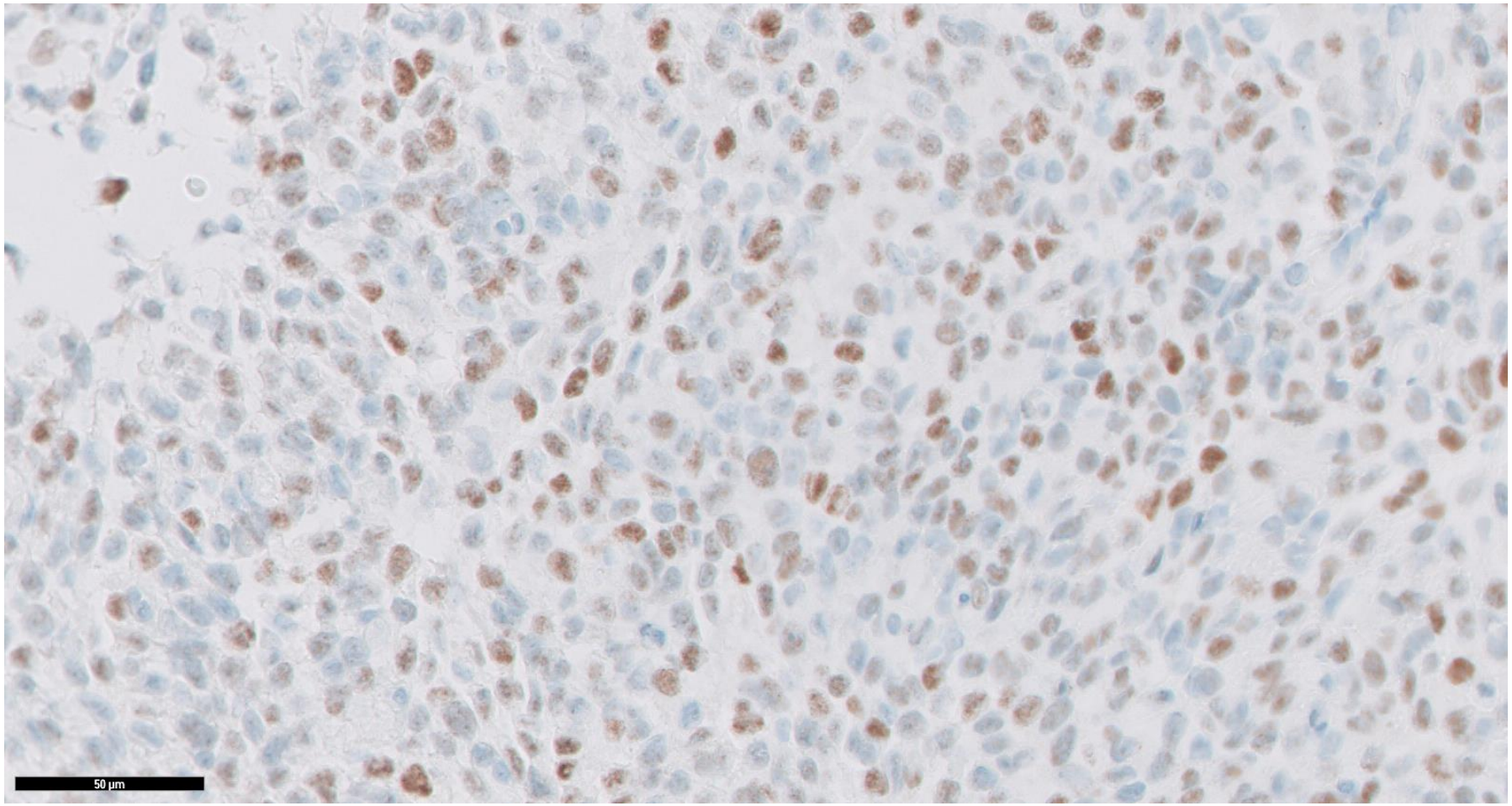

Ki-67

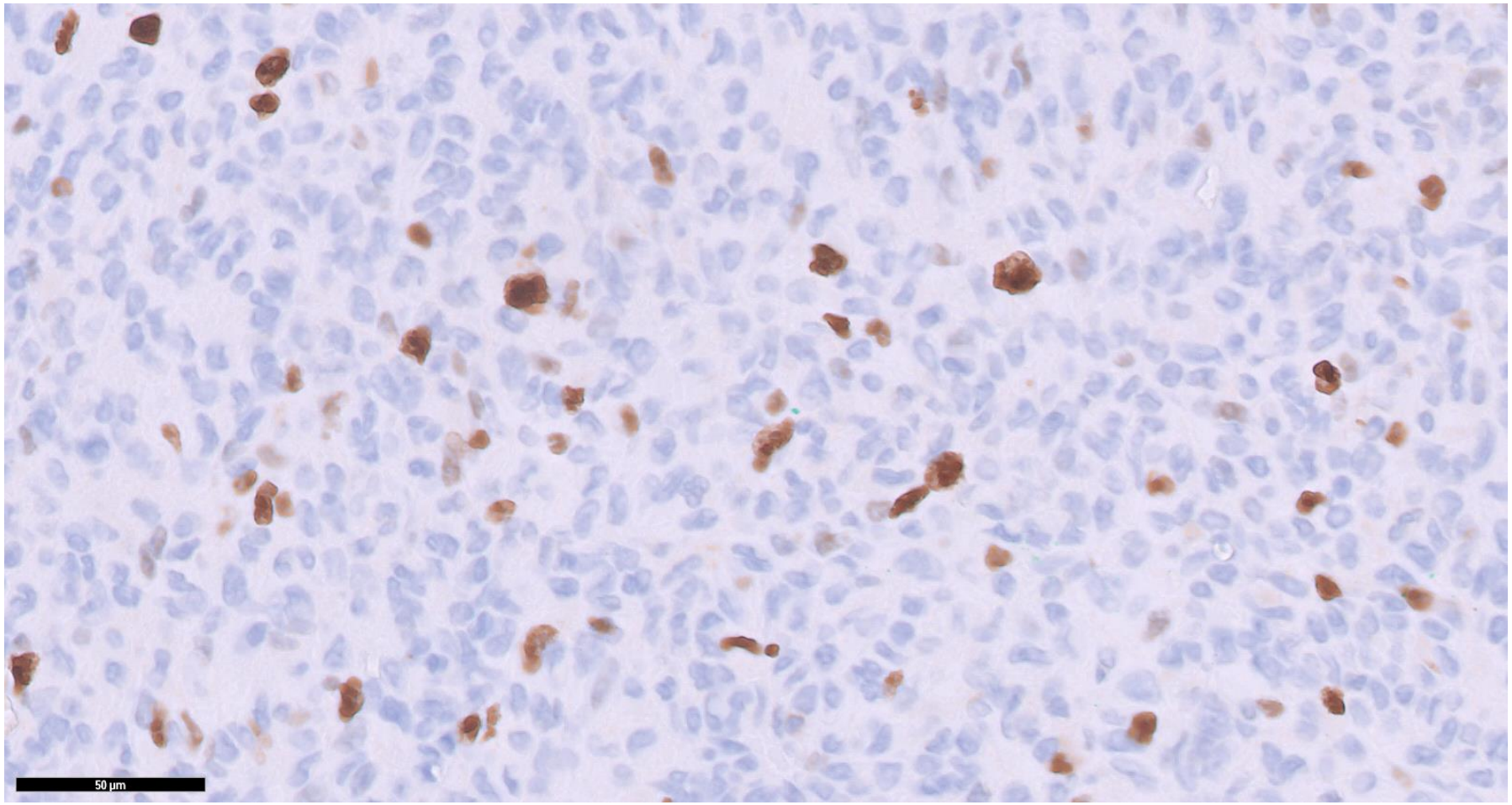

p16

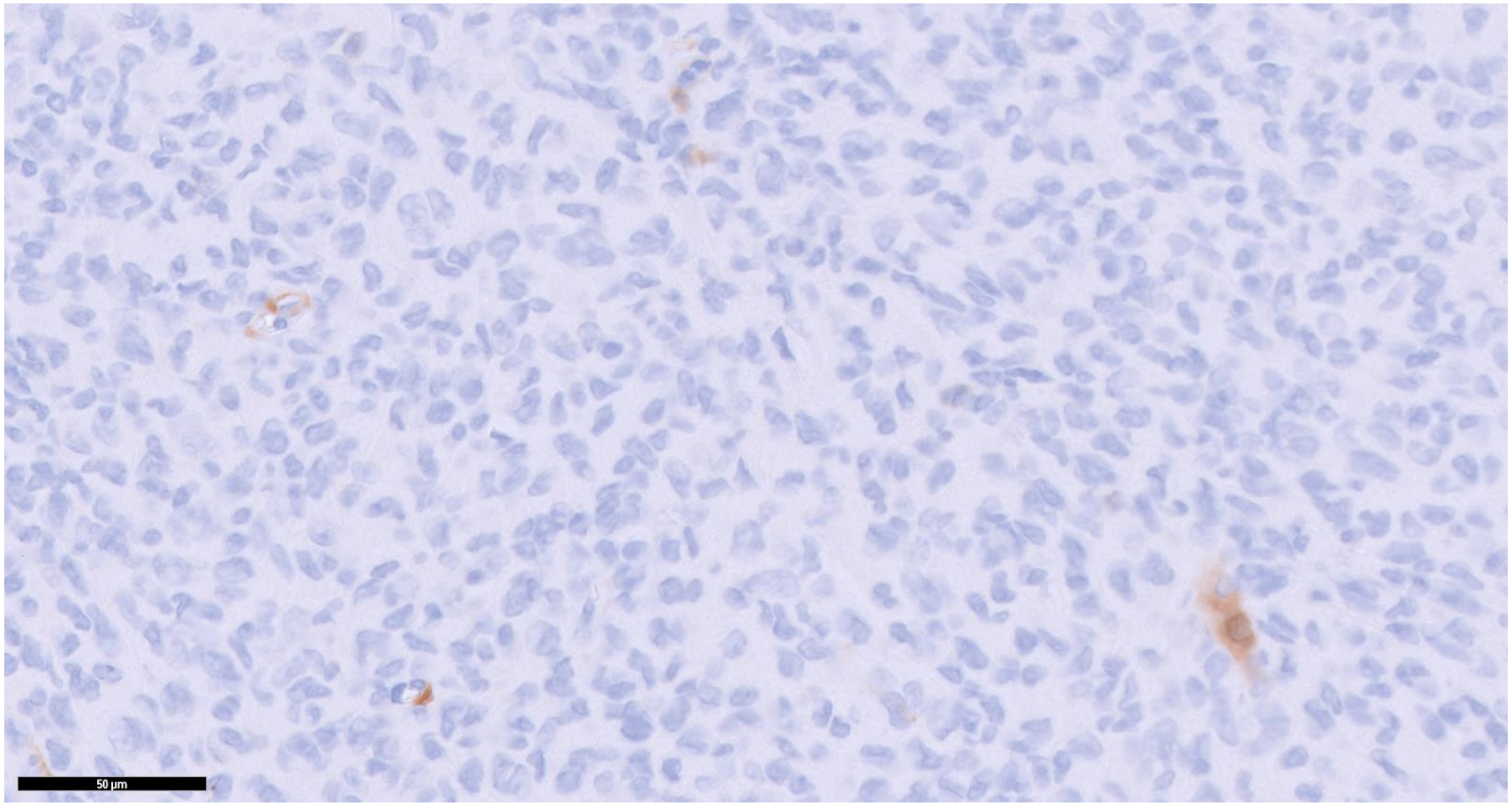

Diagnosis: Rhabdomyosarcoma arising from Inflammatory Rhabdomyoblastic Tumor

Diagnosis: Rhabdomyosarcoma arising from Inflammatory Rhabdomyoblastic Tumor

Inflammatory Rhabdomyoblastic Tumor (IRMT)

- Immunohistochemistry:
  - Diffusely positive for desmin with variable expression of PAX7, MyoD1, and myogenin
  - Negative for caldesmon
  - CD163 highlights reactive histiocytes
- Molecular: near haploidization, with retention of both parental copies of chromosomes 5 and 22, with or without subsequent whole-genome doubling

Inflammatory Rhabdomyoblastic Tumor (IRMT)

- Classification: Skeletal muscle tumor of intermediate malignancy
- Histology:
  - Circumscribed, often with a well-defined fibrous capsule but also showing small foci of infiltration into the surrounding soft tissues
  - Prominent inflammatory infiltrate comprised predominately of histiocytes, small lymphocytes, and plasma cells
  - Neoplastic spindled, epithelioid, and often pleomorphic cells with abundant, deeply eosinophilic, “glassy” cytoplasm
  - Well-differentiated rhabdomyoblasts with cross-striations are absent
  - Low mitotic activity (<1/10 hpfs) and necrosis absent

Modern Pathology (2021) 34:758–769
https://doi.org/10.1038/s41379-020-00703-8

ARTICLE

"Inflammatory Leiomyosarcoma" and "Histiocyte-rich Rhabdomyoblastic Tumor": a clinicopathological, immunohistochemical and genetic study of 13 cases, with a proposal for reclassification as "Inflammatory Rhabdomyoblastic Tumor"

Jeffrey M. Cloutier[1] · Gregory W. Charville[1] · Fredrik Mertens[2] · William Sukov[3] · Karen Fritchie[3] · Kyle D. Perry[4] · Mark Edgar[5] · Ross A. Rowsey[3] · Andrew L. Folpe[3]

Inflammatory Rhabdomyoblastic Tumor (IRMT)

- Historical perspective/terminology:
  - Inflammatory leiomyosarcoma
  - Histiocyte-rich rhabdomyoblastic tumor
  - Low-grade inflammatory myogenic tumor

➢ Preferred new consensus term: IRMT – preserves part of original name, accurately describes line of differentiation, emphasizes borderline behavior

Mod Pathol 37 (2024) 100359

MODERN PATHOLOGY

USCAP UNITED STATES AND CANADIAN ACADEMY OF PATHOLOGY
Creating a Better Pathologist

Journal homepage: https://modernpathology.org/

Research Article

Inflammatory Rhabdomyoblastic Tumor: Clinicopathologic and Molecular Analysis of 13 Cases

Toru Odate[a], Kaishi Satomi[a,b], Takashi Kubo[c], Yuko Matsushita[d,e], Toshihide Ueno[f], Akira Kurose[g], Kohei Shomori[h], Tokiko Nakai[i], Reiko Watanabe[i], Keiko Segawa[j], Shusa Ohshika[k], Naritomo Miyake[l], Sayaka Kudo[m], Tatsunori Shimoi[n,o], Eisuke Kobayashi[o,p], Motokiyo Komiyama[o,q], Seiichi Yoshimoto[o,r], Fumihiko Nakatani[s], Akira Kawai[o,p], Yasushi Yatabe[a], Shinji Kohsaka[f], Koichi Ichimura[d,e], Hitoshi Ichikawa[c], Akihiko Yoshida[a,o,*]

Diagnosis: Rhabdomyosarcoma arising from Inflammatory Rhabdomyoblastic Tumor

Diagnosis: Rhabdomyosarcoma arising from Inflammatory Rhabdomyoblastic Tumor

Mod Pathol 36 (2023) 100131

MODERN PATHOLOGY

USCAP UNITED STATES AND CANADIAN ACADEMY OF PATHOLOGY
Creating a Better Pathologist

Journal homepage: https://modernpathology.org/

Research Article

Rhabdomyosarcoma Arising in Inflammatory Rhabdomyoblastic Tumor: A Genetically Distinctive Subtype of Rhabdomyosarcoma

Carina A. Dehner[a], Katherine Geiersbach[a], Ross Rowsey[a], Paari Murugan[b], Stephen M. Broski[c], Jeanne M. Meis[d], Andrew E. Rosenberg[e], Andrew L. Folpe[a,*]

IRMT with progression to Rhabdomyosarcoma (RMS)

1. Overgrowth of monomorphic rhabdomyoblasts with diminished histiocytes
2. Monomorphic spindle cell morphology with variably pleomorphic rhabdomyoblasts and low mitotic activity
3. Morphologically undifferentiated spindle cell and epithelioid sarcoma

IRMT with progression to Rhabdomyosarcoma (RMS)

- IHC: Tend to retain diffuse desmin expression with more limited MyoD1 and myogenin expression
- Molecular: Similar near-haploidization, often with additional gains and losses involving loci containing oncogenes/tumor suppressor genes (most often *CDKN2A* and *CDKN2B*)

Differential Diagnosis For This Case

- Metastatic carcinosarcoma
- IRMT vs. RMS arising in IRMT

Differential Diagnosis
For RMS arising in IRMT

- Alveolar RMS: round cell sarcoma, diffuse myogenin expression, *PAX3*/*PAX7*::*FOXO1A* fusions
- Embryonal RMS: young patients, differentiated rhabdomyoblasts, different genetic events
- Spindle cell RMS: similar morphologic and IHC features; may require molecular analysis to distinguish
- Pleomorphic RMS: striking pleomorphism, brisk mitotic activity, large areas of necrosis; complex karyotypes

IRMT Take Home Points

- Neoplastic spindled, epithelioid, and often pleomorphic cells with deeply eosinophilic cytoplasm and prominent histiocytic infiltrate
- Low mitotic activity and no necrosis
- Diffuse desmin expression with more PAX7 and less or no myogenin/MyoD1 by IHC
- Near haploidization
- Can progress to rhabdomyosarcoma

23-1208

Tyler Paul Jankowski/Ankur Sangoi; Stanford

63-year-old man with a testicular mass

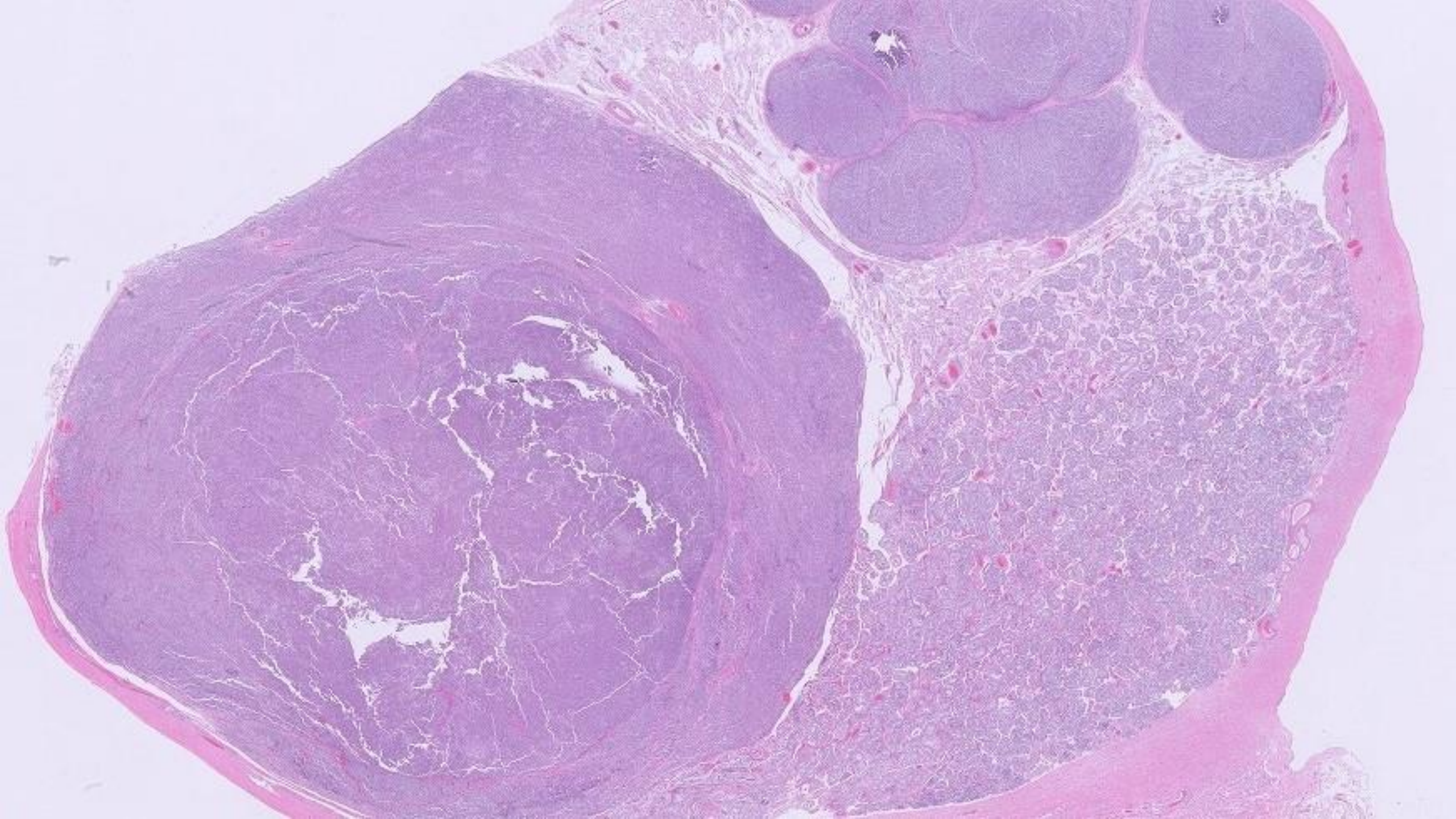

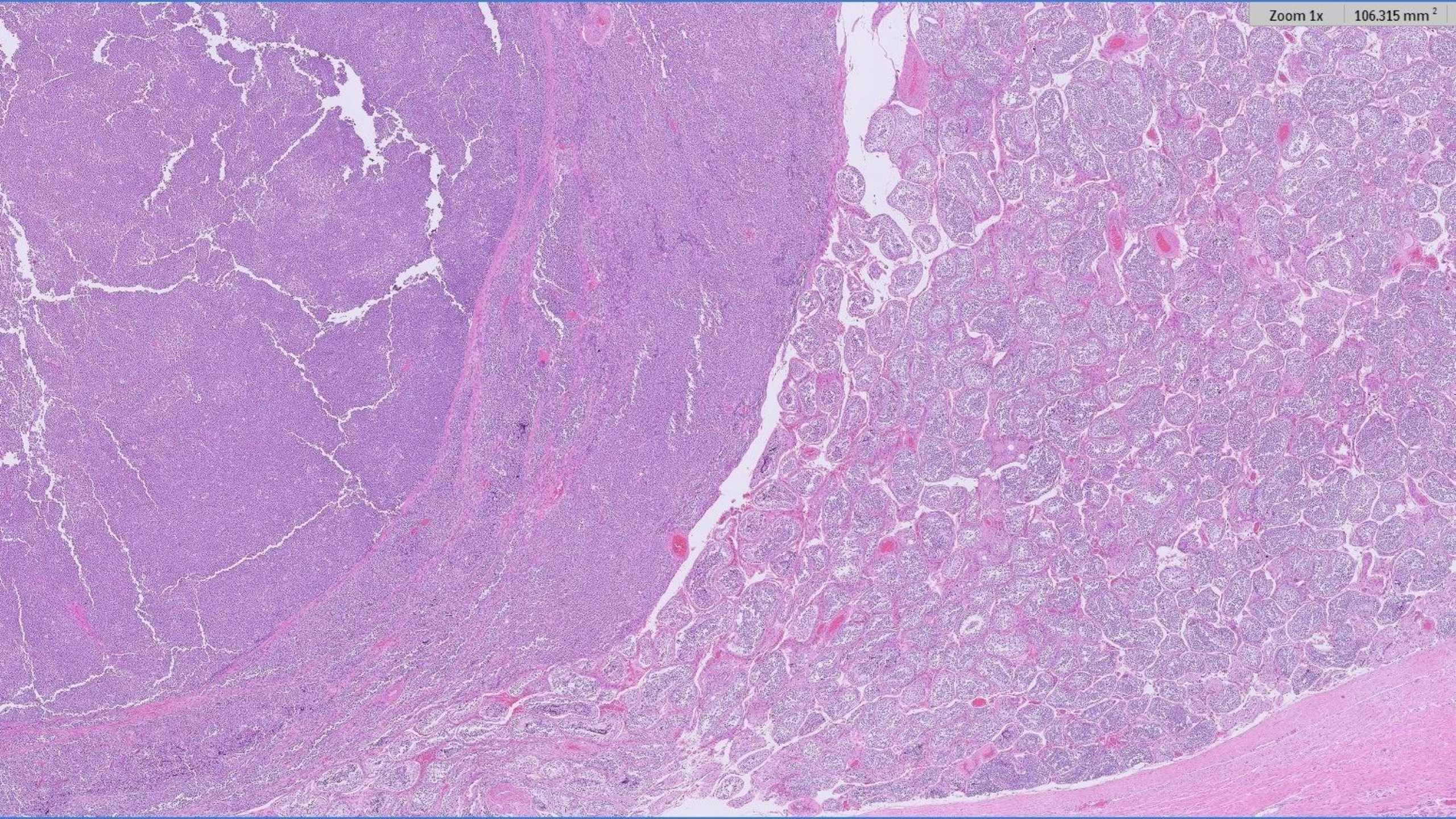
Zoom 1x
106.315 mm 2

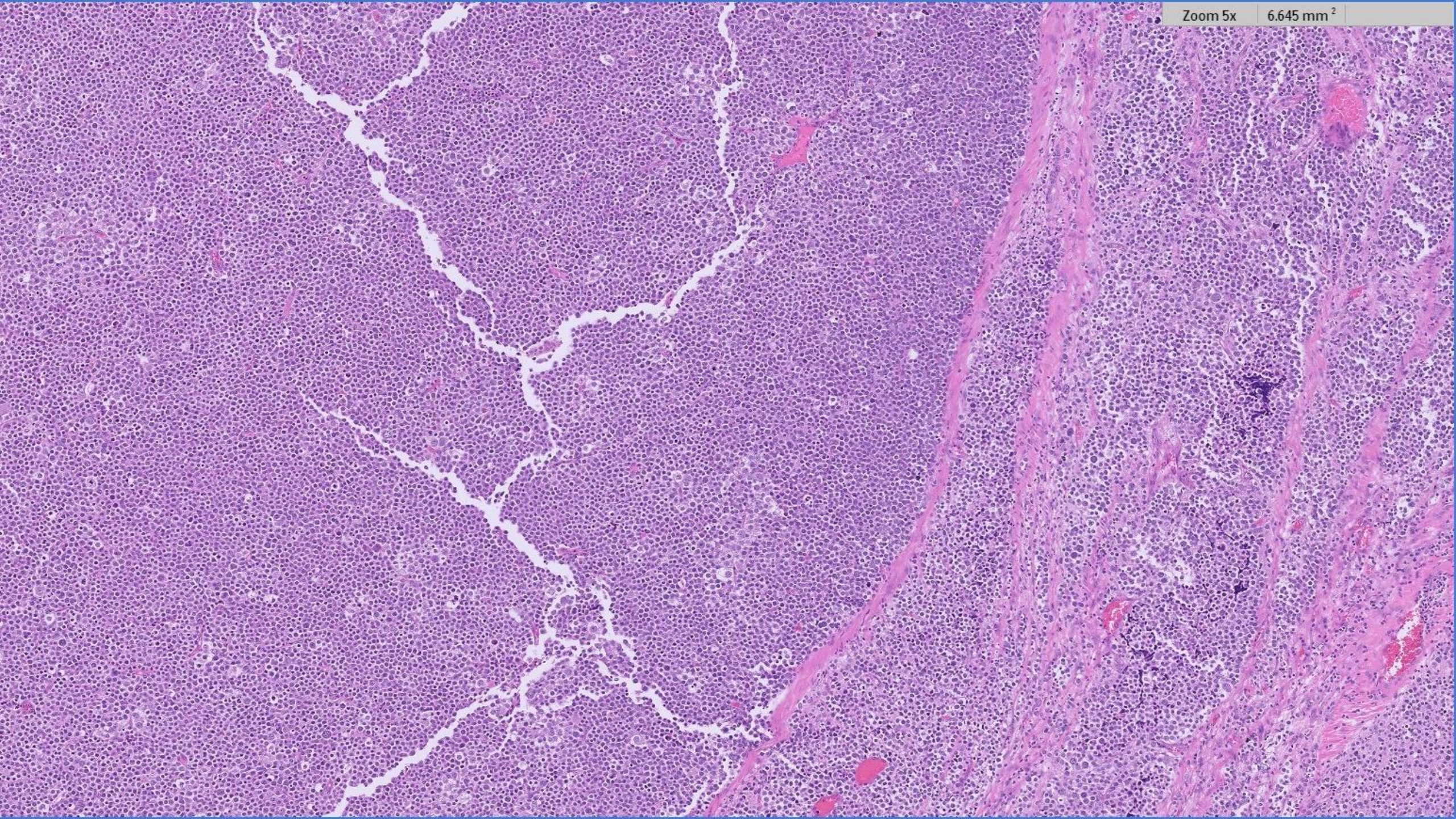
Zoom 5x
6.645 mm 2

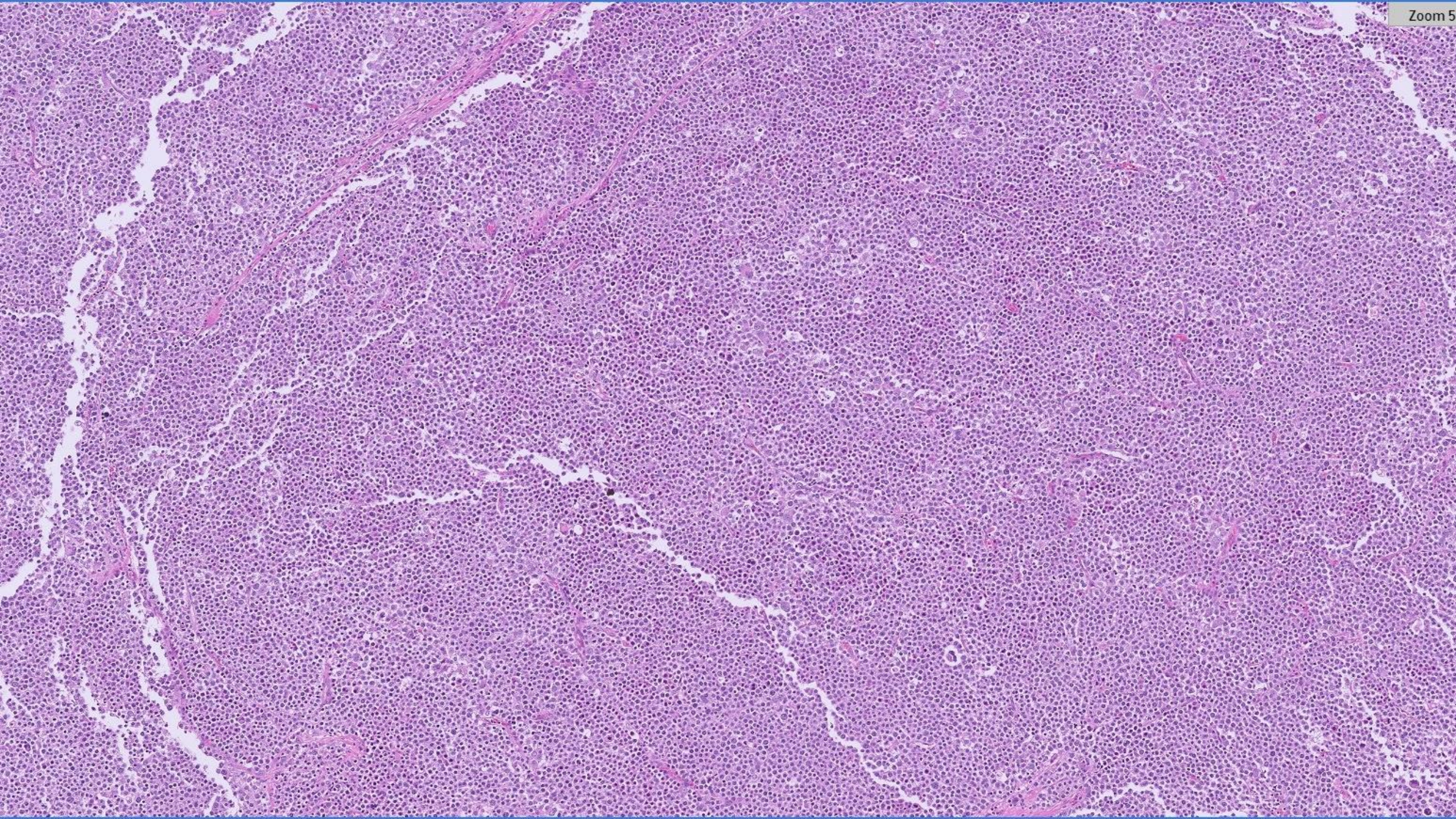
Zoom 5

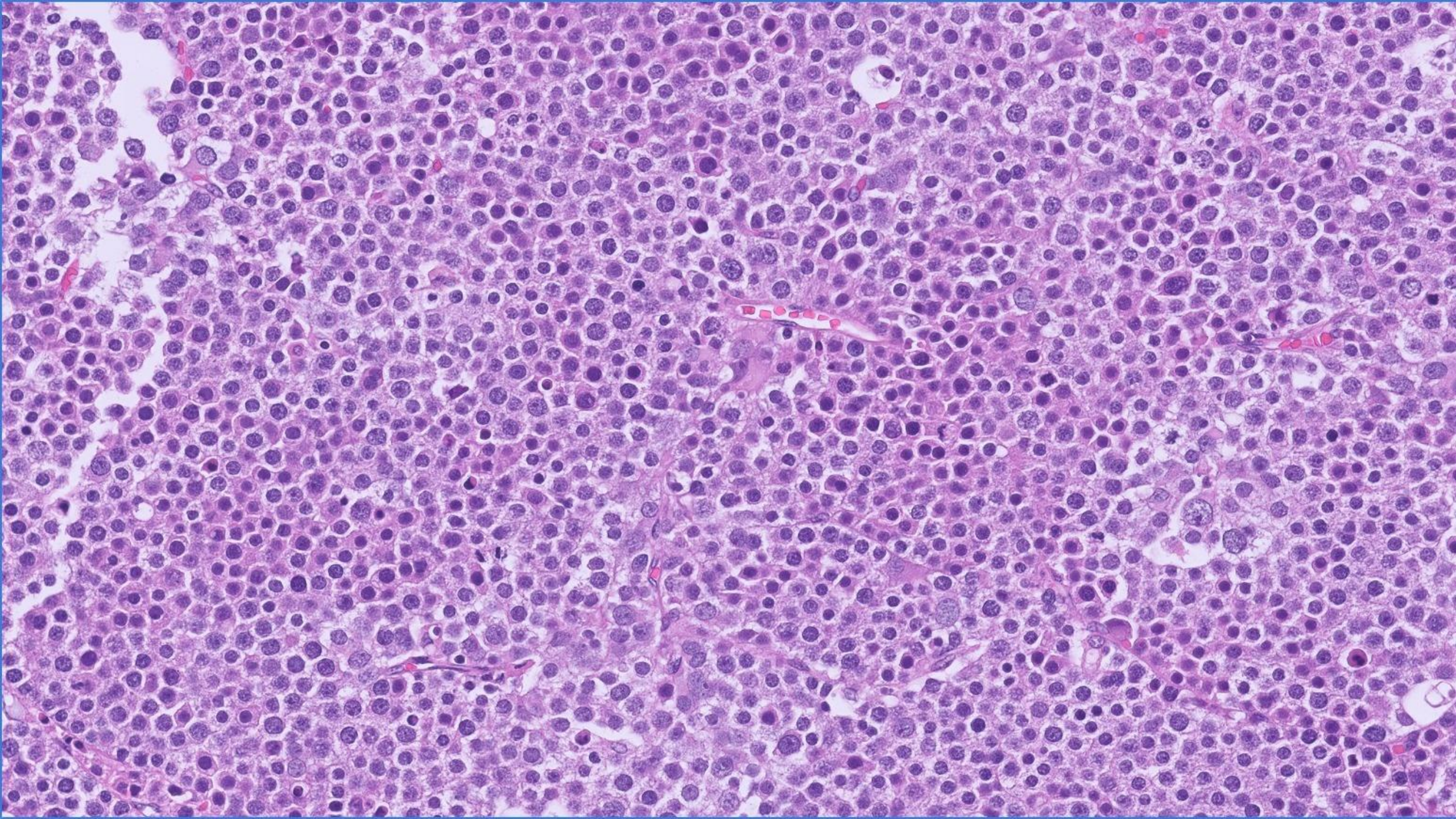

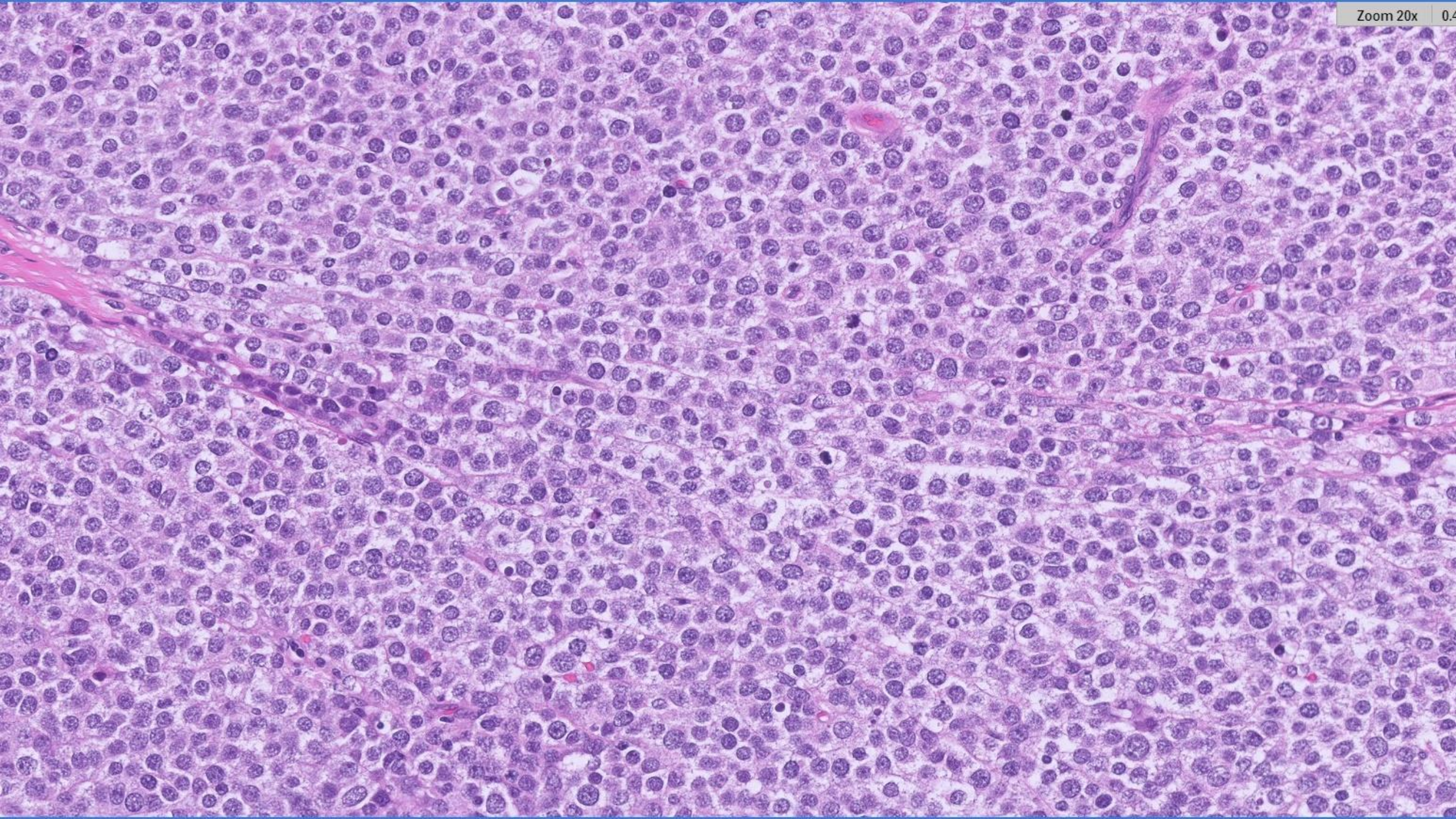
Zoom 20x
0.4

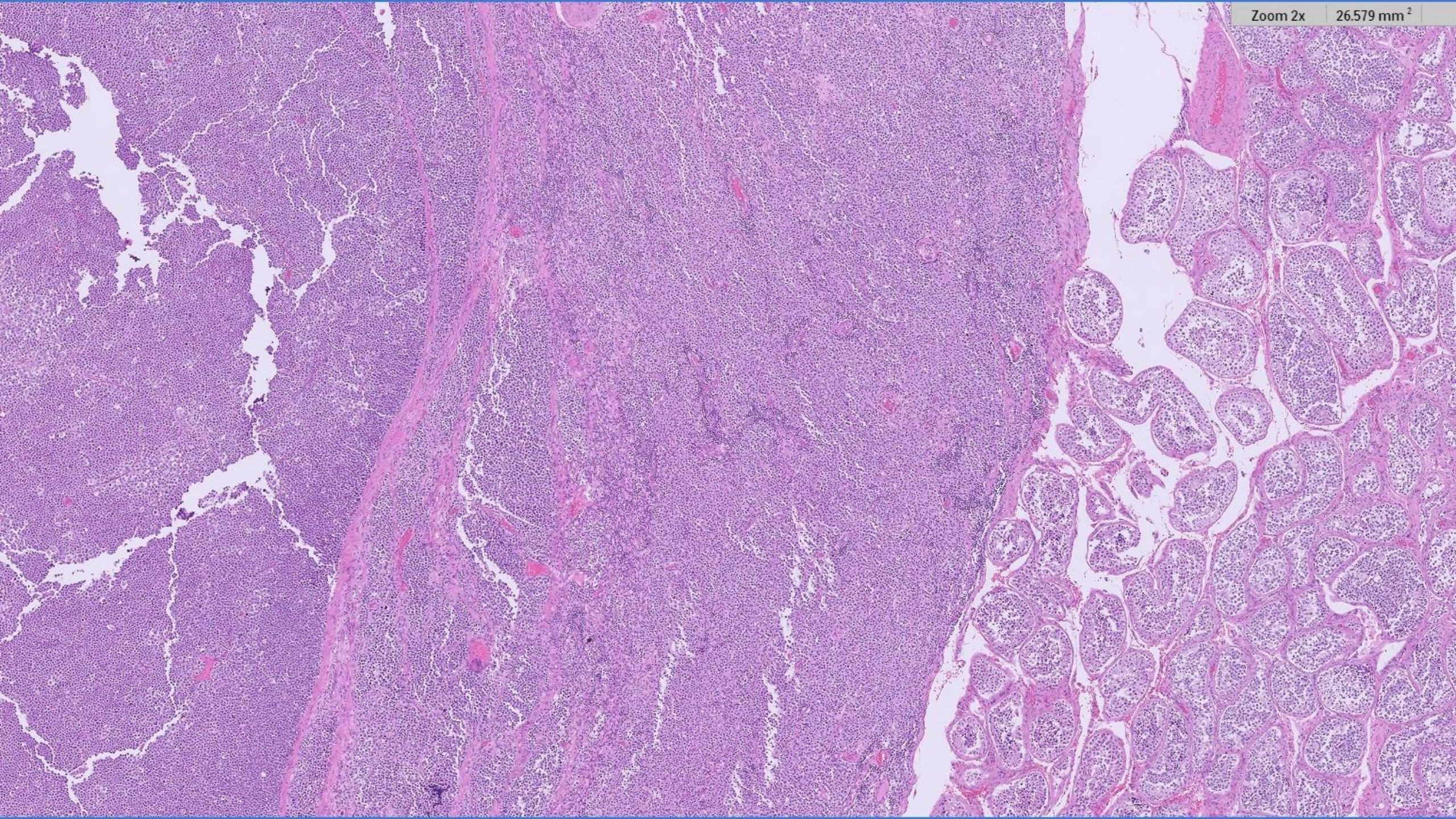
Zoom 2x
26.579 mm ²

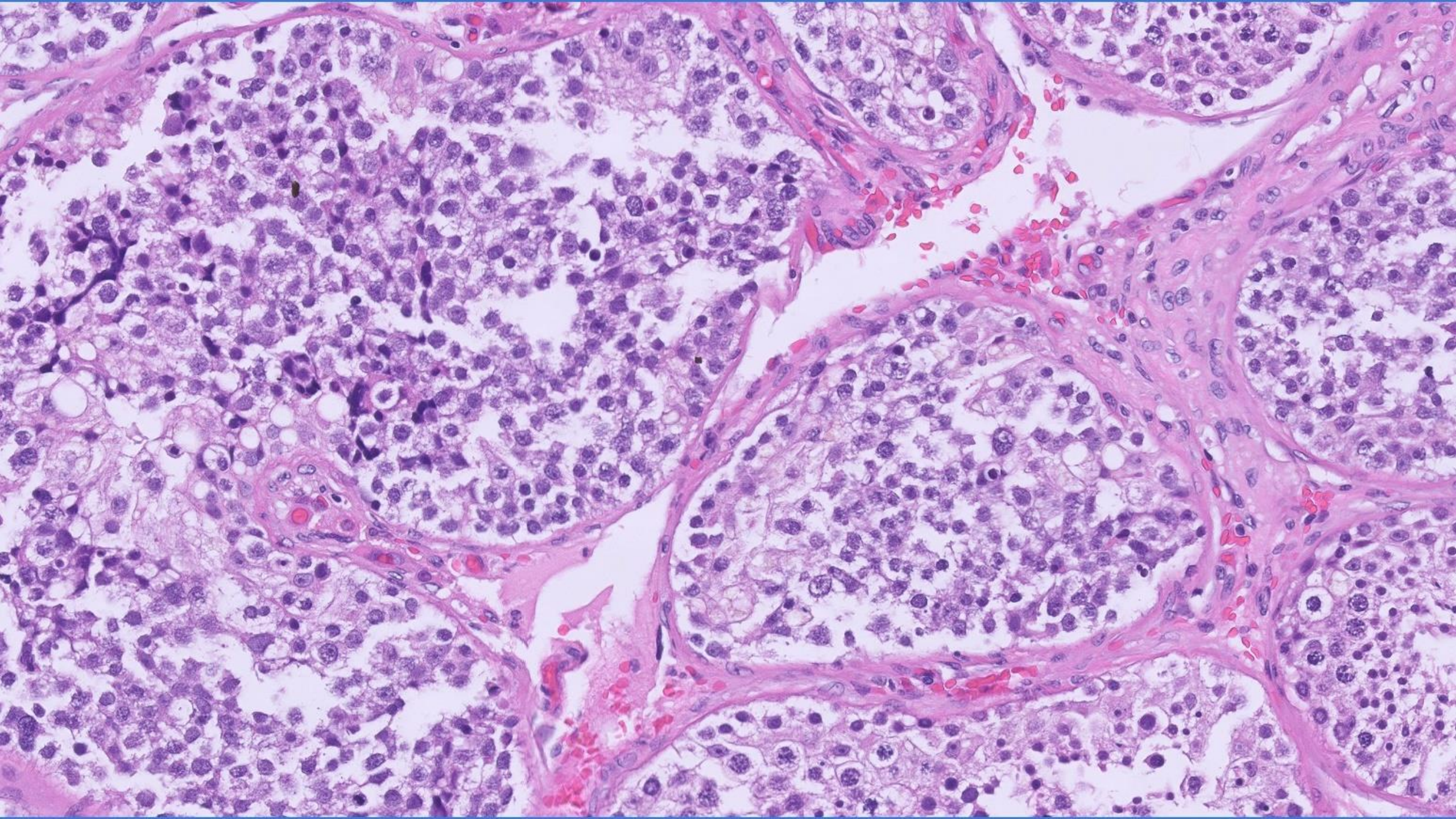

DIAGNOSIS?

Differential Diagnosis:

- Germ Cell Tumor- [Seminoma] vs Other
- Spermatocytic Tumor
- Hematolymphoid Malignancy
- Sex-Cord Stromal Tumor
- Desmoplastic Small Round Cell Tumor
- Metastasis of Unknown Primary

- Additional IHC Work-Up Pursued…

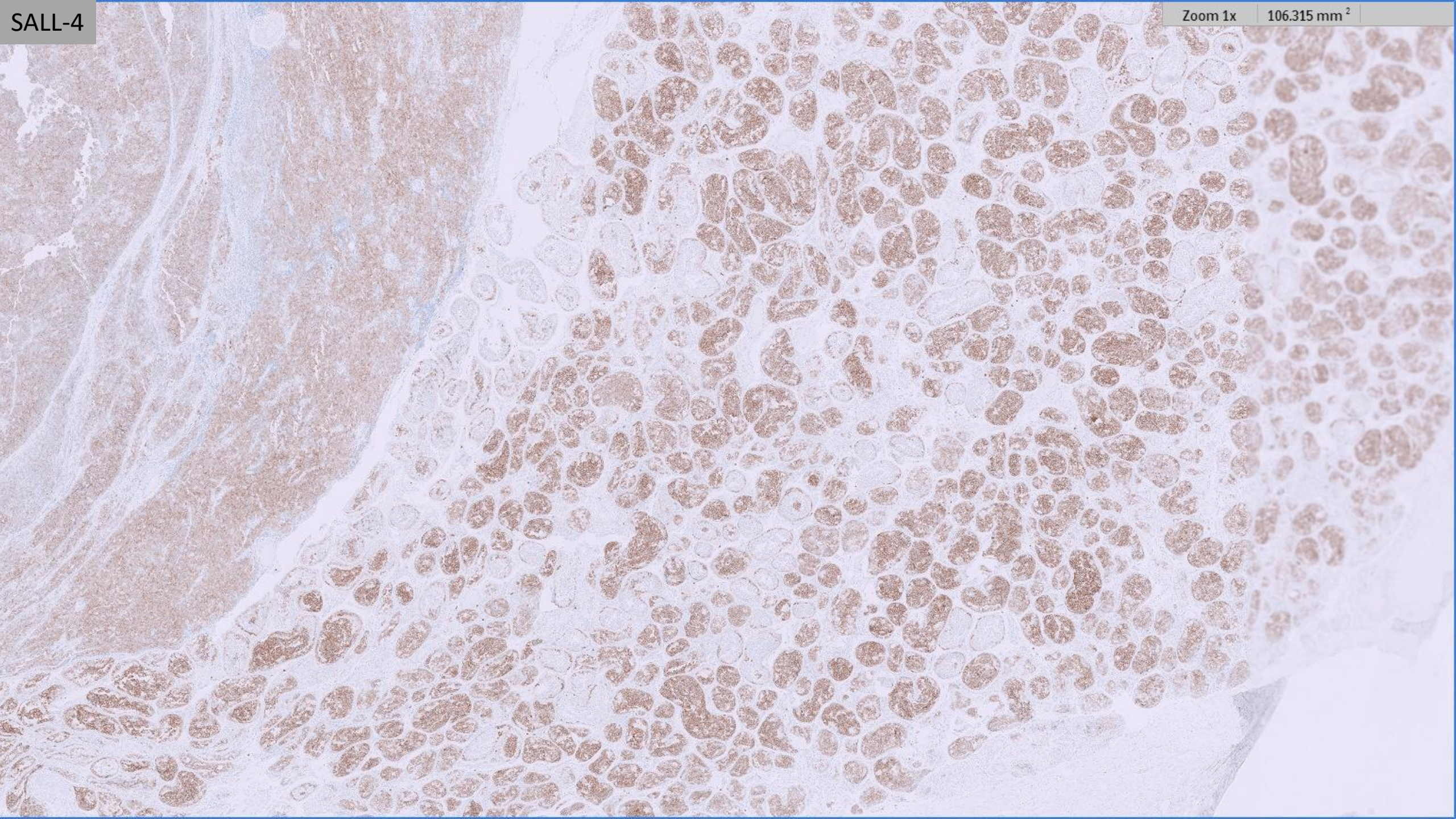
SALL-4
Zoom 1x
106.315 mm 2

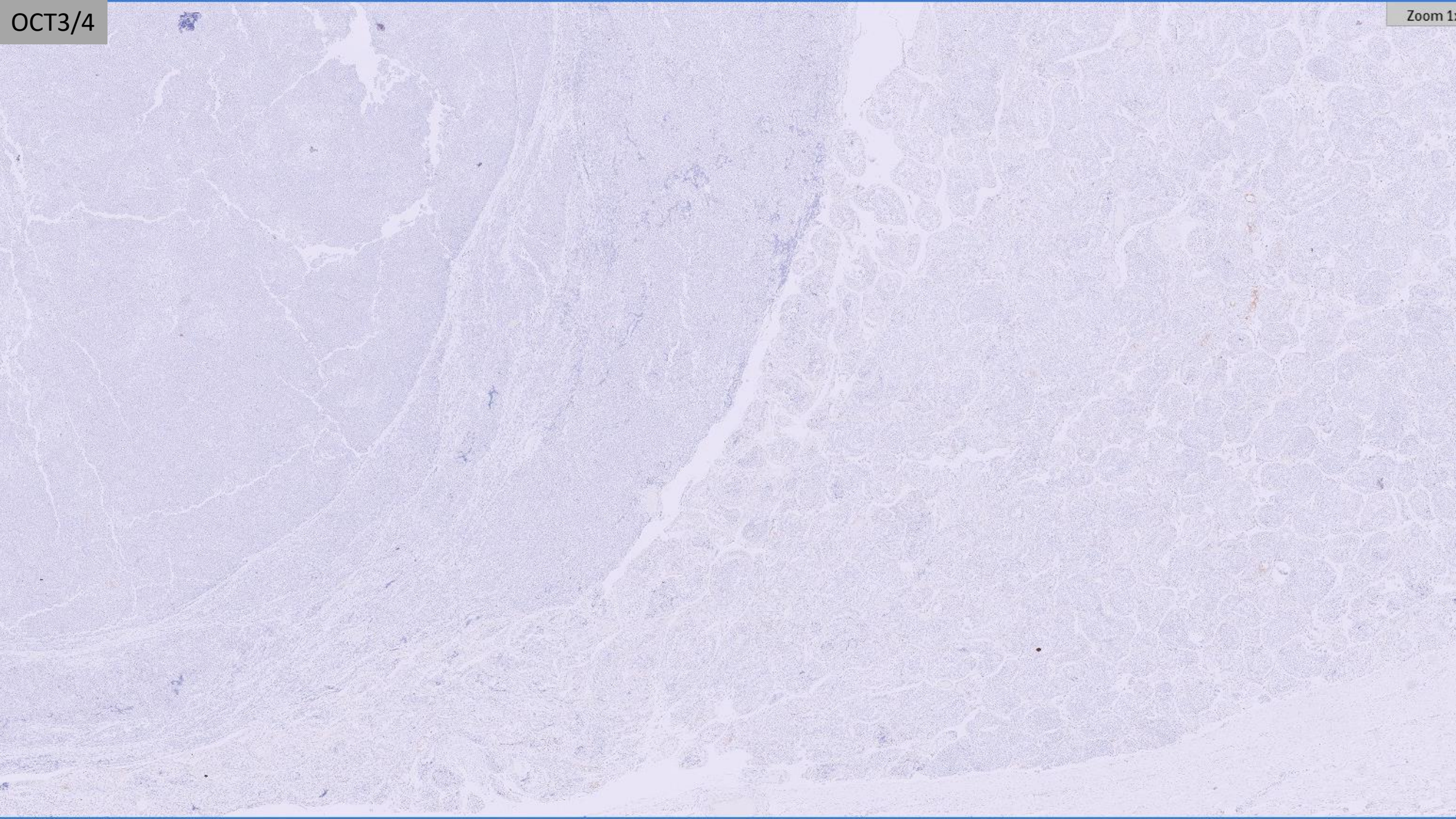
OCT3/4
Zoom 1

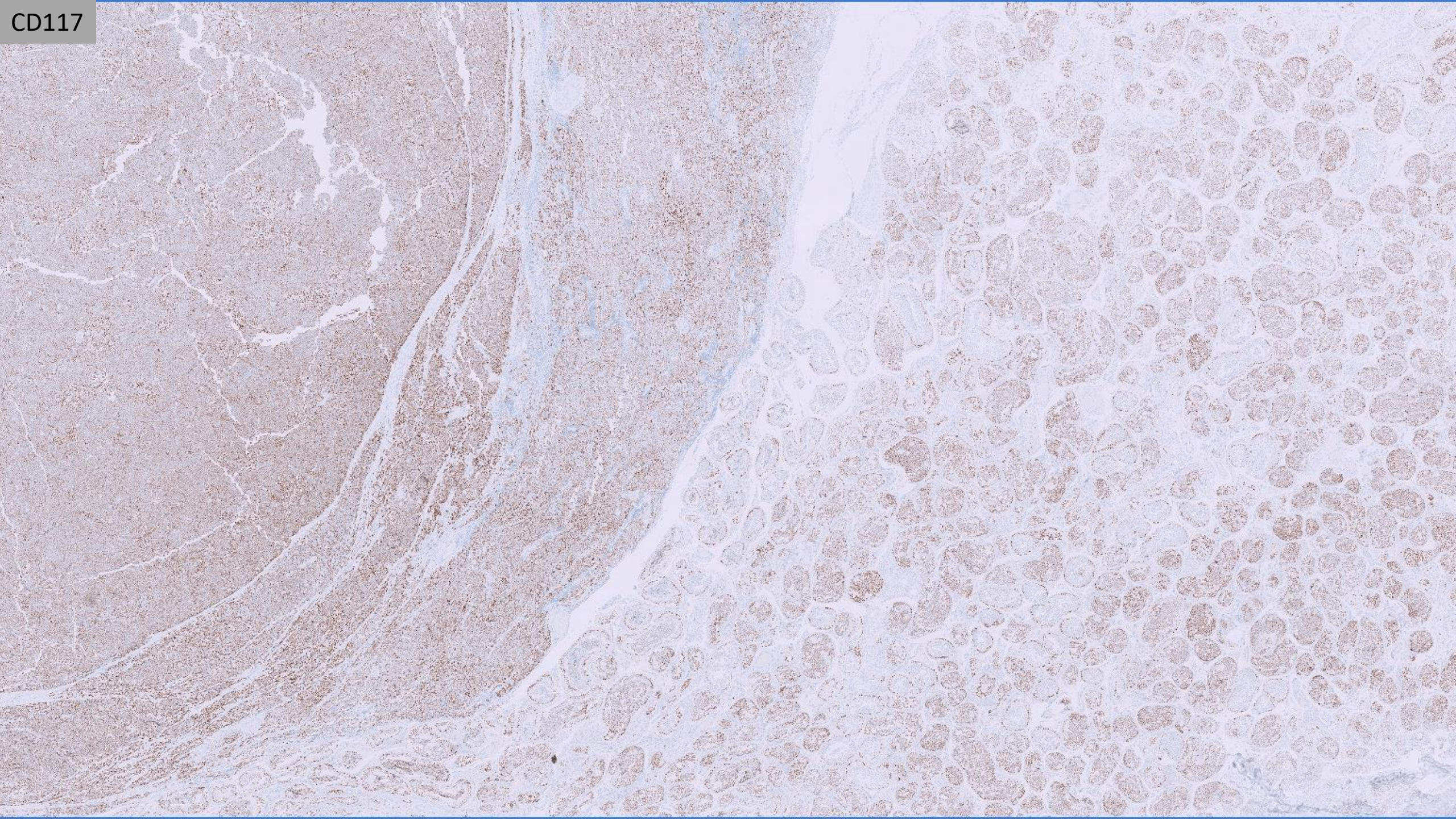
CD117

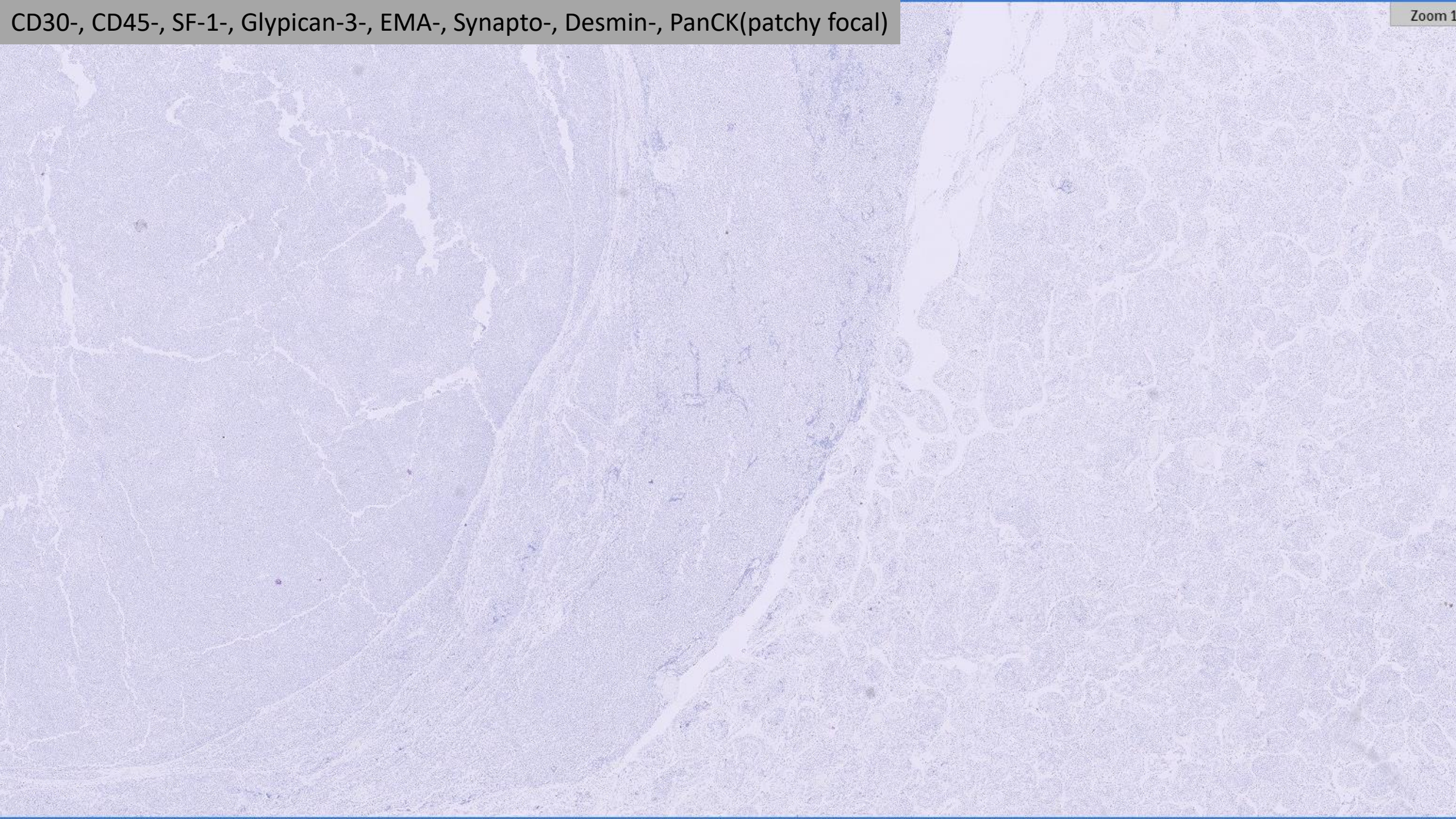
CD30-, CD45-, SF-1-, Glypican-3-, EMA-, Synapto-, Desmin-, PanCK(patchy focal)
Zoom 1

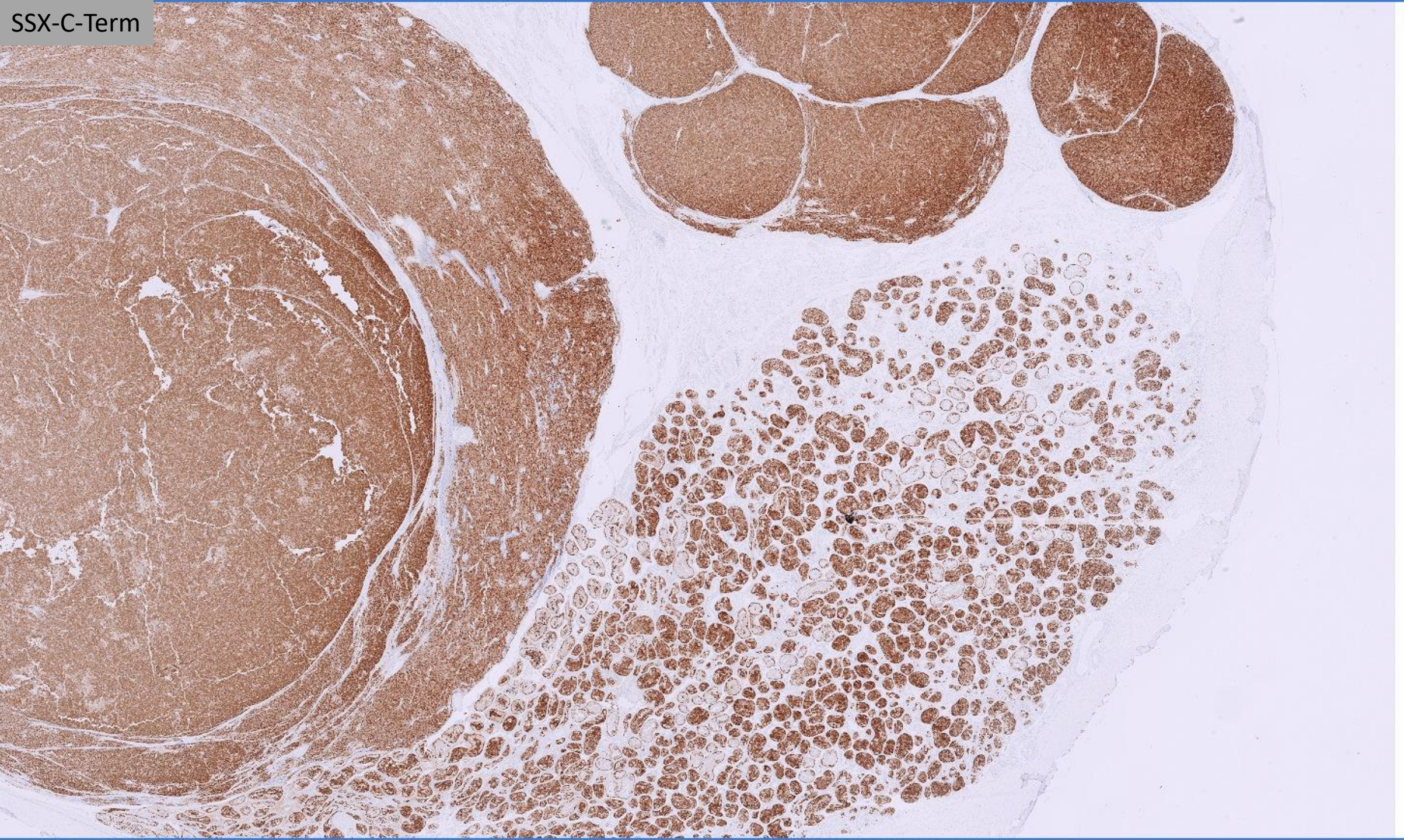
SSX-C-Term
Zoom 0.5x

Final Diagnosis:

- Spermatocytic tumor, 4.0 cm, confined to testis, negative margins

Discussion

Clinical

- Spermatocytic tumor is a GCT derived from post-pubertal germ cells
- Typically presents as painless mass in 6th decade of life
- Serum markers typically NOT elevated
- Not associated with GCNIS- rarely metastasize (5 reported cases)
- Orchiectomy usually curative

Discussion

Pathology

- Most have diffuse multinodular appearance with stromal edema
- Classic polymorphous cells population
  - Tripartite: small, intermediate (usually predominate), and giant cells
- Mitotic figures (including atypical forms) and apoptosis common

Of Note:

- "Anaplastic" variant not evidenced to be of worse clinical prognosis
- Intratubular growth (as opposed to GCNIS) is common
- Can have concurrent sarcomatous component- *worse prognosis!*

Cytogenetic Analysis

- Isochromosome 12p analysis
  - Can help differentiate spermatocytic tumor from seminoma
    - STs hallmark is amplification of *DMRT1* gene on chromosome 9

Genomic analysis of spermatocytic tumors demonstrates recurrent molecular alterations in cases with malignant clinical behavior

Sounak Gupta[1], Lynette M Sholl[2], Yiying Yang[3], Adeboye O Osunkoya[4], Jennifer B Gordetsky[5], Kristine M Cornejo[6], Kvetoslava Michalova[7], Fiona Maclean[8], Eugénia Dvindenko[9], Matija Snuderl[3], Michelle S Hirsch[2], William J Anderson[2], Ross A Rowsey[1], Rafael E Jimenez[1], John C Cheville[1], Peter M Sadow[6], Maurizio Colecchia[10], Costantino Ricci[11,12], Thomas M Ulbright[13], Daniel M Berney[14] and Andres Martin Acosta[2,13*]

Acosta, et. al

- 25 cases of STs analyzed by DNA seq, SNP, methylation, 12p FISH, IHC
  - Analysis revealed 2 subgroups
    - Diploid genomes with hotspot RAS/RAF variants
    - Global ploidy shift and absence of recurrent mutations
  - Gain of chr. 9 was consistent in both groups
  - Clinically aggressive behavior was associated with acquired TP53 mutations
    - Gains of 12p also noted as well as TP53 associated with sarcomatoid histology

Conclusion:

- STs with relative 12p gain suggest they may exhibit biologic characteristics similar to GCT with GCNIS.

Immunohistochemistry

Histopathology

Histopathology 2021, **79**, 700–707. DOI: 10.1111/his.14398

Expression of the C-terminal region of the SSX protein is a useful diagnostic biomarker for spermatocytic tumour

William J Anderson,[1] Fiona M Maclean,[2] Andres M Acosta[1] & Michelle S Hirsch[1]

[1]*Department of Pathology, Brigham and Women's Hospital and Harvard Medical School, Boston, MA, USA, and*

[2]*Department of Anatomical Pathology, Douglass Hanly Moir Pathology, Macquarie Park, New South Wales, Australia*

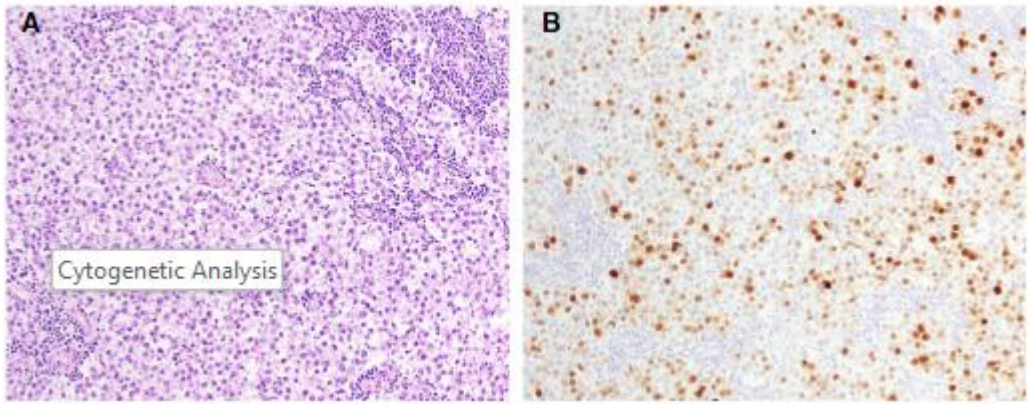

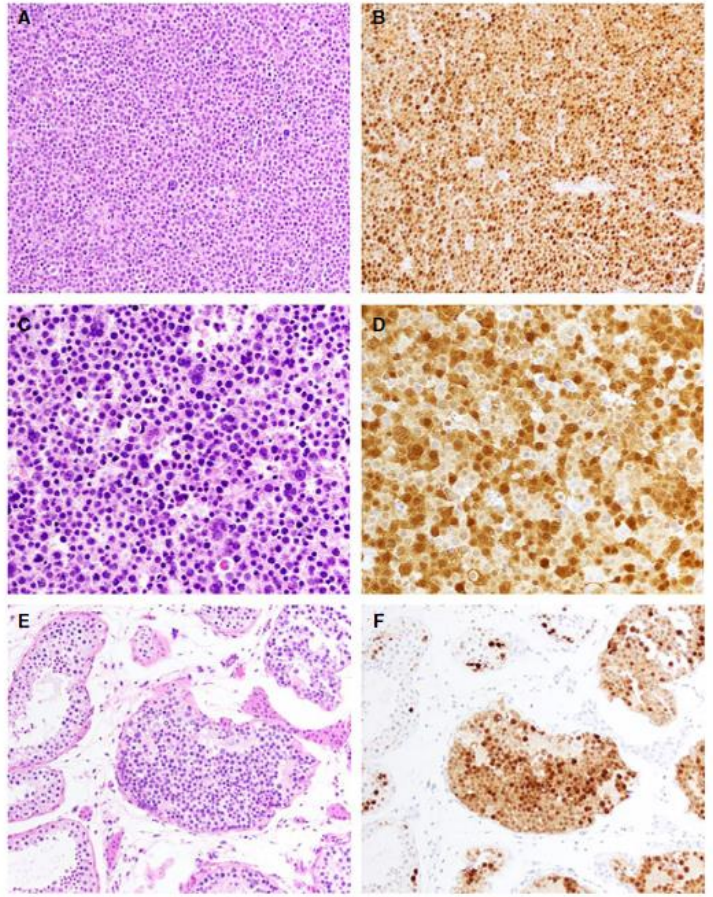

Immunohistochemistry

Table 1. Immunohistochemical expression for the C-terminal region of SSX (SSX_CT) in testicular tumours

Tumour type	Total no. of cases	SSX_CT positive, *n* (%)	0, *n* (%)	1+, *n* (%)	2+, *n* (%)	3+, *n* (%)
Spermatocytic tumour	15	15 (100)	0	0	1 (7)	14 (93)
Pure seminoma (total)	34	20 (59)	14 (41)	15 (44)	3 (9)	2 (6)
Seminoma (age ≤50 years)	22	13 (59)	9 (41)	10 (45)	1 (5)	2 (9)
Seminoma (age >50 years)	12	7 (58)	5 (42)	5 (42)	2 (16)	0
MGCT components (total)	39	2 (5)	37 (94)	1 (3)	1 (3)	0
Seminoma	4	2 (50)	2 (50)	1 (25)	1 (25)	0
Embryonal carcinoma	13	0	13 (100)	0	0	0
Yolk sac tumour	12	0	12 (100)	0	0	0
Choriocarcinoma	6	0	6 (100)	0	0	0
Teratoma	4	0	4 (100)	0	0	0
Sertoli cell tumour	7	0	7 (100)	0	0	0
Lymphoma (DLBCL)	6	0	6 (100)	0	0	0

Southbay Treasurer 2023 Year End Update

- Membership ($300/member):
  - 8 trainees (3 UCSF and 5 Stanford)
  - 65 full members (about the same from 2022)
- Starting Balance: $40,768
- Current Balance: $38,533 (December meeting and Webmaster pending)
- Expenses
  - Bi-monthly Meetings: $22,232.11 (plus December)
  - Spring Meeting: $10,426.52
  - Tax Accountant: $1,200
  - Survey Monkey: $372
  - Zoom: $150
  - CME: $999